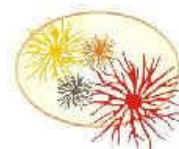




UNIVERSIDADE FEDERAL DO RIO GRANDE - FURG

INSTITUTO DE CIÊNCIAS BIOLÓGICAS

PROGRAMA DE PÓS-GRADUAÇÃO EM CIÊNCIAS FISIOLÓGICAS



**INTERAÇÕES FARMACODINÂMICAS ENTRE QUIMIOTERÁPICOS  
USADOS NO TRATAMENTO DA LEUCEMIA: ABORDAGENS *IN VITRO* E *IN  
SILICO* SOBRE ASPECTOS DAS DEFESAS ANTIOXIDANTES, SISTEMA DE  
FOSFORILAÇÃO E FENÓTIPO DE RESISTÊNCIA A MÚLTIPLAS DROGAS**

**Maiara Bernardes Marques**

Orientador: Dr. Luis Fernando Marins

Co-orientadora: Dr<sup>a</sup>. Daniela Volcan Almeida

Tese de doutorado apresentada ao Programa de Pós-Graduação em Ciências Fisiológicas da Universidade Federal do Rio Grande como requisito parcial para a obtenção do Título de Doutora.

**Rio Grande, 2018**

*Ainda que eu falasse a língua dos  
homens e dos anjos, sem amor  
eu nada seria.*

*1 Coríntios 13:1*

*Dedico essa tese aos meus pais, meu irmão,  
minha vó Odete e a todas as pessoas que me  
ajudaram a chegar até o final, que agora, já é um novo início...*

## **Agradecimentos**

Eu poderia escrever inúmeras páginas somente com os agradecimentos as várias pessoas que me ajudaram a chegar até aqui e entregar a tese, o que representa um marco na vida de qualquer pesquisador. Acho importante a gratidão e o reconhecimento de que ninguém consegue realizar um sonho sozinho.

Inicialmente, agradeço à banca por aceitar colaborar com essa Tese.

Agradeço à Fabiana Seixas e à Karina Machado por se disponibilizarem a participar de um momento importante para minha formação.

Agradeço à Ana Votto pela paciência, ajuda e contribuição significativa em vários momentos ao longo de todos estes anos.

Ao Michel por ter sido um super parceiro nessa tese, colaborando com meu crescimento profissional e pessoal. Pessoa maravilhosa que cruzou meu caminho, só gratidão!

Ao Carioca, por ser um exemplo de profissional, professor e pessoa do nosso PPG-Ciências Fisiológicas. Obrigada por aceitar o convite da compor a banca, precisei insistir!!

À Dani Volcan pela ajuda, paciência e formação, principalmente sobre os ensinamentos básicos no campo da biologia molecular.

Agradeço ao Luf, pela orientação, por se desafiar junto comigo nos diversos temas que estudamos ao longo desses anos. Agradeço por me ensinar tanto, pela paciência em explicar várias vezes, de diversas formas até conseguir se fazer entender. Muito além da formação acadêmica, aprendi contigo sobre autonomia, sobre buscar com as próprias mãos e isso eu levarei para vida toda. Obrigada!

Agradeço ao pessoal do Legene, em especial ao Bruno Oliveira pela troca e amizade durante todos esses anos. Às meninas Jade, Raiza, Kamila e Luíza por tornarem os dias mais alegres. E também à Bruna por me ajudar nessa reta final, obrigada!

Agradeço à FURG pela oportunidade de estudar por 10 anos e meio em uma Universidade Pública e de qualidade.

E também a CAPES pela bolsa de estudo [O presente trabalho foi realizado com apoio da Coordenação de Aperfeiçoamento de Pessoal de Nível Superior - Brasil (CAPES) - Código de Financiamento 001]

Agradeço à todos professores, comissão acadêmica do PPG-Ciências Fisiológicas em especial à Marta e Juh por sempre se disponibilizarem a ajudar. Também agradeço à todos funcionários em especial à Loraine, Maria e Inês.

Ao longo destes anos fui agraciada com muitos amigos.

Agradeço a todos eles em especial a Carol Peixoto por tudo. É difícil até encontrar palavras para mensurar a importância da tua amizade e apoio durante todos esses anos.

À Gisele, por ser uma amiga tão leal. Por me ensinar sobre as operações Jack Bauer, sobre como ser gentil e amável, entre tantas outras coisas mais. Sem palavras para te agradecer.

As minhas amigas de sempre e às amigas da dança por acompanharem e apoiarem minha trajetória acadêmica.

Agradeço diversos colegas e amigos Ayane, Roberta, Aline, Renatinha, Juh, Sil, Marcelinho, Lidi, Elita, Pri, Fernanda, Anahy, Laís, Cris, Bruno, Dedi, Laura, Jose, Carol Reyes e Marina por vários momentos felizes que já passamos juntos.

À Barbosa, em especial à Janice e aos meus olhinhos brilhantes, por me renovarem, ajudarem e por toda paciência nessa reta final.

Aos meus amores Vó Odete, Isadora, Gabi, Adriana e demais familiares por sempre me ajudarem e se preocuparem comigo.

Ao Roger, por ter sido muito mais do que um namorado, um companheiro de verdade, que me ajudou todos os dias nesses últimos 9 meses. Nosso amor foi nascendo e florescendo junto com a Tese. Obrigada por me apoiar, acalmar, acreditar em mim e organizar meus pensamentos quando eu estava perdida. Fostes essencial para a finalização serena e confiante dessa etapa da minha vida.

Agradeço ao meu irmão Matheus por todo apoio, por me ajudar em tudo, por ser meu melhor amigo, meu confidente e às vezes meu escravo. Te amo

Aos meus pais (Graça e Nedi) que me ensinaram que estudar é o bem maior que se leva dessa vida. Devo tudo à vocês e fiz tudo por vocês. Vocês são a razão de tudo.

À Deus, pelas coincidências que não são só coincidências, são Tua sutil presença, pulsante, vibrante e forte.

## Sumário

Rio Grande, 2018.....	i
Agradecimentos .....	4
Lista de abreviaturas .....	7
Lista de Figuras.....	8
Lista de Tabelas .....	9
Resumo .....	10
Abstract.....	11
<b>1. Introdução.....</b>	<b>112</b>
1.1 Câncer .....	12
1.2 Interações entre quimioterápicos .....	13
1.3 Leucemia .....	17
1.4 As principais características da resistência a múltiplas drogas (MDR) .....	19
1.5 Metabolismo tumoral e fenótipo MDR.....	22
1.6 Bombas de extrusão e o fenótipo MDR.....	25
1.7 Relação entre a quinase PIM-1 e o fenótipo MDR.....	26
1.8 Novo inibidor de quinase PIM-1: AZD1208.....	32
1.9 Modelos estudados in vitro .....	33
1.10 Bioinformática no Câncer .....	34
<b>2. OBJETIVOS.....</b>	<b>35</b>
2.1 Objetivo Geral .....	35
<b>3. RESULTADOS .....</b>	<b>36</b>
3.1 Manuscrito 1 .....	36
3.2 Manuscrito 2 .....	59
3.3 Artigo 3 .....	96
<b>4. DISCUSSÃO GERAL E CONCLUSÕES .....</b>	<b>11</b>
<b>REFERÊNCIAS GERAIS .....</b>	<b>14</b>

## **Lista de abreviaturas**

ABC - ATP binding cassette

ABCB1- ou MDR1, codifica a Glicoproteína-P

ABCC1- ou MRP1, codifica a glicoproteína MRP1

ABCG2- codifica a Glicoproteína ABCG2 ou BCRP

ARE - elementos de resposta antioxidante

CAT- catalase

DNR - daunorubicina

FEPS - Linhagem resistente à daunorubicina

GLUT1 - Transportador de glicose 1

GSTM4 - glutathione-S-transferase

H<sub>2</sub>O<sub>2</sub> - peróxido de hidrogênio

HIF-1 $\alpha$  - fator-1  $\alpha$  de indução a hipoxia

K562- Linhagem celular sensível à quimioterapia (não-MDR)

K562/Lucena 1 (Lucena) - Linhagem celular MDR resistente à Vincristina

LMA - Leucemia Mielóide Aguda

LMC - Leucemia Mielóide Crônica

MDR - Resistência a Múltiplas Drogas

MTT - Brometo de (3- (4 5-dimetiltiazol-2-yl)-2 5-difeniltetrazólio

NRF2 - Fator nuclear (derivado de eritróide 2)

Ph1 - Cromossomo Philadelphia

ROS - Espécies Reativas de Oxigênio

SOD - Superóxido dismutase

VCR- Vincristina

## Lista de Figuras

Figura 1: Figura esquemática demonstrando que agentes quimioterápicos utilizados no tratamento do câncer podem levar à interações farmacodinâmicas. ....	14
Figura 2: Estrutura química dos quimioterápicos estudados. Vincristina, Daunorrubicina e AZD1208. ....	17
Figura 3: Leucemia Mieloide Crônica apresentando translocação dos cromossomos 9 e 22, denominado cromossomo Filadélfia. ....	19
Figura 4: Categorias que podem ativar ou promover a resistência direta ou indireta a múltiplas drogas em células tumorais. ....	20
Figura 5: Ilustração esquemática do sistema de defesa antioxidante contra o estresse oxidativo intracelular. ....	24
Figura 6: Estrutura 3D da ABCB1 (figura oriunda da tese).....	26
Figura 7: Estrutura da quinase PIM-1 (figura oriunda da tese).....	29
Figura 8: Processos celulares regulados por PIM que são críticos para a resistência e progressão tumoral, tornando PIM alvo promissor para terapia contra o câncer.....	30
Figura 9: Aspectos da PIM-1 que estão relacionado com o fenótipo MDR.....	32
Figura 10: Demonstração farmacodinâmica entre proteína e fármaco formada com a utilização de ferramenta de bioinformática.....	35



## **Lista de Tabelas**

Tabela 1: Principais classes de quimioterápicos e seus efeitos nas células tumorais.....	16
--	----

## Resumo

O câncer é um dos maiores problemas de saúde pública do mundo. Dos tratamentos usados para combater o câncer a combinação de quimioterápicos é ainda o mais utilizado. No entanto, a combinação destes quimioterápicos podem gerar interações farmacodinâmicas que podem causar resistência a múltiplas drogas (MDR). A Leucemia Mielóide Crônica (LMC) é um tipo de câncer do sistema hematopoiético e essa doença apresenta a MDR à vários quimioterápicos o que torna urgente a pesquisa por as interações farmacodinâmicas entre os quimioterápicos usados na clínica. O fenótipo MDR, pode levar a alterações no metabolismo celular com consequente desregulação de vias oxidativas, que estão relacionadas à agressividade tumoral e ao baixo prognóstico do câncer. Nessa tese estudamos três linhagens, a K562 que apresenta sensibilidade ao fenótipo MDR, e outras duas resistentes. A Lucena foi selecionada resistente à vincristina (VCR) e a FEPS selecionada através do quimioterápico daunorubicina (DNR). O objetivo desta tese foi estudar se agentes quimioterápicos diferentes poderiam selecionar células com capacidades antioxidantes diferentes, atuar sobre o sistema de fosforilação e interagir sobre o fenótipo de resistência a múltiplas drogas (MDR) em linhagens eritroleucêmicas humanas. No artigo um, identificamos pela primeira vez que os quimioterápicos vincristina (VCR) e daunorubicina (DNR) podem selecionar células com diferentes capacidades antioxidantes. É provável que a seleção com DNR favoreça células com expressão constitutiva dos principais fatores de transcrição que controlam genes relacionados ao suprimento de energia, sistema de defesas antioxidantes e fenótipo MDR. No artigo dois, propusemos um novo mecanismo farmacodinâmico envolvendo o AZD1208, inibidor específico da quinase PIM-1, sob interação com agentes quimioterápicos, como VCR ou DNR, *in vitro* e *in silico*. Nossos resultados *in vitro* mostraram que a co-exposição do AZD1208 com o agente quimioterápico VCR ou DNR aumenta a viabilidade de células resistentes (Lucena e FEPS, respectivamente), o que contrapõem os resultados das células tratadas somente com AZD1208, onde ocorre diminuição de proliferação celular. Com base nisso, é provável que os agentes quimioterápicos possuam alguma interação farmacodinâmica e, para testar essa hipótese, realizamos uma simulação de *docking molecular* no sítio de ligação ao ATP na proteína PIM-1. Os resultados *in silico* sugerem que o AZD1208 pode, teoricamente, induzir a interação farmacodinâmica com VCR ou DNR enfraquecendo o potencial citotóxico, justificando o que observamos nos resultados *in vitro*. No terceiro artigo combinamos duas abordagens *in silico*: *docking molecular* e *teoria de densidade funcional* (DFT *ab initio*) para explicar o mecanismo de interação farmacodinâmica dos mesmos três ligantes quimioterápicos aos domínios transmembrânicos (TMD) da proteína ABCB1. Observamos diferentes intensidades de ligação energética entre os agentes quimioterápicos, sendo AZD1208/Vincristina > AZD1208/Daunorubicina. Com isso, nessa tese propomos um novo mecanismo de ação de interação farmacodinâmica entre quimioterápicos que podem selecionar células com diferentes capacidades antioxidantes, atuar sobre o mecanismo de fosforilação de uma importante quinase, PIM-1, interagindo sobre a principal característica do fenótipo MDR, a proteína ABCB1.

**Palavras chaves:** quimioresistência, vincristina, daunorubicina, ABCB1, AZD1208, PIM-1.

## **Abstract**

Cancer is one of the biggest public health problems in the world. Of the treatments used to combat cancer the combination of chemotherapy is still the most used. However, the combination of these chemotherapeutics can generate pharmacodynamic interactions that can cause resistance to multiple drugs (MDR). Chronic Myeloid Leukemia (CML) is a type of cancer of the hematopoietic system and this disease presents the MDR to several chemotherapeutic agents, which makes research urgent because of the pharmacodynamic interactions between the chemotherapeutic agents used in the clinic. The MDR phenotype can lead to alterations in cellular metabolism with consequent deregulation of oxidative pathways, which are related to tumor aggressiveness and low prognosis of cancer. In this thesis we studied three strains, the K562 that shows sensitivity to the MDR phenotype, and two other resistant ones. Lucena was selected to be resistant to vincristine (VCR) and FEPS selected through chemotherapy daunorubicin (DNR). The objective of this thesis was to study whether different chemotherapeutic agents could select cells with different antioxidant capacities, to act on the phosphorylation system and to interact on the multidrug resistance phenotype (MDR) in human erythroleukemic strains. In article one, we identified for the first time that the chemotherapeutic vincristine (VCR) and daunorubicina (DNR) can select cells with different antioxidant capacities. DNR selection favors cells with constitutive expression of the main transcription factors that control genes related to energy supply, antioxidant defense system and MDR phenotype. In article 2, we proposed a new pharmacodynamic mechanism involving AZD1208, a specific inhibitor of PIM-1 kinase, in interaction with chemotherapeutic agents, such as VCR or DNR, in vitro and in silico. Our in vitro results have shown that the coexistence of AZD1208 with the chemotherapeutic agent VCR or DNR increases the viability of resistant cells (Lucena and FEPS, respectively), which counteract the results of cells treated with AZD1208 only, where there is a decrease in proliferation cell phone. Based on this, it is likely that the chemotherapeutic agents have some pharmacodynamic interaction and, to test this hypothesis, we performed a molecular docking simulation at the ATP binding site in the PIM-1 protein. In silico results suggest that AZD1208 may theoretically induce pharmacodynamic interaction with VCR or DNR, weakening the cytotoxic potential, justifying what we observed in the in vitro results. In the third article we combine two in silico approaches: molecular docking and functional density theory (DFT ab initio) to explain the mechanism of pharmacodynamic interaction of the same three chemotherapeutic ligands to the transmembrane domains (TMD) of the ABCB1 protein. We observed different intensities of energy binding between the chemotherapeutic agents, being AZD1208/Vincristina > AZD1208/Daunorubicina. In this thesis, we propose a new mechanism of action of pharmacodynamic interaction between chemotherapeutic agents that can select cells with different antioxidant capacities, acting on the phosphorylation mechanism of an important kinase, PIM-1, interacting on the main characteristic of the MDR phenotype, ABCB1 protein.

**Keywords:** chemoresistance, vincristine, daunorubicin, ABCB1, AZD1208, PIM-1

# 1. Introdução

## Câncer

O câncer é uma doença causada por padrões aberrantes na expressão de genes. É a segunda doença que mais mata no mundo, após doenças cardiovasculares, e em 2016 foi responsável por 8,9 milhões de mortes. Em nível global, uma em cada seis mortes é devida ao câncer (HANAHAHAN et al., 2000). O Instituto Nacional do Câncer (NIH) define câncer como coleção de doenças em que células anormais podem se dividir e invadir outros tecidos, causando metástase (ROSER et al., 2018). O processo pelo qual as células normais se tornam progressivamente malignas é conhecido por requerer a aquisição sequencial de mutações que surgem como consequência de danos ao genoma (HANAHAHAN e WEINBERG, 2011; BERTRAM, 2000).

Os danos que acometem o genoma e ocasionam o câncer podem ser causados por processos endógenos, como erros na replicação do DNA, a instabilidade química intrínseca de certas bases de DNA ou de ataque por radicais livres gerados durante o metabolismo. Danos no DNA também podem resultar de interações com agentes exógenos, como radiação ionizante, radiação UV e carcinogênicos químicos. As células desenvolveram meios para reparar tais danos, mas por várias razões ocorrem erros e mudanças permanentes no genoma, onde as mutações são introduzidas (BERTRAM, 2000).

Em geral, os genes afetados podem ser divididos em dois grupos: os oncogenes e os genes supressores de tumor. Oncogenes sofrem ativação e são fenotipicamente dominantes, estimulam basicamente a proliferação celular; enquanto os genes supressores de tumor

sofrem inativação e são fenotipicamente recessivos que normalmente inibiriam a proliferação (como a p53) (HANAHAN et al., 2000; HANAHAN e WEINBERG, 2011; BERTRAM, 2000).

## 1.2 Interações entre quimioterápicos

Para o tratamento clínico do câncer em geral é utilizado principalmente combinações de quimioterápicos na quimioterapia. E como fruto dessas combinações entre os quimioterápicos. O estudo das interações entre quimioterápicos em oncologia são de particular importância devido à toxicidade inerente aos agentes antitumorais. Para que exista uma significativa melhora no tratamento de pacientes com câncer, é necessário o estudo da ação e interação entre quimioterápicos. A administração de dois ou mais fármacos geralmente leva a uma interação fármaco-fármaco. Essa interação pode ser uma interação farmacocinética, quando a interação medicamentosa afeta a concentração do fármaco por influenciar os processos de sua absorção, distribuição e metabolismo; ou pode ser uma interação farmacodinâmica, quando ocorre um aumento ou atenuação dos efeitos farmacológicos dos fármacos estudados (Figura 1) (SCRIPTURE e FIGG, 2006).

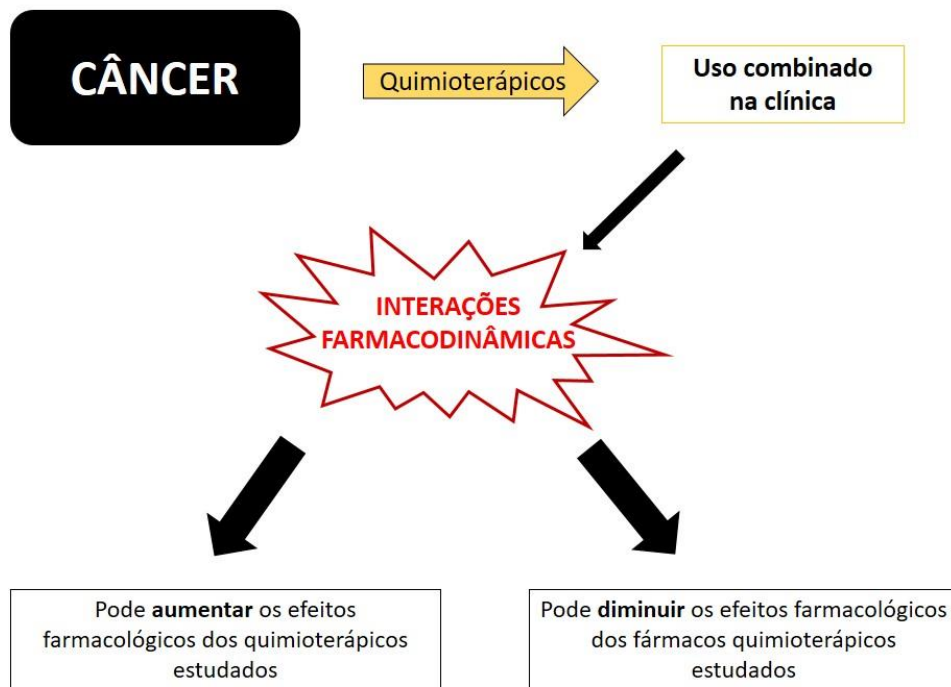


*Figura 1: Figura esquemática demonstrando que agentes quimioterápicos utilizados no tratamento do câncer podem levar à interações farmacodinâmicas.*

Agentes quimioterápicos podem levar à interações farmacodinâmicas e assim, resultar em um dos maiores problemas clínicos do câncer, a resistência a múltiplas drogas (MDR). Dentro da espectro de importância do tema dessa tese, destacamos a necessidade de estudar agentes quimioterápicos tanto de maneira isolada, quando combinados, a fim de entender o mecanismo de ação dos mesmos e com isso, ajudar a ultrapassar o fenótipo MDR.

Existem mais de 100 tipos de quimioterápicos utilizados nos tratamentos contra o câncer. Esses quimioterápicos podem ser usados isolados, ou como na maioria dos casos, combinados. Essas drogas são diferentes em relação a sua composição química, sua utilidade no tratamento de tipos específicos de câncer e nos seus efeitos colaterais. A quimioterapia, de uma forma geral, trabalha basicamente nas diferentes fases do ciclo

celular, por isso que é extremamente importante entender como essas drogas funcionam e como interagem entre si. A forma com que os quimioterápicos atuam e funcionam nas células tumorais é diferente. Assim, eles são classificados em grupos distintos (Tabela 1).

**Tabela 1:** Principais classes de quimioterápicos e seus efeitos nas células tumorais.

<b>CLASSE DO QUIMIOTERÁPICO</b>	<b>PRINCIPAIS EFEITOS</b>	<b>EXEMPLO DE QUIMIOTERÁPICOS</b>
<i>AGENTES ALQUILANTES</i>	Agentes alquilantes impedem a célula de se dividir, danificando o DNA. Estas drogas atuam em todas as fases do ciclo celular e são usadas para tratar muitos tipos diferentes de câncer.	Altretamina Carboplatina Cisplatina Ciclofosfamida Dacarbazina
<i>ANTIMETABÓLITOS</i>	Geralmente, os antimetabólitos induzem a morte celular durante a fase S quando incorporados no RNA, no DNA ou inibem as enzimas necessárias para a divisão celular. Esses compostos têm estruturas químicas semelhantes às moléculas que as células usam na síntese dos ácidos nucleicos (DNA e RNA), como purina ou pirimidina.	5-fluorouracil (5-FU) 6-mercaptopurina (6-MP) Capecitabina (Xeloda®) Gemcitabina (Gemzar®)
<i>ANTIBIÓTICOS ANTITUMORAIS</i>	Essas drogas não são como os antibióticos usados para tratar infecções. Esses antibióticos antitumorais atuam diretamente no DNA. Isso retarda ou impede que as células tumorais cresçam e se multipliquem.	<b>Daunorrubicina</b> Doxorrubicina (Adriamycin®)
<i>INIBIDORES MITÓTICOS</i>	Um inibidor mitótico é uma droga que inibe a mitose ou a divisão celular. Essas drogas atrapalham, por exemplo, a formação dos microtúbulos.	Paclitaxel Vinblastina <b>Vincristina</b>

Dentre os quimioterápicos descritos acima, nessa tese estudamos dois clássicos: a vincristina (VCR) e a daunorrubicina (DNR); e um quimioterápico novo, o AZD1208. A VCR é um alcaloide da família Vinca, possui alguns mecanismos de ação conhecidos, como a inibição dos fusos mitóticos com consequente inibição da divisão celular, especificamente na fase G2. A DNR é um dos antibióticos da classe das antraciclinas, com principais resultados encontrados em leucemias linfoides e mieloides. Dentre os mecanismos descritos podemos destacar a intercalação ao DNA com consequente inibição da síntese de macromoléculas, formação de radicais livres e a iniciação de dano ao DNA por inibição da topoisomerases II (GEWIRTZ, 1999). O AZD1208 ((5Z)-5-[[2-[(3R)-3-aminopiperidin-1-yl]-3-phenylphenyl]methylidene]-1,3-thiazolidine-2,4-dione) é um composto químico novo, por isso os seus mecanismos de ação ainda estão sendo estudados. No entanto, um dos mecanismos proposto pra esse inibidor é a modulação de substratos de sinalização de PIM-1 ((Poviral integration site for Moloney murine) (como caspases, levando à apoptose) que contribuem para a inibição do crescimento tumoral (KEETON et al., 2014). **Figura 2** apresenta a estrutura química dos quimioterápicos estudados.



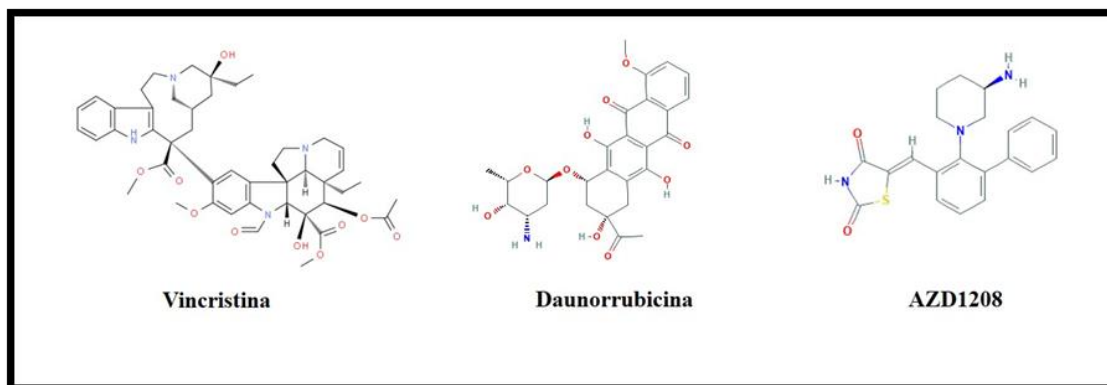


*Figura 2: Estrutura química dos quimioterápicos estudados. Vincristina, Daunorrubicina e AZD1208. Estruturas retiradas do banco de dados PubChem (<https://pubchem.ncbi.nlm.nih.gov/>).*

### 1.3 Leucemia

Dentre os vários tipos de câncer que existem, estudamos aqui a leucemia. As células sanguíneas realizam uma variedade de funções para manterem a homeostase e sobrevivência dos organismos, assim como os outros tipos celulares. Além disso, estas células exibem certas características que as tornam completamente diferentes de outros tipos celulares conhecidos, como a multiplicidade dos tipos celulares e a enorme dispersão destas em todo o corpo. A hematopoiese, processo de contínua formação das células sanguíneas, ocorre na medula óssea, através de células tronco hematopoiéticas. A leucemia é um tipo de câncer que se caracteriza pelo acúmulo de células jovens anormais na medula óssea. A estimativa de novos casos por ano de leucemias no Brasil é de aproximadamente 10.800 (INCA, 2018).

A Leucemia Mieloide Crônica (LMC) é uma desordem clonal mieloproliferativa envolvendo células tronco hematopoiéticas e consistentemente associada ao gene

fusionado BCR-ABL1 conhecido com Cromossomo Philadelphia (Ph1). Essa leucemia é caracterizada por uma translocação recíproca entre os cromossomos 9 e 22  $t(9,22)(q34;q11)$ , onde parte do cromossomo 9 denominado ABL1 é transferido para o gene BCR junto ao cromossomo 22. O cromossomo 22 anormal é o cromossomo Ph1. Na translocação anormal Ph1, o éxon 5' do BCR é fundido ao éxon 3' do ABL1 (**Figura 1**). O gene quimérico BCR-ABL1 resultante codifica excessivamente uma proteína tirosina quinase em relação ao seu produto normal, descontrolando o ciclo celular (LOZZIO e LOZZIO, 1975; NOWELL, 1976). Infelizmente, ainda observamos em LMC resistência a quimioterápicos e fenótipo MDR. Isso justifica a importância de estudar esse tipo de câncer e a relação entre os quimioterápicos que ainda são utilizados no tratamento clínico de LMC, embora sejam altamente citotóxicos a células saudáveis.

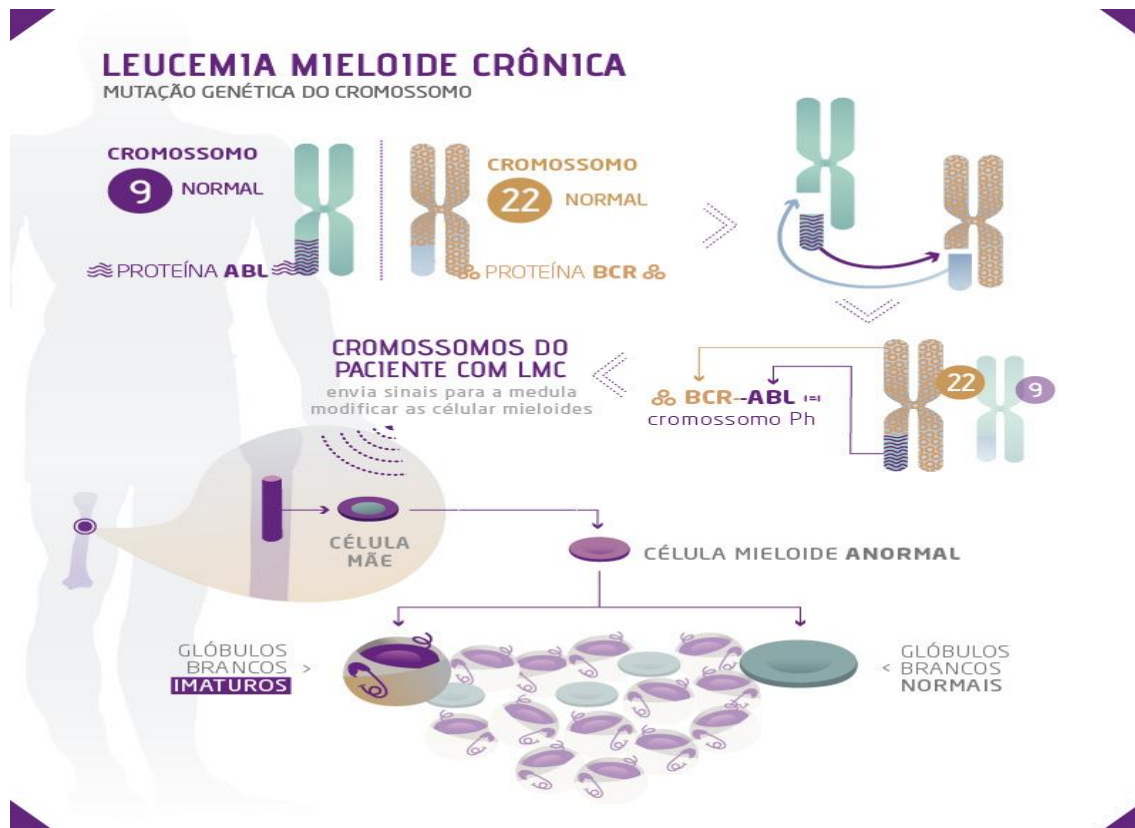


Figura 3: Leucemia Mieloide Crônica apresentando translocação dos cromossomos 9 e 22, denominado cromossomo Philadelphia. (Fonte <https://www.venceroancer.org.br/noticias-lmc/leucemia-mieloide-chronica-requer-persistencia-durante-o-tratamento/>)

## 1.4 As principais características da resistência a múltiplas drogas (MDR)

A resistência à múltiplas drogas infelizmente ainda é um dos grandes problemas das terapias contra o câncer. Quase qualquer terapia (exceto cirurgia) que está sendo usada no tratamento do câncer pode resultar em resistência. Infelizmente, há um grande grupo de pacientes que não respondem à terapia aplicada (resistência intrínseca) ou se tornarão resistentes durante a terapia (resistência adquirida). Às vezes, os pacientes podem se tornar resistentes a uma droga específica e permanecer sensíveis a outras drogas (resistência a

uma droga); outro grupo de pacientes pode tornar-se resistente a um fármaco e também será resistente a outros fármacos não relacionados (resistência múltipla a drogas, MDR).

As principais características que podem levar à ao fenótipo MDR estão destacadas na

**Figura 4.**

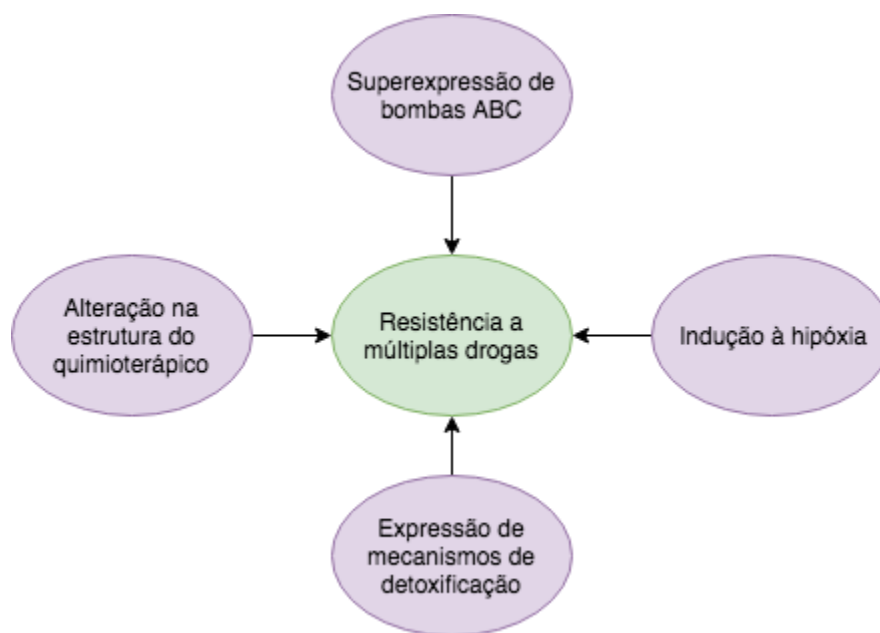


*Figura 4: Categorias que podem ativar ou promover a resistência direta ou indireta a múltiplas drogas em células tumorais. Estes mecanismos podem agir de forma independente ou em combinação e através de várias vias de transdução de sinal.*

Estes mecanismos podem agir de forma independente ou cooperar no desenvolvimento de MDR em relação ao caráter específico das células tumorais (HOUSMAN et al., 2014; WU et al., 2014). Essas características da MDR são brevemente relatadas abaixo:

(1) **Supereexpressão de bombas ABC:** A expressão dos transportadores de fármacos representa a causalidade molecular mais observada da MDR. Pelo menos três transportadores estão envolvidos na redução da sensibilidade a drogas de células

neoplásicas. A mais conhecida é a glicoproteína-P (P-gp ou ABCB1 ou MDR) que representa um membro ABCB1 da família de transportadores ABC. A P-gp pode eliminar da célula uma grande escala de diferentes substâncias, medicamentos, agentes quimioterápicos, xenobióticos entre outros. Outros transportadores importantes envolvidos na MDR são os membros ABCC1, também conhecidos como proteínas associadas multirresistentes 1–3 (MRP1-MRP3) que, em contraste com a P-gp, são específicos para ânions orgânicos. O transportador ABCG2 também é frequentemente descrito como envolvido em MDR. Este transportador também é conhecido como proteína resistente do câncer de mama (BCRP).

(2) **Alteração na estrutura do quimioterápico:** Muitos medicamentos antineoplásicos passam por diversas ativações metabólicas para adquirir eficácia clínica. Essas ativações das drogas *in vivo* envolvem mecanismos complexos em que substâncias interagem com diferentes proteínas-alvo. As interações químicas podem modificar e degradar parcialmente ou completamente a droga, levando à sua inativação com consequente MDR nas células tumorais. Um exemplo é observado no tratamento da LMA com o quimioterápico citarabina. Essa droga ativa uma série de outras proteínas que mudam a estrutura do quimioterápico tornando a LMA multirresistente à citarabina.

(3) **Indução à hipóxia:** Uma célula tumoral está em constante proliferação celular, necessitando de alta demanda de ATP e por isso pode possuir déficit de oxigênio. Quando o tumor está em hipóxia, ocorre aumento na expressão do fator de indução a hipóxia 1- (HIF-1), aumento de genes transportadores de glicose, fatores de crescimento e de angiogênese, resultando em consequente aumento da massa/volume tumoral. No entanto, no fenótipo MDR muitos desses fatores citados acima estão superexpressos. Como por exemplo em células de câncer gástrico resistentes à VCR (SGC7901/VCR). Nesta

linhagem o *hif-1* está superexpresso, inibindo a apoptose e diminuindo o acúmulo intracelular de VCR através extrusão da droga pela da P-gp. Essa relação, entre o *hif-1* e proteínas MDR, também é observada em outros tipos de câncer sugerindo que o *hif-1* é um importante fator que regula a MDR (LIU et al., 2008).

(4) **Expressão de mecanismos de detoxificação:** A droga pode ser detoxificada por enzimas de detoxificação como as glutathione-S-transferases (GSTs). As GSTs representam um grupo de enzimas que estão frequentemente envolvidas na proteção de células contra o estresse tóxico. As ações das GSTs são frequentemente associadas com as proteínas MRPs (ABCC1 ou ABCC3), da família ABC. Em células MDRs a enzima GST e outras do sistema antioxidante estão superexpressas. As células MDRs adquirem uma maior capacidade de respostas aos xenobióticos por conta desse mecanismos de detoxificação estarem superexpressos nessas células.

## 1.5 Metabolismo tumoral e fenótipo MDR

Todas as células do corpo humano precisam constantemente de suprimento externo de oxigênio e nutrientes para manter as condições fisiológicas em homeostase. A principal organela celular envolvida no processo de respiração celular é a mitocôndria. Esta respiração aeróbica gera energia e como resultado desse metabolismo oxidativo, vários compostos são produzidos. A energia é necessária para a execução de todas as atividades do sistemas do nosso organismo, como as sinapses, contração muscular, a própria respiração celular e pulmonar, entre outros tantos. Durante as reações metabólicas parte da energia liberada pela glicose é conservada em forma de ATP e NADH.

Como subprodutos dos processos metabólicos as espécies reativas de oxigênio (ROS) são constantemente geradas durante o metabolismo celular. As espécies reativas podem ser classificadas em quatro grupos baseados no átomo principal envolvido: ROS, espécies reativas de nitrogênio (RNS), espécies reativas de enxofre (RSS) e espécies reativas de cloreto (RCS). De todos os compostos derivados do metabolismo oxidativo, as ROS são as mais abundantemente produzidas. As espécies reativas de oxigênio incluem o ânion superóxido ( $O_2^-$ ), o peróxido de hidrogênio ( $H_2O_2$ ), o radical hidroxila ( $OH^-$ ) e o oxigênio singlete ( $^1O_2$ ). O dano que o ROS podem causar à célula não depende apenas da sua concentração intracelular, mas também do equilíbrio entre as espécies ROS e as espécies antioxidantes endógenas. Quando o equilíbrio pró-oxidante/antioxidante é perdido, o estresse oxidativo é gerado, alterando e danificando muitas moléculas intracelulares, incluindo DNA, RNA, lipídios e proteínas, podendo causar doenças, incluindo o câncer (SOSA et al., 2013).

Os antioxidantes são parte dos mecanismos de respostas celulares ao excesso de ROS, e podem ser classificados em diferentes grupos de acordo com suas propriedades: antioxidantes endógenos, antioxidantes naturais e antioxidantes sintéticos. Os antioxidantes endógenos incluem superóxido dismutase (SOD), catalase (CAT), glutathione-S-transferase (GST), glutathione peroxidase (GPXs), entre outros (SOSA et al., 2013)(PAVLOVA e THOMPSON, 2016).

Nas células MDRs, podemos encontrar genes antioxidante alterados, como a CAT, a SOD e a GST. A ação das enzimas antioxidantes contra o ROS está brevemente destacada na **Figura 5**.

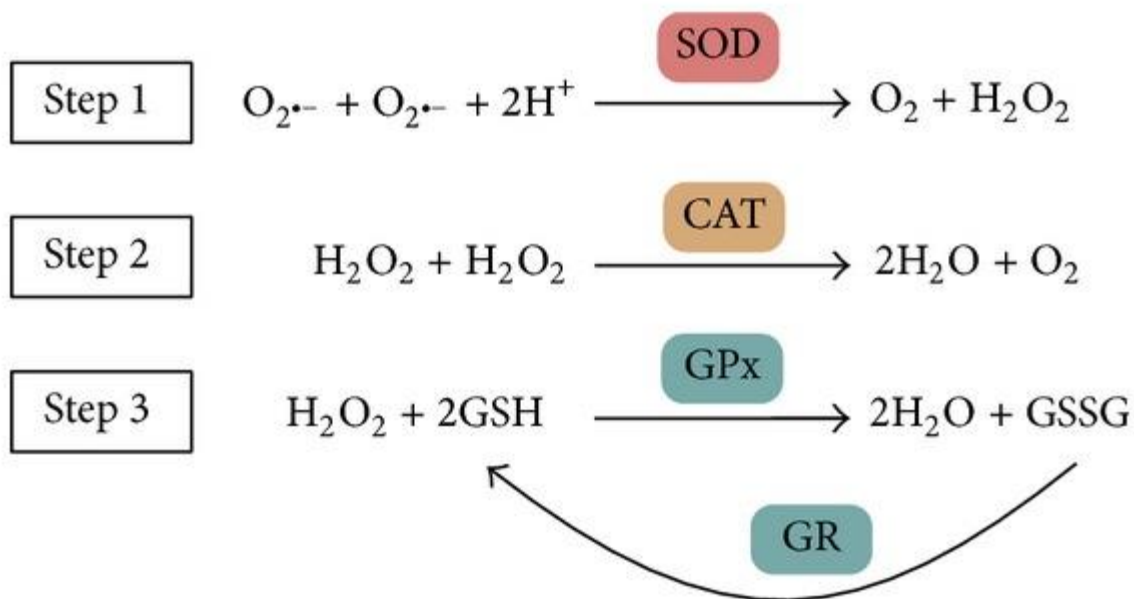


Figura 5: Ilustração esquemática do sistema de defesa antioxidante contra o estresse oxidativo intracelular. SOD: superóxido dismutase, CAT: catalase, GPx: glutatona peroxidase, GR: glutatona redutase, GSH/GSSG: glutatona reduzida/glutatona oxidada. Fonte: PENG et al., (2014).

PAVLOVA et al. (2016) sugerem características centrais do metabolismo tumoral como: 1) absorção desregulada de glicose e aminoácidos; 2) utilização de intermediários da glicólise e do ciclo do ácido cítrico para produção de NADPH; 3) ampliação na demanda de nitrogênio; 4) mudanças na regulação e expressão de genes-chave para a resistência tumoral; 5) mudanças metabólicas no microambiente do câncer.

Nas células com fenótipo MDR, duas principais alterações do metabolismo tumoral são destacadas: a absorção desregulada de glicose e as mudanças na regulação e expressão de genes-chave. Uma das primeiras respostas celulares à produção de ROS é a superexpressão do fator de transcrição HIF-1. O HIF-1 atua no aumento da expressão de muitos genes da



via glicolítica, dentre eles o transportador de glicose (GLUT-1). O HIF-1 e o GLUT estão superexpressos em células resistentes de em LMA (SONG et al., 2014; DIEHN et al., 2009).

Outra alteração em resposta ao altos níveis de ROS acontece através da ativação do fator de transcrição NRF2 (nuclear factor-erythroid-2-related factor), atuando como sensor de estresse oxidativo, sinalizando e ativando a região promotora dos elementos de resposta antioxidante (ARE). O NRF2 atua em conjunto com o NFkB e ambos controlam a progressão do tumor. O NRF2 atua ativando os genes do sistema antioxidante como a glutationa-S-transferase (GST), a CAT e a SOD (e suas três principais isoformas SOD1, SOD2 e SOD3) (JARAMILLO e ZHANG, 2013; HARDER et al., 2015; PAVLOVA e THOMPSON, 2016).

## 1.6 Bombas de extrusão e o fenótipo MDR

O transporte através das membranas celulares é um processo fundamental para todos os organismos vivos e existe um grande número de transportadores específicos que evoluíram para realizar estas funções. No câncer, muitos transportadores transmembrânicos apresentam mutações que em geral, as quais resultam na superexpressão destes com consequente diminuição dos quimioterápicos na célula tumoral. Por essa razão, o fenótipo MDR ainda continua sendo uma das principais causas das falhas no tratamento do câncer (AMBUDKAR et al., 2006; SZAKÁCS et al., 2006). A principal bomba relacionada ao fenótipo MDR é a ABCB1 (ou P-gp).

Do ponto de vista estrutural, o mecanismo molecular de importação de drogas é catalisado pela hidrólise de ATP nos subdomínios de ligação a nucleotídeos (NDBs) da

ABCB1. Enquanto a extrusão da droga é facilitada por um par de domínios transmembrânicos (TMDs) de forma unidirecional, a partir de uma cavidade central entre as TMDs para fora. As  $\alpha$ -hélices estruturalmente conservadas, são parte dos domínios das TMDs e estão presentes em todas as estruturas cristalográficas dos transportadores ABC, que são invariavelmente fusionados aos NDBs (**Figura 6**) (JONES e GEORGE, 2002; HOLLENSTEIN et al., 2007).

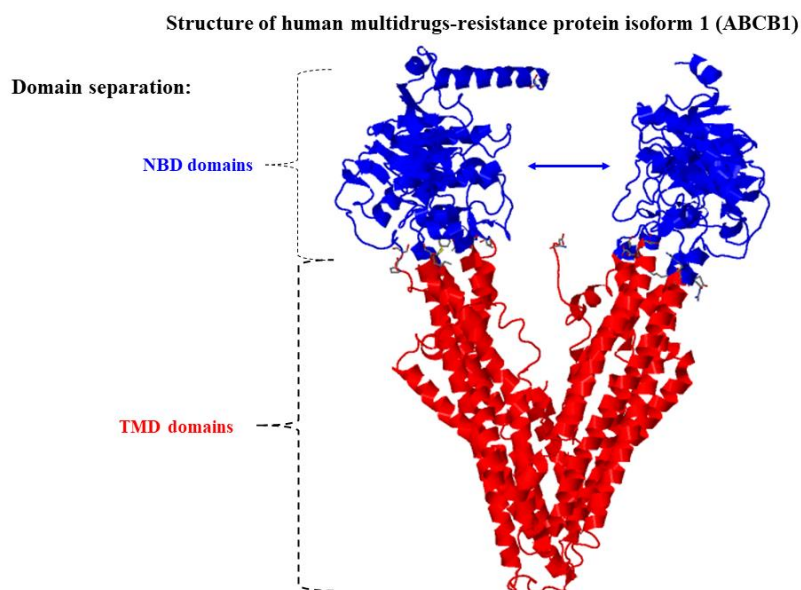


Figura 6: Estrutura 3D da ABCB1 (figura oriunda da tese)

## 1.7 Relação entre a quinase PIM-1 e o fenótipo MDR

A fosforilação é um mecanismo regulatório universal que controla processos fisiológicos como a diferenciação celular, proliferação, sobrevivência entre outros eventos importantes para a sobrevivência celular. Câncer hematopoiéticos e sólidos utilizam cascatas

intercelular de sinalização mediadas por quinases oncogênicas para manter a sobrevivência e o crescimento tumoral. Em células normais, a atividade dessas quinases são extremamente controladas. Entretanto, mutações nessas quinases podem promover resistência apoptótica e a proliferação celular descontrolada (MARMIROLI et al., 2015).

As proteínas quinases (PK) são enzimas que catalisam a fosforilação de proteínas através da transferência de um grupo fosfato de ATP para resíduos de tirosina (Tyr), treonina (Thr) ou serina (Ser). As PKs compõem uma das maiores famílias de proteínas nos eucariontes, e são essenciais para a comunicação celular e transduções de sinais (MARTIN et al., 2010). Essas proteínas tipicamente apresentam um arranjo conservado de estrutura secundária em 12 subdomínios que se enovelam em um núcleo catalítico bilobulado (N-terminal e C-terminal) com o sítio de ligação de ATP (domínio catalítico) numa fenda localizada entre os dois lobos. O lobo N-terminal é composto por cinco fitas- $\beta$  e uma  $\alpha$ -hélice proeminente, enquanto o domínio C-terminal é constituído predominantemente por  $\alpha$ -hélices. Os domínios catalíticos homólogos das quinases consistem de ~250-300 resíduos de aminoácidos (ENGH e BOSSEMEYER, 2001).

A proteína PIM é uma quinase serina/treonina que foi identificada como uma nova classe de quinases constitutivamente ativas e foi inicialmente descoberta através da triagem de inserção viral para descobrir o desenvolvimento de linfoma no modelo de tumor Eumyc (THEO CUYPERS et al., 1984). PIM fosforila inúmeros substratos que ativam cascatas de fosforilação essenciais para os processos fisiológicos como proliferação, sobrevivência e apoptose. A PIM tem sido relacionada ao processo de resistência e oncogênese e aparece superexpressa em muitos tipos de cânceres. A PIM está envolvida em processos críticos nos processos de MDR (TURSUNBAY et al., 2016; ISAAC et al., 2011).

A família PIM apresenta três isoformas (PIM1, PIM2 e PIM3) que são altamente conservadas ao longo da evolução. Os genes estão localizados em diferentes cromossomos humanos e compartilham sequências homólogas entre os aminoácidos; PIM1 e PIM2 são 61% idênticas e PIM1 e PIM3 são 71% idênticas (KEANE et al., 2015). O gene da PIM-1 está localizado no cromossomo 6p21.1-p21.31 e codifica para uma proteína de 313 aminoácidos. Do ponto de vista estrutural, a quinase PIM-1 tem uma dobra que compreende dois domínios: 1) domínio N-terminal (NTD) que consiste em folhas  $\beta$  antiparalelas do resíduo 33 ao 120 e, 2) domínio C-terminal (CTD) formado por  $\alpha$ -hélices, do resíduo 129 ao 305. Esses domínios estão associadas por um motivo de ligação que inclui a Leu120, que atua como uma ‘porteira’ de entrada ao sítio ativo de ATP da quinase PIM-1. Esse sítio de ligação ao ATP possui a sequência consenso ERPEPV. O sítio ativo do ATP está circundado por uma alça rica em glicina (G-alça, do resíduo 46 ao 54) e uma alça de ativação A (resíduo 191 ao 202). As regiões de ligação à adenosina são importantes para analisar as propriedades dos homólogos de PIM-1 e construir inibidores eficientes (**Figura 7**)(WANG et al., 2001; ZHUKOVA et al., 2011; BACHMANN e MÖRÖY, 2005).

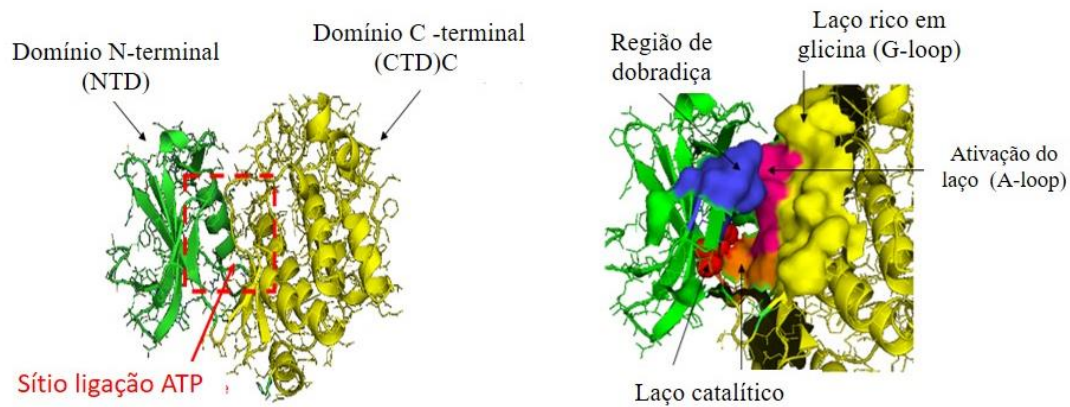


Figura 7: Estrutura da quinase PIM-1 (figura oriunda da tese)

Geralmente a transcrição de PIM-1 é ativada por interleucinas (IL-2, IL-3 e IL-6), por via de transdução de sinalização por duas famílias de proteínas: Jak Quinases (JAKs) e os Transdutores de Sinal e Ativadores de Transcrição (STATs). Muitos substratos de fosforilação de PIM-1 estão sendo identificados, os quais estão envolvidos no ciclo celular, crescimento celular e sobrevivência celular. A PIM-1 fosforila o regulador do ciclo celular, p21, e também fosforila o p27, promovendo a progressão do ciclo celular (WANG et al., 2002). Uns dos principais reguladores da sobrevivência celular é a família de *bcl-2* (B-cell lymphoma 2). Essa família controlam a permeabilidade da membrana externa da mitocôndria e pode então controlar a apoptose. Já se sabe que *bcl-2* é outro substrato de fosforilação da PIM-1 (**Figura 8**) (TURSUNBAY et al., 2016).

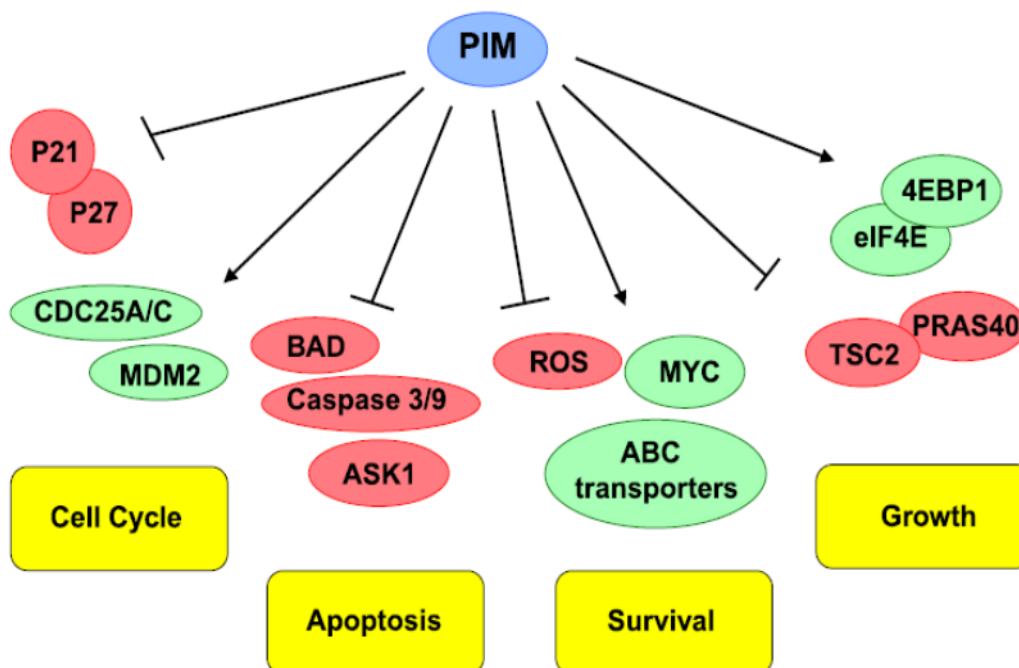


Figura 8: Processos celulares regulados por PIM que são críticos para a resistência e progressão tumoral, tornando PIM alvo promissor para terapia contra o câncer. Adaptada de TURSYNBAY et al. (2016).

PIM-1 apresenta duas isoformas: PIM-1S e PIM-1L. Uma está localizada no núcleo e a outra no citosol/membrana plasmática. Sugere-se que a PIM-1L tenha relação com a ativação das proteínas de efluxo da família ABC (TURSYNBAY et al., 2016). A PIM-1L é a isoforma mais longa com uma massa molecular de 44 kDa, enquanto a PIM-1S é a isoforma mais curta com uma massa molecular de 33 kDa. Notavelmente, a PIM-1S localiza-se predominantemente no núcleo e no citosol, enquanto PIM-1L localiza-se principalmente na membrana plasmática.

Um aspecto pouco compreendido e muito importante nas pesquisas oncológicas é o papel da fosforilação como um mecanismo para regular a função desses transportadores ABC. A PIM-1 parece estar envolvida na expressão e ativação desses transportadores de

efluxo de drogas. Um dos primeiros estudos sobre relação entre fenótipo MDR e a PIM-1L demonstrou o mecanismo molecular em que essa quinase fosforila a proteína BCRP no resíduo Thr-362, resultando na dimerização da proteína BCRP com consequente translocação de BCRP para a membrana plasmática (XIE et al., 2008). Esse resultado apresentou um forte indício da relação de PIM com a super-família-ABC. Isso sugere que para a maturação da glicoproteína e consequente translocação para a membrana plasmática, promovendo então sua ação de extrusão de drogas, é necessário a fosforilação pela PIM-1 (XIE et al., 2010; TURSUNBAY et al., 2016).

A PIM-1 quinase também fosforila a P-gp e protege da degradação proteica por meio da estabilização da P-gp e do aumento de sua expressão na superfície celular. Inibidores combinados de P-gp e PIM-1 aumentam a eficiência do medicamento pelo aumento da apoptose de células tumorais resistentes à VCR (leucemia HL60/VCR) (TURSUNBAY et al., 2016). Por essa razão, entender como essa quinase controla suas vias de sinalização é importante para promover possíveis combinações de drogas que sejam inibidores eficazes de quinases mutadas no câncer, como a PIM-1 (**Figura 9**) (XIE et al., 2010).

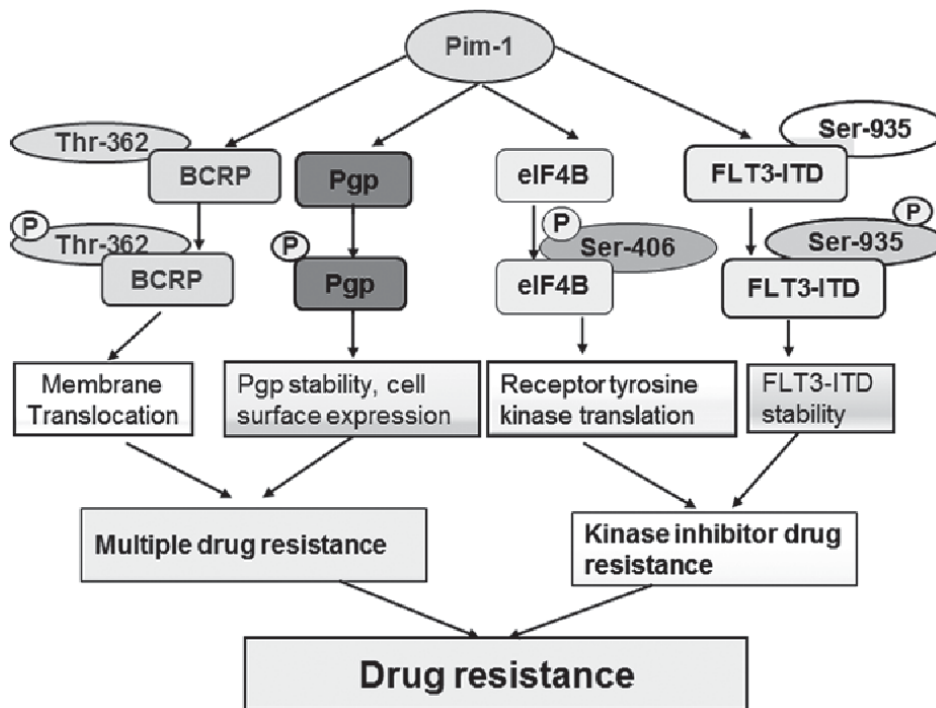


Figura 9: Aspectos da PIM-1 que estão relacionado com o fenótipo MDR. TURSUNBAY et al. (2016)

## 1.8 Novo inibidor de quinase PIM-1: AZD1208

Vários inibidores da quinase PIM-1 estão sendo sintetizados. Alguns derivados da quinona estão sendo estudados para o tratamento do câncer de próstata (LI et al., 2009). Outros, como imidazol [1,2] piridazinas, foram descritos pelos efeitos antiproliferativos na leucemia aguda (POGACIC et al., 2007). No entanto, a resistência a múltiplos fármacos induzida por transportadores (ABC) continua a ser um problema do ponto de vista farmacocinético para garantir a biodisponibilidade no sangue e reduzir os efeitos adversos de agentes quimioterápicos (inibidores da quinase PIM) (POGACIC et al., 2007; ASATI et al., 2018; REN et al., 2011).

Um potente e recente inibidor do PIM-1 conhecido como AZD1208 mostrou eficácia em um modelo pré-clínico na inibição do crescimento celular e levou à apoptose



por inibir a supressão da fosforilação através dos substratos p70S6K e 4EBP128 em amostras de pacientes (REN et al., 2011; KEETON et al., 2014). Embora já existam vários inibidores de PIM-1 e pesquisas usando AZD1208, mais estudos são necessários para identificar as possíveis interações de AZD1208 com diferentes classes de agentes quimioterápicos. Precisamente porque a maioria dos tratamentos clínicos inclui a combinação de dois ou mais medicamentos para superar o baixo prognóstico dos pacientes com câncer. Portanto, é crucial a possibilidade de descobrir novos ligantes e bloqueadores do PIM-1 (GARRAWAY et al., 2013).

## 1.9 Modelos estudados *in vitro*

A K562 foi a primeira linhagem celular estabelecida disponível *in vitro* para pesquisa com a persistência do cromossomo Ph1 depois de prolongadas passagens celulares (LOZZIO e LOZZIO, 1975). As células foram retiradas a partir da efusão pleural de uma mulher com 53 anos que veio a falecer após 4 anos com a doença. A K562 também possui cromossomo Ph1, como característica da leucemia mielocítica. A linhagem K562 tem a característica de ser sensível à quimioterapia. A fim de se ter um modelo biológico de estudo com fenótipo MDR, RUMJANEK et al. (2001) utilizaram o quimioterápico VCR para induzir a K562, linhagem eritroleucêmica sensível, a se tornar um modelo experimental de estudo celular MDR. À essa linhagem foi dado o nome de K562-Lucena-1 (Lucena). DAFLON-YUNES e colaboradores (2013) selecionaram outra linhagem MDR, também derivada da parental K562, através do quimioterápico DNR. O nome dado à esta linhagem foi FEPS.

## 1.10 Bioinformática no Câncer

A bioinformática é uma nova e complexa área que abrange diversos conhecimentos e, por isso, necessita da integração de diferentes profissionais, sendo considerada uma área multidisciplinar. A modelagem molecular é uma área que investiga as estruturas e as propriedades moleculares pelo uso da química computacional. O objetivo do docking é prever a melhor orientação de ajuste de um ligante em uma proteína (como as proteínas PIM-1 e ABCB1) (MENG et al., 2011).

Os métodos de investigações de modelagem molecular determinam em geral a energia de ligação levando em consideração parâmetros eletrostáticos, como as ligações de Van der Waals, as ligações entre hidrogênios, caracterização do ligante mais ou menos hidrofóbico, aos quais geram modelos matemáticos que preveem melhores orientações do ligante, segundo escores de energia. A química computacional vem oferecendo um excelente direcionamento no planejamento racional de fármacos (MENG et al., 2011).

Por essa razão, a docagem molecular tem sido alvo de intensos estudos na área do câncer, principalmente para desenhar e identificar propriedades de novas drogas que ultrapassem o fenótipo MDR. Uma característica importante da bioinformática é fornecer dados de forma mais rápida e eficiente, sem grandes custos. Além disso, é uma importante alternativa as pesquisas, *in vitro* ou *in vivo*, pois as pesquisas *in silico* estão cada vez assertivas e utilizando menos testes em modelos de animais. A partir dessas novas estratégias é possível selecionar por virtual screening – triagem virtual compostos em bases de dados antes que eles sejam sintetizados, eliminando compostos não promissores (**Figura 10**).

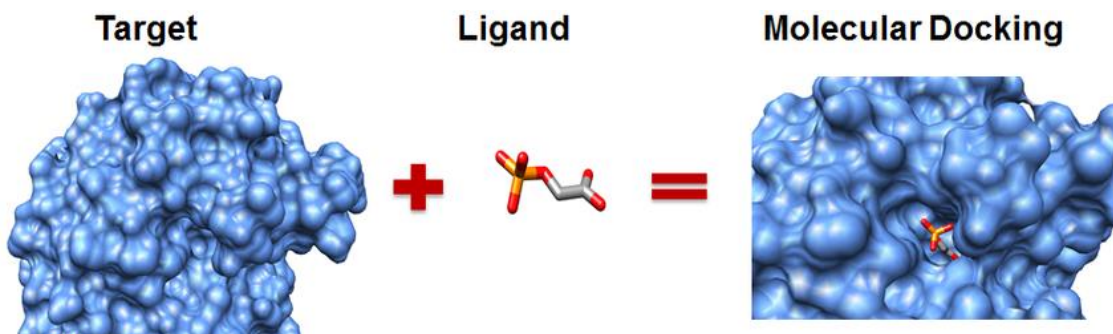


Figura 10: Demonstração entre proteína e fármaco formada com a utilização de ferramenta de bioinformática e que propicia o docking molecular. Fonte: [https://www.researchgate.net/figure/Elements-in-molecular-docking\\_fig1\\_237012127](https://www.researchgate.net/figure/Elements-in-molecular-docking_fig1_237012127)

## 2. OBJETIVOS

### 2.1 Objetivo Geral

O objetivo desta tese foi avaliar, através de abordagens *in vitro* e *in silico*, se agentes quimioterápicos diferentes poderiam selecionar células com capacidades antioxidantes diferentes, atuar sobre o sistema de sistema de fosforilação e interagir sobre o fenótipo de resistência a múltiplas drogas (MDR) em linhagens eritroleucêmicas humanas.

### 2.2 Objetivos Específicos

- ✓ Avaliar se agentes quimioterápicos diferentes (VCR ou DNR) podem gerar células com capacidades antioxidantes diferentes nas linhagens leucêmicas: Lucena (resistente a VCR) e FEPS (resistente a DNR);
- ✓ Verificar se a permanência ou ausência dos quimioterápicos VCR e DNR interferem na viabilidade de celular e na produção de ROS nas linhagens

leucêmicas: Lucena (resistente a VCR) e FEPS (resistente a DNR)), após serem expostas a um agente estressor (H<sub>2</sub>O<sub>2</sub>);

- ✓ Estudar a relação dos quimioterápicos VCR e DNR sobre a perspectiva do fenótipo MDR e a expressão de genes relacionados ao metabolismo tumoral;
- ✓ Verificar se o AZD1208 (inibidor de PIM-1) sozinho ou em co-tratamento com VCR ou DNR diminui a viabilidade celular das linhagens tumorais sensíveis (K562) e resistentes a múltiplas drogas (Lucena e FEPS).
- ✓ Avaliar se o AZD1208 mais o co-tratamento dos quimioterápicos (VCR ou DNR) pode inibir a atividade da glicoproteína-P (ABCB1);
- ✓ Aplicar técnicas de bioinformática para propor, teoricamente, um mecanismo de interação farmacodinâmica entre os ligantes VCR, DNR e AZD1208 ao sítio ativo de duas proteínas relacionadas ao fenótipo MDR, a quinase PIM-1 e a bomba de extrusão ABCB1.
- ✓ Examinar a interação farmacodinâmica entre o AZD1208 e os quimioterápicos VCR e DNR no sítio de ligação ao ATP da proteína PIM-1 através de docking molecular;
- ✓ Identificar a interação farmacodinâmica entre o AZD1208 e os quimioterápicos VCR e DNR no sítio de ligação ao TMD da glicoproteína ABCB1 através de docking molecular e a interação entre AZD1208 e VCR e AZD1208 e DNR através de DTF *ab initio*.

### **3. RESULTADOS**

#### 3.1 Manuscrito 1

**EFFECTS OF CHEMOTHERAPEUTIC DRUGS ON THE ANTIOXIDANT  
CAPACITY OF HUMAN ERYTHROLEUKEMIA CELLS WITH MDR  
PHENOTYPE**

Maiara Bernardes Marques<sup>a</sup>, Bruno Rodrigues Oliveira<sup>a</sup>, Daniela Volcan Almeida<sup>a</sup>, Ana  
Paula de Souza Votto<sup>b</sup>, Luis Fernando Marins<sup>a\*</sup>

<sup>a</sup>Laboratory of Molecular Biology, Institute of Biological Sciences, Federal University of Rio Grande -FURG, Rio Grande, RS, Brazil.

<sup>b</sup>Laboratory of Cell Culture, Institute of Biological Sciences, Federal University of Rio Grande -FURG, Rio Grande, RS, Brazil.

\*Correspondence: Institute of Biological Sciences, Federal University of Rio Grande - FURG, Av. Itália, Km 8, 96201-900 Rio Grande, Brazil. E-mail address: dqmluf@furg.br (L.F. Marins). Phone: +55 53 32935191.

## ABSTRACT

In this work, we identified that different chemotherapeutic drugs may select cells with different antioxidant capacities. For this, we evaluated the sensitivity of two multidrug resistant (MDR) erythroleukemia cell lines: Lucena (resistant to vincristine, VCR) and FEPS (resistant to daunorubicin, DNR) derived from the same sensitive cell K562 (non-MDR) to hydrogen peroxide. In addition, we evaluated how the cell lines respond to the oxidizing agent in the absence of VCR/DNR. In absence of VCR, Lucena drastically decreases cell viability when exposed to hydrogen peroxide, while FEPS is not affected even without DNR. To analyze whether selection by different chemotherapeutic agents may generate altered energetic demands, we analyzed the production of reactive oxygen species (ROS) and the relative expression of the glucose transporter 1 gene (*glut-1*). We observed that the selection through DNR apparently generates a higher energy demand than VCR. High levels of transcription factors genes expression (*nrf2*, *hif-1 $\alpha$*  and *oct4*) were kept even when the DNR is withdrawn from the FEPS culture for one month. This same expression pattern was observed for genes related to the detoxification system (*cat*, *gstm4*, *sod1*, *sod2* and *sod3*) and extrusion pump (*abcb1*). Together, these results indicate that DNR selects cells with greater ability to express the major transcription factors related to the antioxidant defense system and to the main extrusion pump (ABCB1) related to the MDR phenotype. Taking into account that the antioxidant capacity of tumor cells is closely related to resistance to multiple drugs, it is evident that endogenous antioxidant molecules may be targets for the development of new anticancer drugs.

**Palavras chaves:** antioxidant defense system; MDR phenotype; *abcb1*; VCR; DNR.

## 1. INTRODUCTION

Multiple drug resistance (MDR) is one of the major causes of cancer treatment failure leading to changes in cellular metabolism and consequent redox status deregulation, which are being related to tumor aggressiveness and unfavorable cancer prognosis [1]. Chemotherapy continues to be one of the main ways to treat different types of cancers. However, it is also observed as a result of chemotherapy, low prognosis, metabolic dysfunctions, poor effectiveness of systemic action, cytotoxicity and MDR phenotype [2].

The selective events of chemotherapeutic agents usually cause changes in classic pathways of tumor metabolism. Among these altered pathways, the overexpression of key genes that regulate cell metabolism and deregulated glucose uptake are hot spots [2; 3]. As byproducts of the metabolic processes, the reactive oxygen species (ROS) are constantly generated in a wide variety of changes to cellular metabolic responses [4] and oxidative stress, in turn, is characterized as a metabolic imbalance between the formation and detoxification of ROS.

Chemotherapy drugs such as daunorubicin (DNR) and vincristin (VCR) may alter the levels of transcription factors that regulate the levels of energy supply, extrusion pump related to the MDR phenotype (ABCB1), activate response elements that are responsible for increasing or decreasing levels of antioxidant gene expression. One of the cellular responses to these alterations is overexpression of the transcription factor known as hypoxia-1 induction factor (HIF-1 $\alpha$ ) [3]. HIF-1 $\alpha$  plays an important role in increasing one of the major indicator genes of tumor metabolism, the glucose transporter 1 (*glut-1*) encoded by *slc2a1* gene [4]. In this context, overexpression of *glut-1* and *hif-1 $\alpha$*  have been

observed in acute myeloid leukemia, being also related to the MDR phenotype and metabolic processes [5]. *hif-1 $\alpha$*  also appears mutated in breast cancer [6].

Another alteration in response to different chemotherapeutic agents occurs through the activation of the transcription factor NRF2 (nuclear factor-erythroid-2-related factor 2), acting as an oxidative stress sensor, signaling and activating the promoter region of the antioxidant response elements (ARE) [7]. The antioxidant genes code for enzymes of stage II of cellular detoxification like glutathione-S-transferase (GSTM4), catalase (CAT) and superoxide dismutase (SOD1, SOD2 and SOD3) [8][9]. NRF2 has been associated to the MDR phenotype by regulating the expression of multidrug-resistance-associated protein-1 gene (*mrp1*). Resistant cells from lung cancer (H69AR) have high levels of MRP1 in relation to the sensitive lineage (H69) [10]. NRF2 also presents relationship with *abcf2* gene (subgroup of ABC family) in ovarian cancer [11].

The transcription factor OCT4 is normally associated with pluripotency and is responsible for maintaining cells with undifferentiated embryonic characteristics. This transcription factor is related to the MDR phenotype and is already known to activate extrusion glycoproteins genes like *abcb1* [12]. Other studies have reported the association of OCT4 with prostate cancer [13] and lung cancer [14]. Although there are many studies on the MDR phenotype, few of them relate the resistance to the antioxidant capacity coming from the selective effect of the chemotherapeutic agents.

In this context, we studied chronic myeloid leukemia (CML) cell lines selected resistant by different selective agents. The major molecular feature of CML is a reciprocal translocation of chromosomes 9 to 22 (t (9:22) (q34; q11)), known as Philadelphia chromosome (Ph1). This mutation generates the fusion of two genes BCR and ABL, which



fuse and give rise to oncoprotein BCR-ABL, a protein tyrosine kinase [15]. Rumjanek et al. [16] established the cell line K562-Lucena-1 (Lucena), which was selected resistant from the K562 erythroleukemic lineage, through increasing doses of the VCR chemotherapy. The same research group also selected another resistant line from K562. The FEPS line was selected resistant through DNR chemotherapy [17].

Although the parental origin is the same (K562), those lineages have phenotypic and genotypic differences that make them an excellent model for research on the MDR phenotype [19]. In this work, we identified, for the first time, that different chemotherapeutic drugs (VCR and DNR) may select cells with different antioxidant capacities in human erythroleukemic lines with multidrug resistance phenotype (Lucena and FEPS).

## **2. Materials and methods**

### *2.1 Cells and culture procedures*

The cell lines were provided of Immunology Laboratory at the Medical Biochemistry Institute Leopoldo de Meis of the Federal University of Rio de Janeiro (Brazil). Lucena was maintained with 60 nM of VCR (Sigma, Brazil) and FEPS with 300 ng/ml of DNR (Sigma, Brazil). The cells were grown at 37°C in 5% CO<sub>2</sub> in disposable plastic flasks containing RPMI1640 (Gibco, Brazil), medium supplemented with sodium bicarbonate (2.0 g/L) (Vetec, Brazil), l-glutamine (0.3 g/L) (Vetec, Brazil), Hepes (25 mM) (Acros, Belgium), 10% fetal bovine serum (Gibco, Brazil), 1% antibiotic (penicillin, 100 U/mL and streptomycin 100 mg/mL) (Gibco, Brazil) and antimycotic (amphotericin B 0.25 mg/mL - Sigma, Brazil). All experiments were performed with six samples from each cell line.

## 2.2 Vincristine (VCR) and daunorubicin (DNR) treatment

The cell lines were cultured in the Cell Culture Laboratory of the Federal University of Rio Grande in presence of the chemotherapeutic – Lucena with VCR (60 nM) and FEPS (300 ng/ml) with DNR or 30 days without the presence of chemotherapeutic agents. Subsequently, the cells of each treatment (with or without the chemotherapeutic drug) were used for the analyses of cell viability, reactive oxygen species levels and gene expression. K562 was used as control.

## 2.3 Treatment with hydrogen peroxide (H<sub>2</sub>O<sub>2</sub>)

K562, Lucena with or without VCR and FEPS with or without DNR ( $2,5 \times 10^5$  cell/ml) were spun down, washed twice and diluted in medium RPMI1640 (Gibco, Brazil). The cells were then incubated for 30 min with hydrogen peroxide (H<sub>2</sub>O<sub>2</sub>) in two concentrations: 20 mM and 60 mM. After incubation, the suspensions were centrifuged, washed and resuspended in medium. Cells were then incubated in 96 well plates for 24 h. Cell viability was measured by MTT (3-(4,5-dimethylthiazol-2-yl), 2,5-diphenyltetrazolium) according to Trindade et al. (1999)[18].

## 2.4 Evaluation of Reactive oxygen species (ROS) levels

K562, Lucena with or without VCR and FEPS with or without DNR ( $2,5 \times 10^5$  cell/mL) were washed with PBS and incubated for 30 min at 37°C with the fluorogenic compound 2',7'-dichlorofluorescein diacetate (H<sub>2</sub>DCF-DA) at a final concentration of 40 μM. After

loading with H<sub>2</sub>DCF-DA, the cells were washed with PBS and then resuspended in fresh PBS. Five replicates of 160 µL aliquots of each sample were placed into an ELISA plate, and the fluorescence intensity was determined during 90 min at 37°C, using a fluorometer (FilterMax F5), with excitation and emission wavelengths of 485 and 520 nm, respectively. The ROS levels were expressed in terms of fluorescence area, after fitting fluorescence data to a second-order polynomial and integrating between 0 and 90 min to obtain the area.

### 2.5 Total RNA extraction and cDNA synthesis

Total RNA (2x10<sup>6</sup> cell/mL) was extracted by Trizol reagent method, according to manufacturer's instructions (Invitrogen, Brazil), the lineages K562, Lucena with or without VCR and FEPS with or without DNR using six samples, collected from each cell lineage. RNA was quantified by BioDrop µLite (England). RNA integrity was confirmed by electrophoresis in agarose gel (1%) stained with 0.5 µg/mL of ethidium bromide. The RNA was then treated with Dnase1 (Invitrogen) and 2 µg of total RNA, following the manufacturer's instructions of reverse transcriptase (RT High capacity, Applied Biosystems, Brazil).

### 2.6 Gene expression - Real-time quantitative PCR

The gene expression analysis was performed using a Real-time PCR System 7500 (Applied Biosystems) through the SYBR Green PCR Master Mix kit (Applied Biosystems). Specific primers were designed for each gene analyzed using the Primer-Blast tool from the NCBI website (<http://www.ncbi.nlm.nih.gov>). The analyzed genes

(**Table 1**) were from antioxidant system (*cat*, *gstm4*, *sod1*, *sod2* and *sod3*), glucose transporter (*glut1*), member of ABC family (*abcb1*) and transcription factors (*nrf2*, *hif-1 $\alpha$*  and *oct4*). The *ef1 $\alpha$*  and *b2m* genes were used as internal controls for data normalization. geNorm applet [19] was used to validate the reference genes through a normalization factor, which was calculated as the geometric mean of the expression values of the reference genes. Relative expression levels of the target genes were calculated by dividing the expression value of the target gene by the normalization factor.

## 2.7 Statistical analysis

All experiments were repeated at least three times. Statistical significance between groups was determined by one-way ANOVA, followed by Tukey's *post hoc* test. The results are expressed as mean  $\pm$  S.E.M. P values  $< 0.05$  were considered statistically significant.

## 3 Results

### 3.1 Cell Viability Assay

K562 decrease cell viability after 24 h exposure to H<sub>2</sub>O<sub>2</sub> at concentrations of 20 mM and 60 mM, when compared to the control (**Figure 1**). Both cell lines exposed in the presence of the chemotherapeutic agent VCR or DNR did not present a significant difference after 24 h exposure to H<sub>2</sub>O<sub>2</sub>. However, in the absence of the chemotherapeutic VCR Lucena has a decrease in cell viability of 69% in both concentrations of H<sub>2</sub>O<sub>2</sub> (20 mM e 60 mM) in relation to control. FEPS is not affect by H<sub>2</sub>O<sub>2</sub>.

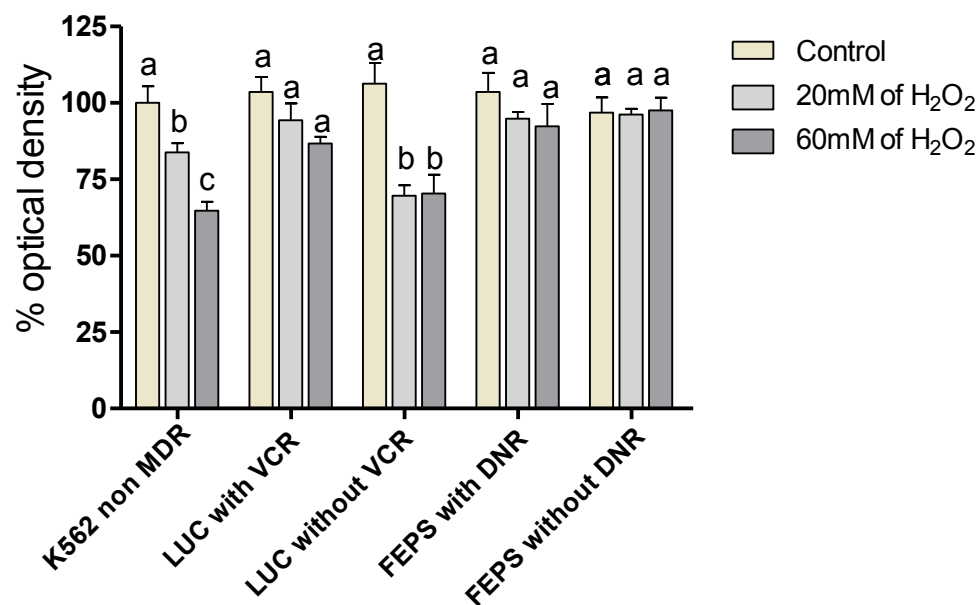


**Figure 1:** Sensitivity (%) of K562 (non-MDR), Lucena (with or without VCR) and FEPS (with or without DNR) to H<sub>2</sub>O<sub>2</sub> (20 mM and 60 mM) 24 h after incubation. The data are expressed as the mean  $\pm$  standard error. The different letters indicate a significant difference for each cell line ( $p < 0.05$ ).

### 3.2 Intracellular levels of ROS and relative gene expression of glucose transporter 1 (*glut1*)

In the absence of chemotherapeutics, both MDR lineages decrease ROS levels. However, this decrease is more pronounced in FEPS (Figure 2A). For *glut1* expression, we observed that FEPS has higher level of expression in relation the other cell lines (K562 and Lucena), independently of DNR presence (Figure 2B).

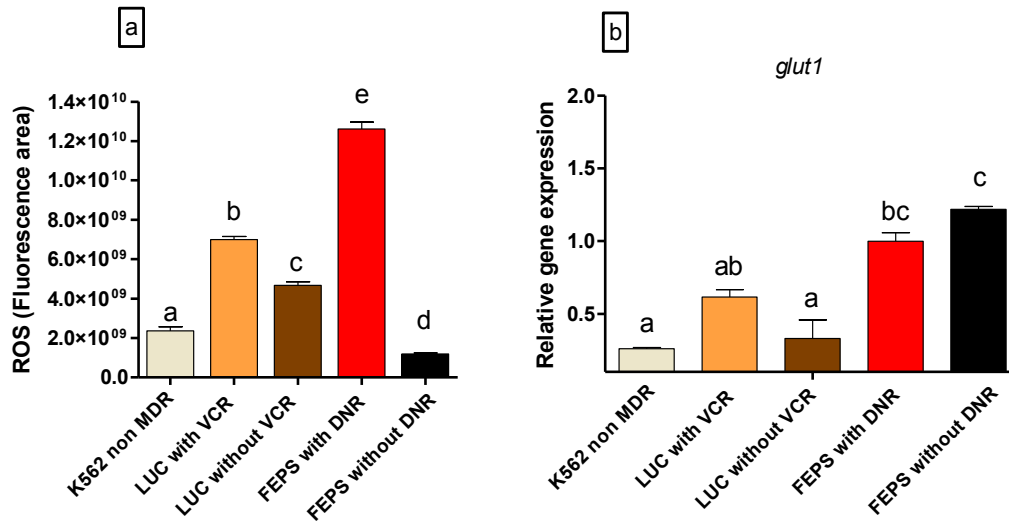


**Figure 2:** (A) The intracellular levels of reactive oxygen species (ROS); (B) relative glucose transporter 1 (*glut1*) gene expression in K562 (non-MDR), Lucena (with or without VCR) and FEPS (with or without DNR). The data are expressed as the mean  $\pm$  standard error. The different letters indicate a significant difference in ROS levels for each cell line ( $p < 0.05$ ).

### 3.3 Transcriptions factors expression

VCR induces the expression of *nrf2*, *oct4* and *hif-1 $\alpha$*  in relation to K562. The same does not happen with DNR, being only *hif-1 $\alpha$*  increased by this chemoterapeutic. In the absence of VCR, only *hif-1 $\alpha$*  remains high while the other two genes return to the control level. Diferently, in the DNR absence all genes remain in high expression level (**Figure 3**).

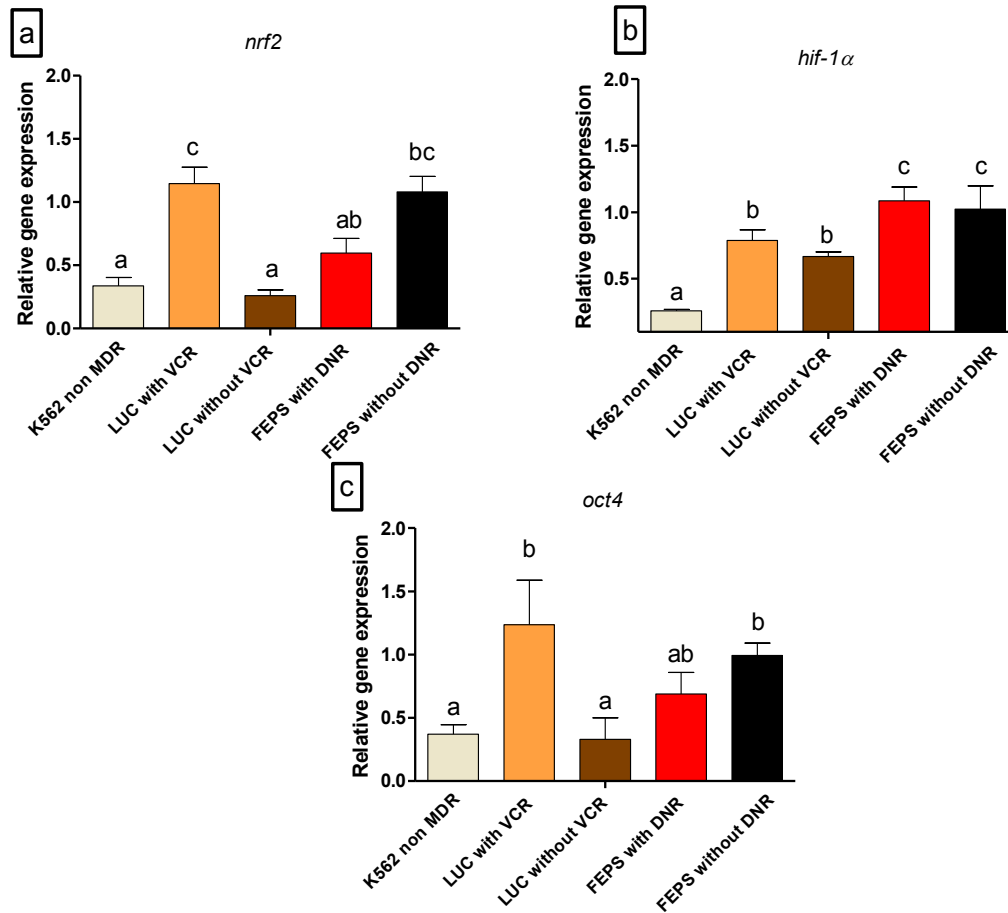


**Figure 3:** Relative gene expression of transcription factors genes *nrf2* (A), *hif-1α* (B) and *oct4* (C) were analyzed in K562 (non-MDR), Lucena (with or without VCR) and FEPS (with or without DNR). The data are expressed as the mean  $\pm$  standard error. The different letters indicate a significant difference for each cell line ( $p < 0.05$ ).

### 3.4. Antioxidant genes and extrusion pump expression

All genes analysed (*cat*, *gstm4*, *sod1*, *sod2*, *sod3* and *abcb1*) showed a consistent pattern of expression. VCR induces all six genes in high level, while the absence of this

chemotherapeutic reduces significantly their expression to the control level or below. In contrast, DNR absence keeps all genes with elevated expression in relation the levels observed when VCR was withdraw (Figure 4).

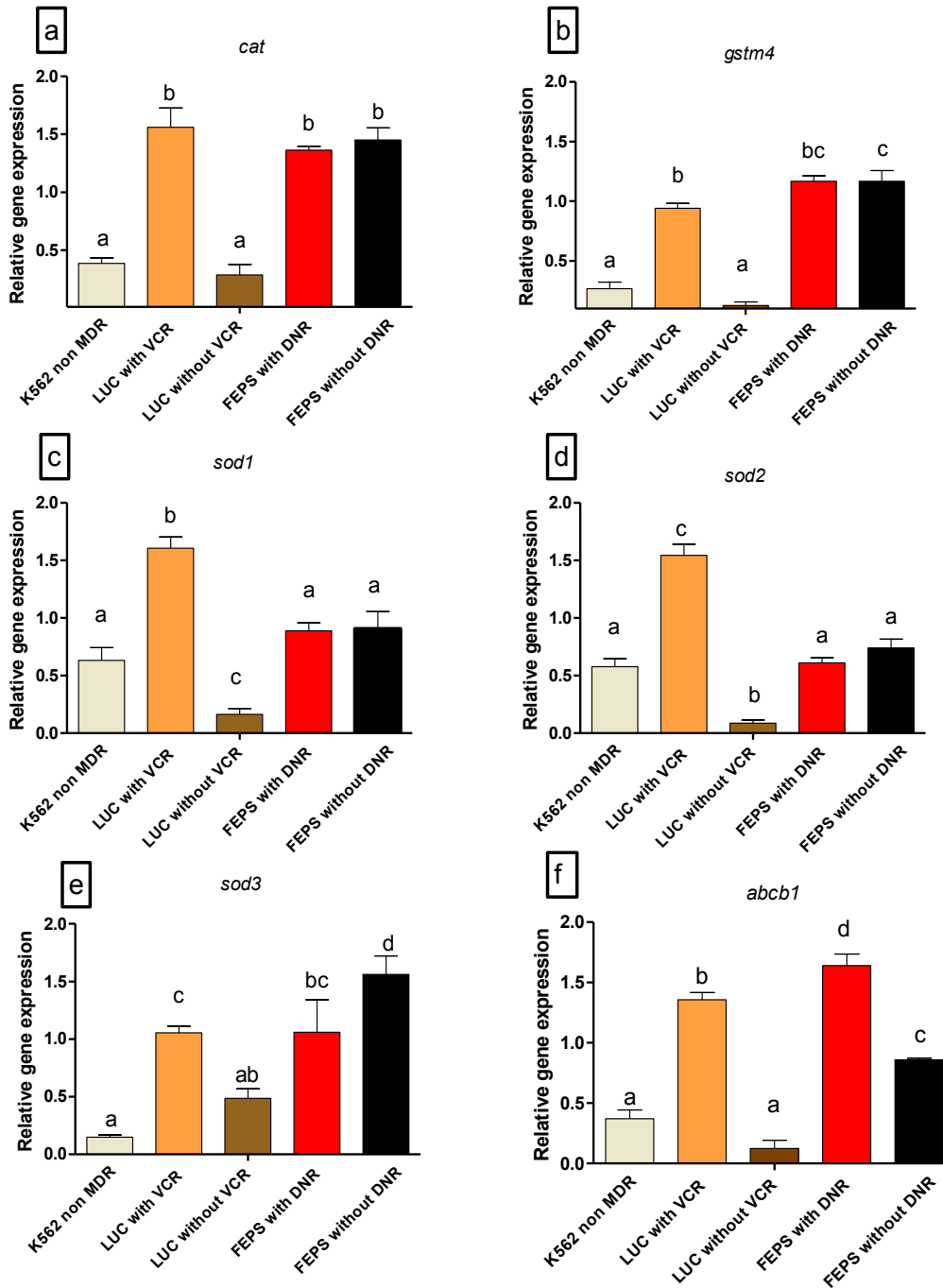




**Figure 4:** Relative gene expression of antioxidant genes *cat* (A), *gstm4* (B), *sod1*(C), *sod2* (D), *sod3* (E) and extrusion pump *abcb1* (F) in K562 (non-MDR), Lucena (with or without VCR) and FEPS (with or without DNR). The data are expressed as the mean  $\pm$  standard error. The different letters indicate a significant difference for each cell line ( $p < 0.05$ ).

#### 4 DISCUSSION

In this work, we identified that the effect of different chemotherapeutic drugs may select cells with different antioxidant capacities. At first, we compared the sensibility of the two resistant lines (MDR) against an oxidant agent ( $H_2O_2$ ). The cell lines used were selected by different chemotherapeutics. Lucena is resistant to VCR and FEPS is resistant to DNR. The cell lines were analyzed in the presence of their respective chemotherapeutics (VCR or DNR) and in the absence of them (for one month). Our results show that cell lines have different sensitivities when exposed to  $H_2O_2$ . In the presence of VCR Lucena maintains the cellular viability in both concentrations of  $H_2O_2$ . When the VCR is removed, viability of Lucena cells is drastically reduced (69%) (**Figure 1A**), while FEPS cells maintain high viability (100%) even in the absence of DNR. These data suggest that the selective effect of DNR generates a population of cells resistant to chemotherapy, but with increased antioxidant capacity. This feature does not appear to be dependent on the DNR because it is maintained even when the cells are cultured for a month without this chemotherapeutic agent.

The increased antioxidant capacity observed for FEPS cells may be related to the need for increased cell energy to cope with DNR. This chemotherapeutic belongs to a family of anthracyclines drugs and is used to treat some types of cancers, including myeloid and

lymphoid leukemias [20]. There are two main mechanisms proposed for the effect of DNR in tumor cells. The first is the intercalation of DNR to the double helix and the interruption of DNA repair mediated through topoisomerase II. The second mechanism is the generation of oxidative stress. DNR is oxidized to semiquinone, an extremely unstable metabolite, and the semiquinone is converted back into DNR in a process that releases reactive oxygen species [21]. Thus, DNR appears to be more stressful for cells than the VCR, which has as its main mechanism of action the binding to the tubulin protein, which affects chromosomes separation during the metaphase and induces apoptosis [22].

The results obtained from the exposure of the Lucena and FEPS cells to the oxidizing agent suggest that chemotherapeutic agents are acting differently on the oxidative metabolism. So what is the mechanism behind it? Was the energy expenditure of the two lineages selected by different chemotherapeutic drugs the same? To answer those questions we evaluated the levels of ROS and the relative expression of *glut1*. Taking into account that ROS are byproducts generated during the production of ATP in the respiratory chain that occurs in the mitochondria, we can consider this parameter as an indirect measure of energy demand caused by exposure to DNR. On the other hand, *glut1* is a glucose transporter that has great importance in the entrance of glucose into the cell to supply the energetic demand.

The results obtained in the ROS analyzes in the two resistant cell lines used in this study pointed to a different energy demand caused by exposure to the two chemotherapeutics: VCR and DNR. The withdrawal of VCR in Lucena cell culture causes a 33% decrease in ROS production, whereas the withdrawal of DNR in FEPS cell cultures causes a decrease of approximately 90% in this same parameter (Figure 2A). *glut1*

expression does not demonstrate significant changes in Lucena cells when compared to the K562 control. However, the expression of this transporter increases in FEPS cells, with the peculiarity that this expression remains high even with DNR removal (Figure 2B). This fact demonstrates that DNR-resistant cells appear to have been selected in order to keep this key gene constitutively high. The question that arises is whether this transcriptional feature extends to other genes related to the antioxidant defense system and the MDR phenotype.

In terms of understanding the transcriptional mechanisms that govern the expression pattern of a given gene, the first step is to analyze the transcription factors. In the case of *glut1*, the main transcription factor that regulates its expression is HIF-1 $\alpha$ . Figure 3B shows relative expression of *hif-1 $\alpha$* , where it is evident that the levels of expression of this transcription factor are higher in FEPS, being maintained this way even in the absence of DNR. Figures 3A and 3C show the same pattern of constitutive expression for two other important transcription factors: *nrf2* (associated with control of expression of genes from the antioxidant defense system), and *oct4* (associated with stem tumor cells and the MDR phenotype). Taken together, these results demonstrate that DNR selects cells with constitutively active transcription factors, resulting in altered control of target genes expression. As *glut1* is controlled by HIF-1 $\alpha$ , NRF2 controls *cat*, *gstm4*, *sod1*, *sod2*, *sod3* and extrusion pump *abcb1*. The extrusion pump is also controlled by OCT4. The results shown in Figure 4 corroborate the hypothesis that constitutively expressed transcription factors alter the expression of target genes. All six genes analyzed maintain their high expression even in the absence of DNR, which can be explained by the maintenance of

*nrf2* expression in this experimental condition. The opposite is observed in the Lucena cells, where the withdrawal of the VCR causes a drastic fall in all analyzed genes.

In conclusion we identified for the first time, that different chemotherapeutic VCR and DNR may select cells with different antioxidant capacities. It seems that selection with DNR favors cells with constitutive expression of the main transcription factors that control genes related to the energy supply, antioxidant defense system and MDR phenotype. The reasons why these transcription factors are altered may be through mutations in their promoters or changes in their methylation patterns. This topic seems to be an interesting research target for the advancement in the knowledge of the mechanisms involved in the development of resistance to chemotherapeutic drugs, which is a great barrier in the treatment of most types of cancers.

### **Conflicts of interest**

The authors declare that they have no competing interests.

### **Acknowledgments**

We thank the Institute of Medical Biochemistry Leopoldo de Meis from the Federal University of Rio de Janeiro (UFRJ) for providing the cell lines used in this study. This study was financed in part by the Coordenação de Aperfeiçoamento de Pessoal de Nível Superior - Brasil (CAPES) - Finance Code 001. This study was carried out in the Post-Graduate Program in Physiological Sciences. L. F. M is a research fellow from CNPq (Proc. No. 305928/2015-5).

## REFERENCES

- [1] A. Cort, T. Ozben, L. Saso, C. De Luca, L. Korkina, Redox Control of Multidrug Resistance and Its Possible Modulation by Antioxidants, *Oxid. Med. Cell. Longev.* 2016 (2016) 1–17. doi:10.1155/2016/4251912.
- [2] K.A. Conklin, Chemotherapy-associated oxidative stress: impact on chemotherapeutic effectiveness., *Integr. Cancer Ther.* 3 (2004) 294–300. doi:10.1177/1534735404270335.
- [3] A. Challapalli, L. Carroll, E.O. Aboagye, Molecular mechanisms of hypoxia in cancer, *Clin. Transl. Imaging.* 5 (2017) 225–253. doi:10.1007/s40336-017-0231-1.
- [4] E.H. Heiss, D. Schachner, K. Zimmermann, V.M. Dirsch, Glucose availability is a decisive factor for Nrf2-mediated gene expression, *Redox Biol.* 1 (2013) 359–365. doi:10.1016/j.redox.2013.06.001.
- [5] K. Song, M. Li, X.J. Xu, L. Xuan, G.N. Huang, X.L. Song, Q.F. Liu, HIF-1a and GLUT1 gene expression is associated with chemoresistance of acute myeloid leukemia, *Asian Pacific J. Cancer Prev.* 15 (2014) 1823–1829. doi:10.7314/APJCP.2014.15.4.1823.
- [6] N.S. Brown, R. Bicknell, Hypoxia and oxidative stress in breast cancer. Oxidative stress: its effects on the growth, metastatic potential and response to therapy of breast cancer., *Breast Cancer Res.* 3 (2001) 323–7. doi:10.1186/bcr315.
- [7] M. Jaramillo, D. Zhang, The emerging role of the Nrf2–Keap1 signaling pathway in

- cancer, *Genes Dev.* 27 (2013) 2179–2191. doi:10.1101/gad.225680.113.
- [8] W.M. Frederiks, K.S. Bosch, K.A. Hoeben, J. van Marle, S. Langbein, Renal cell carcinoma and oxidative stress: The lack of peroxisomes, *Acta Histochem.* 112 (2010) 364–371. doi:10.1016/j.acthis.2009.03.003.
- [9] B. Halliwell, Oxidative stress and cancer: have we moved forward?, *Biochem. J.* 401 (2007) 1–11. doi:10.1042/BJ20061131.
- [10] L. Ji, H. Li, P. Gao, G. Shang, D.D. Zhang, N. Zhang, T. Jiang, Nrf2 Pathway Regulates Multidrug-Resistance-Associated Protein 1 in Small Cell Lung Cancer, *PLoS One.* 8 (2013) e63404. doi:10.1371/journal.pone.0063404.
- [11] L. Bao, J. Wu, M. Dodson, E.M. Rojo de la Vega, Y. Ning, Z. Zhang, M. Yao, D.D. Zhang, C. Xu, X. Yi, ABCF2, an Nrf2 target gene, contributes to cisplatin resistance in ovarian cancer cells., *Mol. Carcinog.* 56 (2017) 1543–1553. doi:10.1002/mc.22615.
- [12] B.R. Oliveira, M.A. Figueiredo, G.S. Trindade, L.F. Marins, OCT4 mutations in human erythroleukemic cells: implications for multiple drug resistance (MDR) phenotype, *Mol. Cell. Biochem.* 400 (2014) 41–50. doi:10.1007/s11010-014-2260-7.
- [13] D.E. Linn, X. Yang, F. Sun, Y. Xie, H. Chen, R. Jiang, H. Chen, S. Chumsri, A.M. Burger, Y. Qiu, A Role for OCT4 in Tumor Initiation of Drug-Resistant Prostate Cancer Cells., *Genes Cancer.* 1 (2010) 908–16. doi:10.1177/1947601910388271.
- [14] X. Wang, J. Dai, Concise review: Isoforms of OCT4 contribute to the confusing diversity in stem cell biology, *Stem Cells.* 28 (2010) 885–893. doi:10.1002/stem.419.

- [15] C.B. Lozzio, B.B.L. Information, A. Society, W. Dc, T.A. Society, Human chronic myelogenous leukemia cell-line with positive Philadelphia chromosome, (2012) 321–334.
- [16] V.M. Rumjanek, G.S. Trindade, K. Wagner-souza, Multidrug resistance in tumour cells : characterisation of the multidrug resistant cell line K562-Lucena 1 \*, 73 (2001).
- [17] N. Daflon-Yunes, F.E. Pinto-Silva, R.S. Vidal, B.F. Novis, T. Berguetti, R.R.S. Lopes, C. Polycarpo, V.M. Rumjanek, Characterization of a multidrug-resistant chronic myeloid leukemia cell line presenting multiple resistance mechanisms., *Mol. Cell. Biochem.* 383 (2013) 123–35. doi:10.1007/s11010-013-1761-0.
- [18] G.S. Trindade, M. a Capella, L.S. Capella, O.R. Affonso-Mitidieri, V.M. Rumjanek, Differences in sensitivity to UVC, UVB and UVA radiation of a multidrug-resistant cell line overexpressing P-glycoprotein., *Photochem. Photobiol.* 69 (1999) 694–9. <http://www.ncbi.nlm.nih.gov/pubmed/10378008>.
- [19] J. Vandesompele, K. De Preter, ilip Pattyn, B. Poppe, N. Van Roy, A. De Paepe, rank Speleman, Accurate normalization of real-time quantitative RT-PCR data by geometric averaging of multiple internal control genes, *Genome Biol.* 3 (2002) 34–1. doi:10.1186/gb-2002-3-7-research0034.
- [20] M.G. Côme, A. Skladanowski, A.K. Larsen, G. Laurent, Dual mechanism of daunorubicin-induced cell death in both sensitive and MDR-resistant HL-60 cells., *Br. J. Cancer.* 79 (1999) 1090–7. doi:10.1038/sj.bjc.6690174.
- [21] D.A. Gewirtz, A critical evaluation of the mechanisms of action proposed for the

antitumor effects of the anthracycline antibiotics adriamycin and daunorubicin,  
Biochem. Pharmacol. 57 (1999) 727–741. doi:10.1016/S0006-2952(98)00307-4.

- [22] M.A. Jordan,. Mechanism of action of antitumor drugs that interact with  
microtubules and tubulin". Current Medicinal Chemistry. Anti-cancer Agents. 2  
(1): 1–17



Table 1

Gene	Metabolic pathway	Gene expression	GenBank
EF $\alpha$	Housekeeping gene	hEF1a-FOR: GCCAGTGGAAACCACGGCTGCT hEF1a-REV: ATCTGGAGAGGCAGGGCGCA	NM_001402
B2M	Housekeeping gene	hB2M-FOR: CTCACGTATCCAGCAGAGAA hB2M-REV: TCGGATGGATGAAACCCAGAC	NM_004048.2
OCT4	Octamer-binding transcription factor 4	hOCT4-FOR: TTCCCATGGGGACACCT hOCT4-REV: CCCCTGGCCCATCACCTCCA	NM_002701
NFR2	Nuclear factor, erythroid 2 like 2	hNFR2-FOR: GATGAAAGAGACAGTTGCCCCA hNFR2-REV: TACAAACGGGAATGTCTGGC	NM_001313904.1
ABCB1	ATP binding cassette subfamily B member 1	hABCB1-FOR: TCCTCAGTCAAGTTCAGAGTCTCA hABCB1-REV: TCTCCACTTGATGATGTCTCACT	NM_000927
SOD1	O <sub>2</sub> degradation Conjugation	hSOD1-FOR: GAAAACA CGGTGGGCCAAAAG hSOD1-REV: GCAGTCACATTGCCCAAGTC	NM_000454.4
SOD2	O <sub>2</sub> degradation Conjugation	hSOD2-FOR: AGCGGCTTCAGCAGATCG hSOD2-REV: AACATGCTCTAGTGTGGT	NM_001322816.1
SOD3	O <sub>2</sub> degradation Conjugation	hSOD3-FOR: CTCTGAGGTCTCACCTTCGC hSOD3-REV: TGGTGGGTCTCGGTATAGGG	NM_003102.2
GSTM4	Conjugation of GSH and xenobiotics	hGSTM1-FOR: TGGACGCCTTCCAAATCTGA hGSTM1-REV: GCCACAGGAAACCTCAAAGC	NM_147148.2
CAT	H <sub>2</sub> O <sub>2</sub> degradation	hCAT-FOR: TGAAGATGCGGCGAGACTTT hCAT-REV: GAGGGGTACTTTCCTGTGGC	NM_001752.3

**Table 1:** Gene-specific primers used in analysis via RT-PCR, metabolic pathway and accession number of GenBank

### 3.2 Manuscrito 2

*Manuscript to be submitted to Toxicology and Applied Pharmacology Journal*

**New mechanistic insight on the PIM-1 kinase inhibitor AZD1208 using multidrug resistant human erythroleukemia cell lines and molecular docking simulations**

Maiara Bernardes Marques<sup>a,b\*</sup>, Michael González-Durruthy<sup>c,\*</sup>, Bruna Félix da Silva Nornberg<sup>a</sup>, Bruno Rodrigues Oliveira<sup>a</sup>, Daniela Volcan Almeida<sup>a</sup>, Ana Paula de Souza Votto<sup>b</sup>, Luis Fernando Marins<sup>a,\*</sup>

<sup>a</sup>Laboratory of Molecular Biology, Institute of Biological Sciences, Federal University of Rio Grande - FURG, Rio Grande, RS, Brazil.

<sup>b</sup>Laboratory of Cell Culture, Institute of Biological Sciences, Federal University of Rio Grande - FURG, Rio Grande, RS, Brazil.

<sup>c</sup>Department of Chemistry and Biochemistry, Faculty of Science, University of Porto, Porto, Portugal.

\* Correspondence: Institute of Biological Sciences, Federal University of Rio Grande - FURG, Av. Itália, Km 8, 96203-900 Rio Grande, Brazil. E-mail address: mai.mbio@gmail.com (M.B. Marques) and dqmluf@furg.br (L.F. Marins). Phone: +55 53 32336850; Department of Chemistry and Biochemistry, Faculty of Science, University of Porto, Porto, Portugal. Email: michael.durruthy@fc.up.pt (M. González-Durruthy) Phone: +351920276152.

## Abstract

PIM-1 is a kinase which has been related to the oncogenic processes like cell survival, proliferation and multidrug resistance (MDR). This kinase is known for its ability to phosphorylate the main extrusion pump (ABCB1) related to the MDR phenotype. In the present work, we tested a new mechanistic insight on the AZD1208 (PIM-1 specific inhibitor) under interaction with chemotherapy agents such as Daunorubicin (DNR) and Vincristine (VCR). In order to verify a potential cytotoxic effect based on pharmacological synergism, two MDR cell lines were used: Lucena resistant to VCR) and FEPS (resistant to DNR), both derived from the K562 non-MDR cell line. Our *in vitro* results have shown that AZD1208 alone decreases cell viability of MDR cells. However, co-exposure of AZD1208 and DNR or VCR reverses this effect. When we analyzed the ABCB1 activity AZD1208 alone was not able to affect the pump extrusion. Differently, co-exposure of AZD1208 and DNR or VCR impaired ABCB1 activity, which could be explained by compensatory expression of *abcb1* or other extrusion pumps not analyzed here. Furthermore, we performed a molecular docking simulation to delve into the molecular mechanism of PIM-1. Docking analysis showed that AZD1208 is capable of performing hydrophobic interactions with PIM-1 ATP- binding-site residues with stronger interaction-based negative free energy (FEB, kcal/mol) than the ATP itself, mimicking an ATP-competitive inhibitory pattern of interaction. On the same way, VCR and DNR may theoretically interact at the same biophysical environment of AZD1208 and also compete with ATP by the PIM-1 active site. These evidences suggest that AZD1208 may induce pharmacodynamic interaction with VCR and DNR, weakening its cytotoxic potential in the

ATP-binding site from PIM-1 observed in the *in vitro* experiments. Finally, the current results could have a pre-clinical relevance potential in the rational poly-pharmacology strategies to prevent multiple-drugs resistance in human leukemia cancer therapy.

**Keywords:** PIM-1 kinase, AZD1208, molecular docking, multidrug-resistance.

## 1. Introduction

The Proviral integration site for Moloney murine leukemia virus-1 (PIM-1) is a serine/threonine kinase that regulates multiple cellular functions such as cell cycle, cell survival, and drug resistance. From the structural point of view, PIM-1 has a fold that comprising two domains. The N-terminal domain (NTD) consists of antiparallel  $\beta$ -sheets from residue 33 to 120. The C-terminal domain (CTD) is formed by  $\alpha$ -helices, from residue 129 to 305, which are associated by a hinge region or motif that include the Leu120 as a gatekeeper residue (PIM-1 entry point). Besides, PIM-1 kinase is characterized by the ATP binding pocket (active binding-site) which is between the NTD and CTD domains surrounded by the hinge region, glycine-rich loop (G-loop, from residue 46 to 54, and the activation loop (A-loop, from residue 191 to 202)(Lee et al., 2013).

PIM-1 kinase is overexpressed in numerous types of cancer such as hematopoietic tumors, particularly in acute myelogenous leukemia (AML) (Cheng et al., 2017), lymphoblastic leukemia (ALL) (Amson et al., 1989), chronic lymphocytic leukemia (CLL), non-Hodgkin's lymphoma (Cohen et al., 2004), and also in solid tumors as prostate cancer (Ellwood-Yen et al., 2003) (Jiménez et al., 2017). This makes PIM-1 an attractive target for the development of anti-cancer chemotherapeutic drugs (Nawijn et al., 2011). PIM-1 is involved in a number of signaling pathways that control critical processes in hematopoiesis and lymphopoiesis, including multiple drug resistance (MDR) processes (Tursynbay et al., 2016; Isaac et al., 2011). The cell lines used in the present study were selected resistant from the human erythroleukemic cell line sensitive to chemotherapy, K562 (Lozzio et al.,

2012). The K562-Lucena (Lucena) cell line was selected resistant to vincristine (VCR) (Rumjanek et al., 2001) and FEPS to the daunorubicin (DNR) (Daflon-Yunes et al., 2013).

From the clinical point of view, AZD1208 is an orally available molecule of AZD1208 (benzylidene-1,3-thiazolidine-2,4-dione), recognized as a potent PIM kinases inhibitor, with an excellent selectivity profile, low nanomolar activity against all three PIM isoforms (PIM-1, PIM-2 and PIM-3). AZD1208 induces the G1/S phase cell cycle transition breaking off, thereby inducing cell cycle arrest and apoptosis in cells that overexpresses PIMs (Keeton et al., 2014) (Dakin et al., 2012). The growth inhibition of several leukemia cell lines by AZD1208 usually is correlated with the PIM-1 expression (Bachmann and Möröy, 2005).

Commonly, the PIM inhibitors are part of the combination chemotherapeutic drugs of broad-spectrum. Despite extensive studies of new PIM inhibitors, it is still unclear how the AZD1208 molecule interacts with other anti-cancer molecules. The interaction between antitumor agents usually leads to an additive to synergistic cytotoxic effect in tumoral cell lines, causing multidrug resistance. Therefore, it is important to access the possible interaction among chemotherapeutic drugs and consequent cell cytotoxicity before the clinical treatments. In this sense, the use of molecular docking is a powerful and bioinformatic tools for the study of the relevant binding interactions of multiple xenobiotics (ligands) with a specific target-protein high cytotoxicity potential. Furthermore, the implementation of *in silico* tools based on molecular docking mechanisms appears to be an efficient strategy for the predictive purposes and rational drug design of new PIM-1 inhibitors pharmacodynamic efficacy when this theoretical data is supported by experimental *in vitro* evidences (Aouidate et al., 2018).

In this context, we hypothesized that AZD1208 probably interacts pharmacodynamically with the chemotherapeutic agents Vincristine (VCR) and Daunorubicin (DNR) and that this fact, could lead to a competitive inhibitory effect in the active binding-site of PIM-1 kinase with a potential loss of its specific cytotoxic effect (PIM-1 inhibition). Thus, the main objective of this work was to evaluate the interaction of AZD1208 with other drugs commonly used for human erythroleukemia treatment. We performed *in vitro* cytotoxicity assays by using human erythroleukemia MDR cell lines (Lucena/VCR and FEPS/DNR) and molecular docking to evaluate potential pharmacodynamic interactions between chemotherapeutic agents.

## **2. Materials and methods**

### **2.1 Experimental procedures**

#### **2.1.1 Cells and culture procedures**

The cell lines were provided of Immunology Laboratory at the Medical Biochemistry Institute Leopoldo de Meis of the Federal University of Rio de Janeiro (Brazil). Lucena was maintained with 60 nM of VCR (Sigma, Brazil) and FEPS with 300 ng/ml of DNR (Sigma, Brazil). The cells were grown at 37°C in 5% CO<sub>2</sub> in disposable plastic flasks containing RPMI1640 (Gibco, Brazil), medium supplemented with sodium bicarbonate (2.0 g/L) (Vetec, Brazil), l-glutamine (0.3 g/L) (Vetec, Brazil), Hepes (25 mM) (Acros, Belgium), 10% fetal bovine serum (Gibco, Brazil), 1% antibiotic (penicillin, 100 U/mL and streptomycin 100 mg/mL) (Gibco, Brazil) and antimycotic (amphotericin B 0.25 mg/mL - Sigma, Brazil). All experiments were performed with six samples from each cell line.



### 2.1.2 Treatment of cells with AZD1208, Vincristine and Daunorubicin

The K562 (non-MDR), Lucena and FEPS were cultured ( $2,5 \times 10^5$  cells/mL) in presence of 1  $\mu$ M of AZD1208 alone or 1  $\mu$ M of AZD1208 plus 60 nM of VCR; or 1  $\mu$ M of AZD1208 plus 300 nM of DNR for 24, 48 and 72 h. The control cells (not treated) received DMSO at 0.01% (final concentration used in the treatment with AZD1208).

### 2.1.3 MTT Assay

Briefly, the cell lines were incubated in 96 well plates for for 24, 48 and 72 h as described in topic 2.1.2. Cell viability was measured by the MTT (3-(4,5-dimethylthiazol-2-yl), 2,5-diphenyltetrazolium) according to Trindade et al. (1999)[18]

### 2.1.4 Activity of the P-gp transporter

For the transport activity measurements, the accumulation of Rho-123 was observed. The cell lines ( $2,5 \times 10^5$  cells/mL) were treated with 1  $\mu$ M AZD1208, 1  $\mu$ M AZD1208 plus VCR (60 nM) or 1  $\mu$ M AZD1208 plus DNR (300 nM) for 24 h in 24-well culture plates, as previously explained. Subsequently, the cells were centrifuged (1,100 rpm for 2 min) and washed with PBS. The cells treated with Rhodamine 123 were washed in PBS and incubated in the dark at 37°C in 5% CO<sub>2</sub>, for 1 h in 1 mL of fresh medium containing Rho-123 (300 ng/mL). Next, cells were washed twice in PBS, resuspended in 1 mL of fresh medium and incubated for 30 min for Rho-123 efflux. Finally, the medium was removed, and the cells were resuspended in PBS. Excitation/emission values were determined using a multiwell plate at 485/590 nm. These experiments were replicated three times. Therefore, efflux transporters activity was expressed as the inverse of Rho-123 fluorescence accumulation per number of cells.

## 2.2 Computational Procedures

### 2.2.1 Performing molecular docking simulation

We evaluate the docking-interaction between the PIM-1 kinase and the different types of chemotherapy ligand substrates (AZD1208, Vincristine and Daunorubicin) interactions through of molecular docking simulations. The first step consists of preparing the PIM-1 -protein structure-file (receptor) like PDB ID:1XWS and resolution of 1.8 Å, which was obtained from Protein Data Bank. Before the docking simulation, the PIM-1 structure was prepared using the AutoDock Tools 4 software for AutoDock Vina. The -hydrogen atoms of PIM-1-protein were added, according to appropriate hybridization geometry, to those atoms based on built-in modules to add partial charges, protonation states followed by bond orders assignment and set up rotatable bonds of the PIM-1 protein like PDB x-ray crystallography-structure (Trott and Olson, 2009).

In the second step, the different types of chemotherapy ligand structures were obtained from Pubchem Data Base Chemical Structure Search as: Vincristine (PubChem CID: 5978), Daunorubicin (PubChem CID: 30323) and AZD1208 (PubChem CID: 58423153). The optimization process of all the PIM-1-chemotherapy ligand structures were performed by using the MOPAC extension for geometry optimization based on the AM1-Hamiltonian method (Forli et al., 2016; Kim et al., 2016).

To study the formed complexes like PIM-1 -chemotherapy ligand interactions the Gibbs free energy of binding or affinity (FEB in kcal/mol) was calculated from Autodock Vina molecular docking, an open source chemoinformatic tool developed by Trott et al. (2009). In this context, the PIM-1-chemotherapy ligand free energy of binding (FEB) were

calculated using a scoring function which approximates the chemical potentials ( $\Delta G_{\text{bind}}$ ) (Trott and Olson, 2009; Forli et al., 2016).

However, the  $\Delta G$  docking scoring function combines the knowledge-based potential and empirical information obtained from experimental binding affinity measurements with Autodock Vina scoring function using default Amber force-field parameters. The conformational relaxation (flexible docking) favors a significant gain of enthalpy of PIM-1-ligand complexes non-associated with ligand intra-molecular deformation or vibrational decrease within PIM-1-protein binding site. The potential PIM-1-protein active binding sites was previously predicted through DeepSite (freely available at [www.playmolecule.org](http://www.playmolecule.org)) (Jiménez et al., 2017). This step is defined as identifying and delimiting PIM-1-protein cavities, potentially at the Van der Waals surface that are likely to bind to a small ligand like Vincristine, Daunorubicin and AZD1208.

Then, DeepSite analyses all the molecular descriptors related to protein (PIM-1 - protein). The implementation of 3D-deep convolutional neural networks (DCNNs) was validate using deep learning library with an extensive test set based on more than 7000 proteins of the scPDB database (Jiménez et al., 2017). The PIM-1 -protein binding-pocket predictions as well as the PIM-1 -protein volumetric map prediction were determined. This establish the cartesian coordinates of docking box simulation like PIM-1 -grid box size, with dimensions of X=22 Å, Y= 22 Å, Z= 22 Å and the PIM-1 - grid box center with dimension of X=-18.2 Å, Y= -37.6 Å, Z= -1.3Å (Feinstein and Brylinski, 2015). Several runs starting from random conformations were carried out, and the iterations number in a run was adapted according with exhaustiveness parameter of 100 (average accuracy) in each docking simulation (Trott and Olson, 2009; Forli et al., 2016).

The binding free energy, of binding output results is defined by  $\Delta G_{\text{bind}}$  values for all docked poses of the formed complexes (PIM-1-ligands) and include the internal steric energy of a given PIM-1-ligands (Vincristine, Daunorubicin and AZD1208) can be expressed as the sum of individual molecular mechanics terms of standard-chemical potentials like: van der Waals interactions ( $\Delta G_{\text{vdW}}$ ), hydrogen bond ( $\Delta G_{\text{H-bond}}$ ), electrostatic interactions ( $\Delta G_{\text{electrost}}$ ), and intra-molecular ligands interactions ( $\Delta G_{\text{internal}}$ ) from empirically validated Autodock Vina scoring function based on default Amber force-field parameters. Besides, Autodock Vina scoring function considers optimal-linear free binding energy coefficients from experimentally determined chemical potentials ( $\Delta G_{\text{internal}}$ ) (Trott and Olson, 2009; Forli et al., 2016).

It is important to highlight that overall parameter of docking experiment are based on distance-dependent atom-pair interactions ( $d_{ij}$ ) according to the general thermodynamic equations depicted below:

$$FEB_{\text{dock}} \approx \Delta G_{\text{bind}} = \Delta G_{\text{vdW}} + \Delta G_{\text{H-bond}} + \Delta G_{\text{electrost}} + \Delta G_{\text{int}} \quad (1)$$

$$FEB_{\text{dock}} \approx \Delta G_{\text{bind}} = \Delta G_{\text{vdW}} \sum_{\text{lig-PIM1}} \left( \frac{A_{ij}}{d_{ij}^{12}} - \frac{B_{ij}}{d_{ij}^6} \right) + \Delta G_{\text{H-bond}} \sum_{\text{lig-PIM1}} E(t) \left( \frac{C_{ij}}{d_{ij}^{12}} - \frac{D_{ij}}{d_{ij}^{10}} \right) + \Delta G_{\text{elec}} \sum_{\text{lig-PIM1}} \frac{q_i q_j}{(d_{ij})^2} +$$

$$\Delta G_{\text{internal}} \left\{ \sum_{\text{lig}} \frac{A_{ii}}{d_{ii}^{12}} - \frac{B_{ii}}{d_{ii}^6} + \sum_{\text{lig}} E(t) \times \left( \frac{C_{ii}}{d_{ii}^{12}} - \frac{D_{ii}}{d_{ii}^{10}} \right) + \sum_{\text{lig}} \frac{q_i q_i}{4(d_{ii})^2} + \sum_{\text{lig}_i} \gamma_k (1 + \cos(\varpi_k \theta_k - \theta_{0k})) \right\}$$

(2)

The  $\Delta G = - RT (\ln K_i)$ ,  $R$  (gas constant) is  $1.98 \text{ cal}*(\text{mol}*K)^{-1}$ , and  $K_i$  represents the predicted PIM-1-inhibition constants at  $T = 298.15 \text{ K}$ . The first term of a 12-6/Lennard-Jones potential describes the *van der Waals* binding-interaction, as  $A_{ij}/d_{ij}^{12}$  and  $B_{ij}/d_{ij}^6$  (hyperbolic function or repulsion term). This represent a typical Lennard-Jones interactions (PIM-1-ligands), provided the Gaussian term is negative and the parabolic positive,  $d_{ij}$  is the surface distance calculated as  $d_{ij} = r_{ij} - R_i - R_j$ , where  $r_{ij}$  is the interatomic distance and  $R_i$  and  $R_j$  are the radii of the atoms in the pair of interaction of PIM-1  $(i)$ -ligands $(j)$  atoms. The second term is the pair consisting of an H-bond donor and an H-bond acceptor as a directional 12-10 hydrogen-bonding potential term such as  $B_{ij}/d_{ij}^{12}$  and  $C_{ij}/d_{ij}^{10}$ , where  $E(t)$  is an angular weight factor which represents the directionality of the hydrogen bonds and  $d_{ij}$  follows the criteria mentioned above. The third term represents the Coulomb electrostatic potential stored in the formed complex (PIM-1 -ligands)  $ij$  of  $N$  charges ( $q_i, q_j$ ) of pairs of charged atoms of PIM-1  $(i)$  and chemotherapy ligand structures $(j)$ . Following this idea, appropriated Gasteiger partial atomic charges of the PIM-1 were assigned (Trott and Olson, 2009)(Kim et al., 2016).

Herein,  $d_{ij}$  is the interatomic distance between the point charges as the reference positions of interaction based on distance-dependent dielectric constant. The fourth term of the equation (3) as ( $\Delta G_{\text{internal}}$ ) was used to validate the internal steric energy of each PIM-1-ligand including dispersion-repulsion energy and a torsional energy through the sum of the default Amber force field parameters (chemotherapy ligand conformation-independent parameters of the Autodock Vina scoring function) (Trott and Olson, 2009).

By the other hand, the electrostatic components were considered, and the ligand-partial atomic charges were properly assigned with the Gasteiger-Huckel algorithm using partial equalization of orbital electronegativities (PEOE) after the addition of polar and

non-polar hydrogen-atoms. The docking dimensionality based on degree of freedom (DOF) of each member of the PIM-1-ligand. They are: ligand-atom position/translation ( $x_i, y_i, z_i = 3$ ), ligand-atom orientation/quaternion ( $q(x_i), q(y_i), q(z_i), q(w_i) = 4$ ), ligand-number of rotatable bonds/torsion ( $tor_1, tor_2, \dots, tor_n = N_{tor}$ ) and ligand-total dimensionality (total DOF =  $3 + 4 + n$ ), do not have a significant weight in the  $FEB_{dock}$  based on the very small intra-molecular contributions of force field parameters of the PIM-1 -ligand which were considered as rigid molecules and considering the aforementioned ligand-geometry optimization based on the  $\Delta G_{internal}$  minimization of all the PIM-1 -ligands used in the present study (Trott and Olson, 2009; de Ruyck et al., 2016; Lee et al., 2006; Kremer et al., 1997).

PIM-1-ligand conformers with the lowest Gibbs docking free energy of binding (FEB negatives value) were obtained. The best root-mean-square deviation (R.M.S.D) was considered as a criterion of correct docking-pose accuracy below 2Å according to the equation (3) (Forli et al 2016)

$$RMSD(pose_{i-ligands}, pose_{j-PIM1}) = \sqrt{\frac{\sum (atom_{(i-ligand)} - atom_{(j-PIM1)})^2}{n}} \quad (3)$$

Lastly, the next step consists of analyzing the interaction data obtained from the molecular docking with respect to the final free energy of binding (FEB values) for the PIM-1-ligand complexes of each docking approach. Besides, the ATP-molecule was used as reference controls on PIM-1 kinase active-binding pocket.

### 2.2.2 Lig-Plot interactions diagrams

To evaluate the non-covalent intermolecular interactions that occur in a given PIM-1 kinase-chemotherapeutic ligand complex (AZD1208, Vincristine and Daunorubicin), we used the software Lig-plot. Lig-Plot is a software that evaluates the non-covalent intermolecular interactions that occur in a given PIM-1 kinase-chemotherapeutic ligand complex. Then, Lig-Plot automatically generates schematic 2D diagrams of interactions showing the type of interaction that took place like (hydrophobic, hydrogen bond and electrostatic interaction) for all the docking simulations and show details describing all the inter-atomic contacts (Laskowski and Swindells, 2011).

## 3. Results and discussion

### 3.1 Cell viability with AZD1208, Vincristine and Daunorubicin

Over the years, clinical research has advanced mainly because of the studies with *in vitro* models. Those tests have been applied in research on the pharmacokinetic interaction of chemotherapeutics in clinical responses, also to help in generating hypotheses about pharmacogenomics and to predict mechanisms associated with multidrug resistance (Niu and Wang, 2015). In this work, we tested an inhibitor of PIM-1 kinase, AZD1208, in two MDR cell lines (Lucena and FEPS) derived from the non-MDR K562 cell line.

Our results from the cell viability (**Figure 1A**) showed that the two resistant cell lines (Lucena and FEPS) exposed to 1  $\mu$ M of AZD1208 decreased viability after 24 h of exposure, as well the non-MDR cell line, K562. Similar results on the AZD1208 cytotoxicity were observed in an acute myeloid leukemia line, where the AZD1208 caused

a decrease in growth to induce cell-cycle arrest and apoptosis (Keeton et al., 2014). However, when we combined AZD1208 with both VCR (**Figure 1B**) or DNR (**Figure 1C**) we did not observe the same effect caused by AZD1208 alone, suggesting a pharmacodynamic effect.

Other studies have emphasized the synergistic relationship of AZD1208, and cytotoxic, with other chemotherapeutics, precisely because AZD1208 appears to be even more potent in clinical treatments when used with a co-treatment (Mazzacurati et al., 2015) (Keeton et al., 2014) (Lee et al., 2018). Studying the synergistic effects between chemotherapeutic agents is very important both to identify possible combinations of more effective treatments and to predict *in vitro* the likely toxicity of chemotherapeutics before treating cancer patients with them.

### 3.2 *P-gp activity and interactions between AZD1208, VCR and DNR*

The multidrug resistance is one of the main reasons for failure of chemotherapy treatment of human erythroleukemia. Overexpression of ABC glycoproteins such as ABCB1 (P-glycoprotein or MDR1), ABCB1 (MRP1) and ABCG2 (BCRP) are the most studied and related to the MDR phenotype (Housman et al., 2014). For this reason, we tested the activity of P-gp (**Figure 2**) and did not observe significant results for the two MDR cell lines in the presence of AZD1208 alone, demonstrating that AZD1208 did not change the P-glycoprotein activity. When we associated the AZD1208 with VCR (**Figure 2A**) or DNR (**Figure 2B**), we observed a significant increase in co-exposition the both cell lines. The results of rhodamine tests show increase of accumulation only when drugs are administered in combination. These results together with the viability results suggest that AZD1208 is neither pump inhibitor nor substrate. An important and poorly understood



aspect of the ABC transporters is the role of phosphorylation as a mechanism to regulate its functions. Xie et al. (2008) suggest that PIM-1 kinase phosphorylates ABCG2 in Thr362 and that this phosphorylation modulates the dimerization of ABCG2 molecules, which is a requirement for adequate function. Mumenthaler et al. (2010) used SGI-1776, a precursor of AZD1208, and showed that this PIM-1 inhibitor was able to decrease the proliferation of prostate cancer cells by inhibiting the activity of multidrug resistance protein 1 (MDR1).

### 3.3 *In silico* results

We studied the specific molecular mechanism involved in the PIM-1 kinase inhibition induced by AZD1208 based on molecular docking approach a non-time-dependent methodology. Then, considering the aforementioned chemotherapy-ligands (Daunorubicin and Vincristine) we explored the potential ability of these ligands to interact at the same biophysical environment as AZD1208 (PIM-1 active binding site). For this reason, an important step to ensure accuracy of docking simulation data consists in the prediction of suitable PIM-1 -active binding sites. Several methodologies for detecting protein-binding cavities have been performed over the years based on structural, geometric, and chemical protein 3D-features (PIM-1). According to this idea, in the present study the prediction of binding active-sites from PIM-1 was performed by using machine learning algorithm-based 3D-deep convolutional neural networks (DeepSite-CNNs chemoinformatic tool) (Jiménez et al., 2017) which was previously validated by providing an extensive test set based > 7000 proteins structure from the scPDB database (Jiménez et

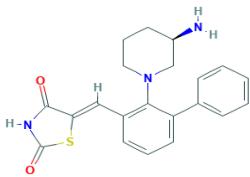
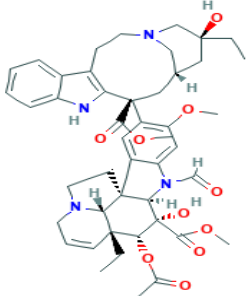
al., 2017). The results on structural identification of the PIM-1 -binding-site are shown in **Figure 3**.

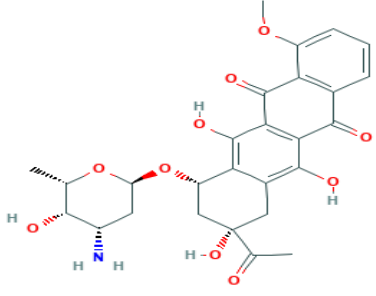
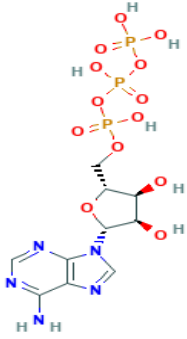
We performed the Ramachandran plot diagram to validate the 3D x-ray crystallographic structure of the PIM-1 kinase. The Ramachandran plot is a 2D-projection on the plane from the three-dimensional structure and all the possible conformations of each PIM-1 kinase-residues, including the ATP-catalytic binding sites residues which are defined based on the torsion dihedral angles (Psi) and (Phi) around the peptide-bond of the PIM-1 kinase residues which can be depicted by 2D-Ramachandran diagrams (Chen et al., 2010). Herein, allowed torsion values of Psi *versus* Phi of a given PIM-1 kinase residue is found within the Ramachandran colored contour PIM-1 kinase correspond to conformationally-favored PIM-1 -residues. Otherwise, is considered as PIM-1 kinase sterically-disallowed residue and the torsion values of dihedral angles Psi versus Phi appear outside of the Ramachandran colored contour (conformationally non-favored residues) (**Figure 4**).

According to this idea, we carried out the molecular docking experiment to obtain the Gibbs free energy of binding (FEB or affinity in kcal/mol) for the complexes formed between the PIM-1 kinase and the chemotherapy agents like (ligand: AZD1208, Vincristine, and Daunorubicin). Theoretical interaction based on the docking simulation results are considered as energetically-unfavorable when the Gibbs free energy of binding for PIM-1 -ligand complexes  $\geq 0$  kcal/mol, pointing either extremely low or complete absence of binding affinity; otherwise is synonymous of the presence of binding interactions from medium to high affinity. The obtained results show that all the tested ligands (AZD1208, Vincristine, Daunorubicin and ATP) were able to interact favorably

with PIM-1 according to spontaneous thermodynamic process ( $\Delta G_{\text{bind}} < 0$  kcal/mol) as shown in **Table 1**.

**Table 1.** Results of *in silico* docking complexes for the best PIM-1 -ligand conformations based on the affinity in kcal/mol. Please, note that the docking simulation of ATP-molecule was used as reference controls on PIM-1 /ATP-binding pockets.

PIM-1 -Ligand Structures	Docking Complexes	Docking Affinity (FEB: kcal/mol)	R.M.S.D (Å)
 <p>The image shows the chemical structure of AZD1208, a thiazolidine derivative. It features a central benzene ring substituted with a thiazolidine ring, a piperidine ring, and a phenyl ring.</p>	AZD1208-PIM-1	- 9.1	2.23
 <p>The image shows the chemical structure of Vincristine, a complex alkaloid. It consists of a complex polycyclic core with multiple nitrogen and oxygen atoms, and various functional groups including hydroxyl, methyl, and acetyl groups.</p>	Vincristine-PIM-1	- 6.1	2.875

 <p>The image shows the chemical structure of Daunorubicin, a tetracycline antibiotic. It consists of a tetracycline core with a daunosamine sugar attached to the 4-position and a daunosonolone aglycone attached to the 12-position. The daunosamine sugar has a methylamino group and a hydroxyl group. The daunosonolone aglycone has a methoxy group and a hydroxyl group.</p>	Daunorubin-PIM-1	- 8.2	2.038
 <p>The image shows the chemical structure of ATP (Adenosine Triphosphate). It consists of an adenine base attached to a ribose sugar, which is further attached to a chain of three phosphate groups. The adenine base is a purine ring system with an amino group at the 6-position. The ribose sugar is a five-membered ring with hydroxyl groups at the 2' and 3' positions. The phosphate groups are linked together by phosphoanhydride bonds.</p>	ATP- PIM-1	- 7.3	1.157

It is well known that PIM-1 kinases are a potential therapeutic target for several hematological tumors. In certain cases, their expression levels are positively correlated with poor clinical outcome. Several selective PIM-1 kinase inhibitors like AZD1208 are under development and a few are in clinical trials. Evaluations of the molecular mechanism of interactions of these drugs have demonstrated that by inhibiting PIM-1, processes such as interruption of the G1/S phase cell cycle transition, thereby inducing cell cycle arrest and apoptosis in cells that overexpress PIM-1. Besides, multiple-drug resistance mechanisms are affected.

The inhibition of growth by this AZD1208 also is usually correlated with the expression levels of PIM-1 in several leukemia cell lines. Interestingly, PIM-1 kinases also

share substrates with these parallel molecular pathways. For this instance, to overcome this challenge, PIM-1 kinase inhibitors-like AZD1208 are frequently tested in combination with a broad-spectrum of chemotherapeutic drugs, including FDA-approved agents like Daunorubicin and Vincristine based on their unique mechanism of actions. Depending on the chemotherapeutic drugs, combination results in sequential or complementary blockage or downregulation of oncogenic pathway to inhibit the PIM-1 kinase.

Our results of molecular docking allowed a mechanistic interpretation from the best PIM-1-chemotherapy ligand conformations from (AZD1208, Vincristine, and Daunorubicin) based on the affinity in kcal/mol allowed to expand our understanding on potential AZD1208 interaction *mechanism with* human PIM-1 kinase in the context of leukemia multiple-drugs resistance. We show for the first-time theoretical evidences to explain the influence of the AZD1208 when combined to VCR and DNR from the pharmacodynamic point of view.

The best docking binding-poses of interaction ( $\text{RMSD} < 2\text{\AA}$ ) for three chemotherapy PIM-1-ligand conformation complexes evaluated suggest strong interactions. The order  $\text{FEB (AZD1208-PIM-1)} > \text{FEB (Daunorubicin-PIM-1)} > \text{FEB (Vincristine-PIM-1)}$  with very close interaction potential energies ( $\Delta G_{\text{bind}}$ ), when compared with the binding affinities (FEB values) of the physiological regulatory substrate of PIM-1 kinase (ATP) used as control of simulations (or theoretical control) for comparison purposes in the ATP-PIM-1 kinase binding-site. These *in silico* results, fit with previous biochemical assays on PIM-1 activity where was proved that AZD1208 molecule inhibit the PIM-1 activity, with an  $\text{IC}_{50}$  of 0.4 nM considering that the high-end of physiologic ATP-concentration the  $\text{IC}_{50}$  values were 2.6 nM for PIM-1 kinase pointing, greater interaction strength (competitive inhibition effect) for AZD1208.

This aspect is very important from the toxicodynamic and clinic, point of view because suggests the presence of AZD1208 interactions, at the same environment biophysical that the ATP, in the PIM-1 kinase. This interaction in binding site is an inhibition constant ( $K_i$ ), demonstrating that competition for the same site of interaction of these chemotherapeutic agents would impair the cytotoxic effect of AZD1208 on resistant leukemic linages. **See Material and Methods** section like  $FEB \text{ (Kcal/mol)} \approx \Delta G = -RT (\ln K_i)$  (**Figure 5**).

The potential pharmacological docking-mechanism of AZD1208 is mainly based on hydrophobic interactions, with ATP-active binding-site residues like: Leu 120 (entry point), Asn 172, Phe 49, Val 52, Leu 174 (G-loop), Ile 185, Asp 186 (A-loop), Leu 44 and Lys 67 from hinge region of the PIM kinase ATP-domains (NTD and CTD). For the chemotherapy ligands (Vincristine and Daunorubicin) the hydrophobic contacts are present in Leu 120 (entry point), Glu 89, Ala 65, Gly 48, from hinge region, Ile 185 (A-loop), and Phe 49, Val 52, Asp 128, Lys 169, Glu 171 (G-loop) as showed in the 2D-Lig-plot diagrams (Supplementary material SM01 and SM02). It is important to highlight that the interactions of the three ligands evaluated with Phe 49-PIM1 residue could have important implications for the mechanism of inhibition of the enzyme. In view of the fact that Phe 49 is involved in the conformational change in the G-loop and A-loop regions through Phe 49 flip according to the pharmacodynamic patterns of interaction that other similar ATP-mimetic PIM1-inhibitors (ATP-competitive inhibitors) (Keeton et al., 2014).

Particularly, for the AZD1208 ligand where the two aromatic rings are less sterically impeded than the Daunorubicin and Vincristine and contributing more significantly to establishing  $\pi$ - $\pi$  hydrophobic interactions with the Phe 49 residue from PIM-1. By the other hand, the presence of hydrogen bond contacts (H-bonds) was

quantitatively different for the three PIM-1 -ligands (AZD1208, Vincristine and Daunorubicin) compared with the ATP molecule (SM01). However, molecular docking results indicates the H-bonds interactions with Lys67 and Asp 186 contribute mainly to the inhibitory activity of PIM-1 inhibitors (Aouidate et al., 2018).

Besides, other interactions contribute to the thermodynamic stability of the formed ligand-PIM-1 complexes following a more heterogeneous pattern of interactions affinity based on non-covalent hydrogen-bond and electrostatic interaction in the ATP-binding site. The results of docking simulations are depicted in the **Figure 6**.

Furthermore, we evaluate the other relevant mechanisms of docking interaction of the aforementioned PIM-1 -ligands with phosphorylation regulatory binding residues. In this regard, we detected high proximity based on inter-atomic distances ( $< 7 \text{ \AA}$ ) of the atoms of PIM-1-ligands (AZD1208, Daunorubicin and Vincristine) with serine regulatory phosphorylation residues like Ser 46, Ser 51, and Ser 54. This distance was chosen because interatomic distances lower than  $7 \text{ \AA}$  imply a high probability of interaction in terms of Gibbs free energy of binding and low probability of obtaining false contacts in the formed docking complexes (Da Silveira et al., 2009) (Xie and Hwang, 2010) .

The inhibition mechanisms of PIM1 are still largely unknown. In this regard, we show that the pharmacological docking-mechanism of AZD1208 is mainly based on hydrophobic interactions with ATP-active binding-site residues with more strong interaction-based negative free energy than the ATP-ligand (a native physiological PIM1 substrate). These *in silico* results fit with the pharmacodynamic patterns of other similar ATP-competitive inhibitors (REN et al., 2011). Besides, and the chemotherapeutic ligand tested like Vincristine and Daunorubicin can theoretically interact in the same biophysical

environment increasing the probability to induce pharmacodynamic interaction in the ATP-binding site from PIM-1 kinase.

Generally, more than one type of chemotherapeutic agent is used in chemotherapy. Our work shows the importance of testing new inhibitors of oncogenes associated with different chemotherapeutics in order to analyze the pharmacodynamic interactions that may occur between them. The competition for the same active site may inhibit the cytotoxic action of chemotherapeutics, which results in resistance to multiple drugs and consequently low prognosis of patients in the treatment of cancer. Concluding, these *in silico* evidences could explain the loss of activity of AZD1208, when there is interaction with chemotherapeutic agents, as observed in the *in vitro* study. Lastly, the current *in silico* results may have a potential pre-clinical relevance in the rational drugs-design and to understand the impact of poly-pharmacology strategies using PIM-1 inhibitors in the context of human leukemia cancer therapy.

### **Acknowledgements**

We thank the Institute of Medical Biochemistry Leopoldo de Meis from the Federal University of Rio de Janeiro (UFRJ) for providing the cell lines used in this study. This study was financed in part by the Coordenação de Aperfeiçoamento de Pessoal de Nível Superior - Brasil (CAPES) - Finance Code 001. This study was carried out in the Post-Graduate Program in Physiological Sciences. L. F. M is a research fellow from CNPq (Proc. No. 305928/2015-5).

### **Conflicts of interest**



The authors declare that they have no competing interests

## References

- Amson, R., Sigaux, F., Przedborski, S., Flandrin, G., Givol, D., Telerman, A., 1989. The human protooncogene product p33pim is expressed during fetal hematopoiesis and in diverse leukemias. *Proc. Natl. Acad. Sci.* 86, 8857–8861.  
<https://doi.org/10.1073/pnas.86.22.8857>
- Aouidate, A., Ghaleb, A., Ghamali, M., Ousaa, A., Choukrad, M., Sbai, A., Bouachrine, M., Lakhlifi, T., 2018. 3D QSAR studies, molecular docking and ADMET evaluation, using thiazolidine derivatives as template to obtain new inhibitors of PIM1 kinase. *Comput. Biol. Chem.* 74, 201–211.  
<https://doi.org/10.1016/j.compbiolchem.2018.03.008>
- Bachmann, M., Möröy, T., 2005. The serine/threonine kinase Pim-1. *Int. J. Biochem. Cell Biol.* 37, 726–730. <https://doi.org/10.1016/j.biocel.2004.11.005>
- Chen, V.B., Arendall, W.B., Headd, J.J., Keedy, D.A., Immormino, R.M., Kapral, G.J., Murray, L.W., Richardson, J.S., Richardson, D.C., 2010. MolProbity: All-atom structure validation for macromolecular crystallography. *Acta Crystallogr. Sect. D Biol. Crystallogr.* 66, 12–21. <https://doi.org/10.1107/S0907444909042073>
- Cheng, H., Huang, C., Xu, X., Hu, X., Gong, S., Tang, G., Song, X., 2017. PIM - 1 mRNA expression is a potential prognostic biomarker in acute myeloid leukemia. *J. Transl. Med.* 1–9. <https://doi.org/10.1186/s12967-017-1287-4>
- Cohen, A.M., Grinblat, B., Bessler, H., Kristt, D.A., Kremer, A., Shalom, S., Schwartz, A., Halperin, M., Merkel, D., Don, J., 2004. Increased Expression of the *hPim-2* Gene In

- Human Chronic lymphocytic Leukemia and Non-Hodgkin Lymphoma. *Leuk. Lymphoma* 45, 951–955. <https://doi.org/10.1080/10428190310001641251>
- Da Silveira, C.H., Pires, D.E.V., Minardi, R.C., Ribeiro, C., Veloso, C.J.M., Lopes, J.C.D., Meira, W., Neshich, G., Ramos, C.H.I., Habesch, R., Santoro, M.M., 2009. Protein cutoff scanning: A comparative analysis of cutoff dependent and cutoff free methods for prospecting contacts in proteins. *Proteins Struct. Funct. Bioinforma.* 74, 727–743. <https://doi.org/10.1002/prot.22187>
- Daflon-Yunes, N., Pinto-Silva, F.E., Vidal, R.S., Novis, B.F., Berguetti, T., Lopes, R.R.S., Polycarpo, C., Rumjanek, V.M., 2013. Characterization of a multidrug-resistant chronic myeloid leukemia cell line presenting multiple resistance mechanisms. *Mol. Cell. Biochem.* 383, 123–35. <https://doi.org/10.1007/s11010-013-1761-0>
- Dakin, L.A., Block, M.H., Chen, H., Code, E., Dowling, J.E., Feng, X., Ferguson, A.D., Green, I., Hird, A.W., Howard, T., Keeton, E.K., Lamb, M.L., Lyne, P.D., Pollard, H., Read, J., Wu, A.J., Zhang, T., Zheng, X., 2012. Discovery of novel benzylidene-1,3-thiazolidine-2,4-diones as potent and selective inhibitors of the PIM-1, PIM-2, and PIM-3 protein kinases. *Bioorganic Med. Chem. Lett.* 22, 4599–4604. <https://doi.org/10.1016/j.bmcl.2012.05.098>
- de Ruyck, J., Brysbaert, G., Blossey, R., Lensink, M.F., 2016. Molecular docking as a popular tool in drug design, an in silico travel. *Adv. Appl. Bioinform. Chem.* 9, 1–11. <https://doi.org/10.2147/AABC.S105289>
- Ellwood-Yen, K., Graeber, T.G., Wongvipat, J., Iruela-Arispe, M.L., Zhang, J., Matusik, R., Thomas, G. V., Sawyers, C.L., 2003. Myc-driven murine prostate cancer shares

molecular features with human prostate tumors. *Cancer Cell* 4, 223–238.

[https://doi.org/10.1016/S1535-6108\(03\)00197-1](https://doi.org/10.1016/S1535-6108(03)00197-1)

Feinstein, W.P., Brylinski, M., 2015. Calculating an optimal box size for ligand docking and virtual screening against experimental and predicted binding pockets. *J. Cheminform.* 7, 18. <https://doi.org/10.1186/s13321-015-0067-5>

<https://doi.org/10.1186/s13321-015-0067-5>

Forli, S., Huey, R., Pique, M.E., Sanner, M., Goodsell, D.S., Arthur, J., 2016. HHS Public Access 11, 905–919. <https://doi.org/10.1038/nprot.2016.051>. Computational

Housman, G., Byler, S., Heerboth, S., Lapinska, K., Longacre, M., Snyder, N., Sarkar, S., 2014. Drug Resistance in Cancer: An Overview. *Cancers (Basel)*. 6, 1769–1792.

<https://doi.org/10.3390/cancers6031769>

Isaac, M., Siu, A., Jongstra, J., 2011. The oncogenic PIM kinase family regulates drug resistance through multiple mechanisms. *Drug Resist. Updat.* 14, 203–211.

<https://doi.org/10.1016/j.drug.2011.04.002>

Jiménez, J., Doerr, S., Martínez-Rosell, G., Rose, A.S., De Fabritiis, G., 2017. DeepSite: Protein-binding site predictor using 3D-convolutional neural networks. *Bioinformatics* 33, 3036–3042. <https://doi.org/10.1093/bioinformatics/btx350>

<https://doi.org/10.1093/bioinformatics/btx350>

Keeton, E.K., Mceachern, K., Dillman, K.S., Palakurthi, S., Cao, Y., Grondine, M.R., Kaur, S., Wang, S., Chen, Y., Wu, A., Shen, M., Gibbons, F.D., Lamb, M.L., Zheng, X., Stone, R.M., Deangelo, D.J., Plataniias, L.C., Dakin, L. a, Chen, H., Lyne, P.D., Huszar, D., 2014. AZD1208 , a potent and selective pan-Pim kinase inhibitor , demonstrates efficacy in preclinical models of acute myeloid leukemia. *Blood* 123, 905–914. <https://doi.org/10.1182/blood-2013-04-495366>. The

Kim, S., Thiessen, P.A., Bolton, E.E., Chen, J., Fu, G., Gindulyte, A., Han, L., He, J., He, S., Shoemaker, B.A., Wang, J., Yu, B., Zhang, J., Bryant, S.H., 2016. PubChem substance and compound databases. *Nucleic Acids Res.* 44, D1202–D1213.

<https://doi.org/10.1093/nar/gkv951>

Laskowski, R.A., Swindells, M.B., 2011. LigPlot+: Multiple Ligand–Protein Interaction Diagrams for Drug Discovery. *J. Chem. Inf. Model.* 51, 2778–2786.

<https://doi.org/10.1021/ci200227u>

Lee, M., Lee, K.-H., Min, A., Kim, J., Kim, S., Jang, H., Lim, J.M., Kim, S.H., Ha, D.-H., Jeong, W.J., Suh, K.J., Yang, Y.-W., Kim, T.Y., Oh, D.-Y., Bang, Y.-J., Im, S.-A., 2018. Pan-Pim Kinase Inhibitor AZD1208 Suppresses Tumor Growth and Synergistically Interacts with Akt Inhibition in Gastric Cancer Cells. *Cancer Res. Treat.* <https://doi.org/10.4143/crt.2017.341>

Lee, S.J., Han, B.G., Cho, J.W., Choi, J.S., Lee, J., Song, H.J., Koh, J.S., Lee, B. II, 2013. Crystal Structure of Pim1 Kinase in Complex with a Pyrido[4,3-D]Pyrimidine Derivative Suggests a Unique Binding Mode. *PLoS One* 8, 1–7.

<https://doi.org/10.1371/journal.pone.0070358>

Lee, T.-J., Kim, O.H., Kim, Y.H., Lim, J.H., Kim, S., Park, J.-W., Kwon, T.K., 2006. Quercetin arrests G2/M phase and induces caspase-dependent cell death in U937 cells. *Cancer Lett.* 240, 234–42. <https://doi.org/10.1016/j.canlet.2005.09.013>

Lozzio, C.B., Information, B.B.L., Society, A., Dc, W., Society, T.A., 2012. Human chronic myelogenous leukemia cell-line with positive Philadelphia chromosome 321–334.

- Mazzacurati, L., Lambert, Q.T., Pradhan, A., Griner, L.N., Huszar, D., Reuther, G.W.,  
2015. The PIM inhibitor AZD1208 synergizes with ruxolitinib to induce apoptosis of  
ruxolitinib sensitive and resistant JAK2-V617F-driven cells and inhibit colony  
formation of primary MPN cells. *Oncotarget* 6.  
<https://doi.org/10.18632/oncotarget.5653>
- Mitternacht, S., Berezovsky, I.N., 2011. Coherent conformational degrees of freedom as a  
structural basis for allosteric communication. *PLoS Comput. Biol.* 7.  
<https://doi.org/10.1371/journal.pcbi.1002301>
- Mizuno, K., Shirogane, T., Shinohara, A., Iwamatsu, A., Hibi, M., Hirano, T., 2001.  
Regulation of Pim-1 by Hsp90. *Biochem. Biophys. Res. Commun.* 281, 663–669.  
<https://doi.org/10.1006/bbrc.2001.4405>
- Mumenthaler, S.M., Ng, P.Y.B., Hodge, A., Bearss, D., Kanekal, S., Redkar, S., Taverna,  
P., Agus, D.B., 2010. NIH Public Access. *Mol. Cancer* 8, 2882–2893.  
<https://doi.org/10.1158/1535-7163.MCT-09-0293>.Pharmacological
- Nawijn, M.C., Alendar, A., Berns, A., 2011. For better or for worse: The role of Pim  
oncogenes in tumorigenesis. *Nat. Rev. Cancer* 11, 23–34.  
<https://doi.org/10.1038/nrc2986>
- Niu, N., Wang, L., 2015. *In vitro* human cell line models to predict clinical response to  
anticancer drugs. *Pharmacogenomics* 16, 273–285. <https://doi.org/10.2217/pgs.14.170>
- Ren, J.X., Li, L.L., Zheng, R.L., Xie, H.Z., Cao, Z.X., Feng, S., Pan, Y.L., Chen, X., Wei,  
Y.Q., Yang, S.Y., 2011. Discovery of novel Pim-1 kinase inhibitors by a hierarchical  
multistage virtual screening approach based on svm model, pharmacophore, and

molecular docking. *J. Chem. Inf. Model.* 51, 1364–1375.

<https://doi.org/10.1021/ci100464b>

Rumjanek, V.M., Trindade, G.S., Wagner-Souza, K., Meletti-De-Oliveira, M.C., Marques-Santos, L.F., Maia, R.C., Capella, M.A.M., 2001. Multidrug resistance in tumour cells: Characterisation of the multidrug resistant cell line K562-Lucena 1. *An. Acad. Bras. Cienc.* 73, 56–69. <https://doi.org/10.1590/S0001-37652001000100007>

Shay, K.P., Wang, Z., Xing, P.-X., Mckenzie, I.F.C., Magnuson, N.S., 2005. Pim-1 Kinase Stability Is Regulated by Heat Shock Proteins and the Ubiquitin-Proteasome Pathway. *Mol Cancer Res* 3, 170–81. <https://doi.org/10.1158/1541-7786.MCR-04-0192>

Stefano Forli, Ruth Huey, Michael E Pique, Michel F Sanner, D.S.G.& A.J.O., Department, 2016. Computational protein–ligand docking and virtual drug screening with the AutoDock suite. *Nat. Methods* 13, 515–520. <https://doi.org/10.1038/nmeth.3838>

Trott, O., Olson, A.J., 2009. AutoDock Vina: Improving the speed and accuracy of docking with a new scoring function, efficient optimization, and multithreading. *J. Comput. Chem.* 30, NA-NA. <https://doi.org/10.1002/jcc.21334>

TURSYNBAY, Y., ZHANG, J., LI, Z., TOKAY, T., ZHUMADILOV, Z., WU, D., XIE, Y., 2016. Pim-1 kinase as cancer drug target: An update. *Biomed. Reports* 4, 140–146. <https://doi.org/10.3892/br.2015.561>

Xie, Y., Xu, K., Linn, D.E., Yang, X., Guo, Z., Shimelis, H., Nakanishi, T., Ross, D.D., Chen, H., Fazli, L., Gleave, M.E., Qiu, Y., 2008. The 44-kDa Pim-1 kinase phosphorylates BCRP/ABCG2 and thereby promotes its multimerization and drug-

resistant activity in human prostate cancer cells. *J. Biol. Chem.* 283, 3349–3356.

<https://doi.org/10.1074/jbc.M707773200>

Xie, Z.R., Hwang, M.J., 2010. An interaction-motif-based scoring function for protein-ligand docking. *BMC Bioinformatics* 11. <https://doi.org/10.1186/1471-2105-11-298>

## CAPTIONS

**Figure 1.** Cell viability (%) measured by MTT assay 24h, 48h and 72h after treatment with 1 $\mu$ M of AZD1208, or 60nM of VCR or 300  $\mu$ M of DNR in K562, non-MDR (**A**), Lucena (**B**) and FEPS (**C**) cells (MDR cells). The group control received 0.01% of DMSO. The data are expressed as the mean + standard error. Graphs represent mean  $\pm$ SD of three biologic replicates. \*,  $P \leq 0.05$ ; \*\*,  $P \leq 0.01$ .

**Figure 2.** Evaluation of P-glycoprotein activity by Rhodamine 123 (Rho) dye extrusion. The Lucena cell line received 1 $\mu$ M of AZD1208, or 60 nM of VCR (**A**) or both co-treatments. To FEPS cell line (**B**), received 1 $\mu$ M of AZD1208 or 300 nM of DNR or both co-treatments for 24 h. The group control received 0.01% of DMSO. The results are expressed as means  $\pm$  S.E.M. Different letters indicate significant differences between means compared to the control group of each cell line ( $p < 0.05$ ).

**Figure 3.** **A)** Representation of x-ray crystallographic molecular structure model from human PIM-1 kinase showing the topological cavities of PIM-1 binding-sites as volumetric orange regions depicted-like Van der Waals surface representation. **B)** Cartoon representation of the main topological cavities of PIM-1 kinase active binding-sites (ATP binding site) and allosteric binding-sites. **C)** Representation of the two main PIM1 kinase

domains as N-terminal domain (NTD: green) and C-terminal domain (CTD: yellow) highlighting the ATP binding-site (marked in red rectangle). **D)** Structural details of ATP binding-site formed by hinge region (purple Van der Waals surface), glycine-rich loop (G-loop: yellow Van der Waals surface), activation loop (A-loop: dark pink Van der Waals surface), the catalytic loop (orange Van der Waals surface) and the PIM1 kinase entry point (Leu 120: red spheres).

**Figure 4. A)** Representation of Ramachandran diagrams and spatial distribution of Ramachandran outliers (none) in the modeled pdb x-ray structure of human PIM-1 kinase. All the possible combinations of dihedral angles of torsion like Psi *versus* Phi of each amino acid residues of PIM-1 kinase are showed. **B)** Results of Ramachandran plot quality assessment (PIM-1 kinase model quality) is measured by the percentage of the PIM-1 kinase-residues that are in the most favored, or core, regions of the Ramachandran plot *versus* resolution (Å). For this instance, is showed a good model structure for PIM-1 kinase, modeled with high resolution of 1.8 Å, with expected percentage of favored region (including the PIM-1 kinase ATP-binding pocket) over 98% (red dotted line).

**Figure 5. A)** Representation of PIM-1 kinase flexibility properties highlighting the ATP-active binding-site (red rectangle). The 3D-colored structure is based on the size of fluctuations-driven by the slowest vibration-modes from PIM-1 kinase-residues from low-flexibility (blue) to high-flexibility (red). **B)** Van der Wall surface representation of the unoccupied ATP-binding-site from PIM-1 kinase. **C)** Van der Wall surface representation of the ATP-PIM-1 kinase docking complex in the ATP-binding-site from PIM-1 kinase like control simulation in the Van der Waals surfaces (red is acidic, blue is basic PIM-1



residues). **D)** Validation-based Ramachandran diagrams for each PIM-1 kinase residue involved in the ATP-docking interaction with the PIM-1 kinase binding-site obtained from 2D Lig-Plot interaction diagrams. Please note that all residues analyzed are conformationally-favored PIM-1 -residues according to the presence in the light green contour into the individual Ramachandran plot.

**Figure 6.** Van der Wall surface representation of PIM-1 -ligand docking complexes in the ATP-binding site considering the best docking pose (RMSD < 2Å) like: **A)** AZD1208-PIM-1 kinase complex (ligand with red label), **B)** Daunorubicin-PIM-1 kinase complex (ligand with yellow label), **C)** Vincristine-PIM-1 kinase complex (ligand with light-blue label). **D)** Superimposed PIM-1 kinase-ligand docking complexes in the ATP-binding site (red, yellow and light blue like AZD1208, Daunorubicin and Vincristine respectively). **E)** Representation of PIM-1 kinase considering dynamic functional properties from residues clusters ATP-binding site linked to their ability to act as allosteric or effector residues. **F)** Superimposed PIM-1 kinase-ligand docking complexes (AZD1208, Daunorubicin and Vincristine) showing a tendency to interact with effector residues in the ATP-binding site according to the bar color (from orange to red).

**Figure 7.** **A)** Cartoon representation of the ATP-binding domain in PIM-1. **B)** The following map show the matrix of perturbations site (j)-residues vs. (i)-response site based on strength of response (as indicated by the scales on the right of the maps) for all PIM-1 residue pairs (i, j) from the unoccupied ATP-binding domain. The strength of communication is measured between perturbations site in (j)-allosteric residues vs.

response triggered by the (i)-effector residues. The blue to orange regions correspond to weak to moderate strength of inter-residue communication (weak cross correlation) between two (i, j)-residues, and the orange to dark red regions represent strong inter-residue communication (high cross correlation) with high propensity to local-perturbation induced by ligand docking interactions like **C**) ATP-PIM-1 kinase docking complex, **D**) AZD1208-PIM-1 kinase docking complex, Daunorubicin-PIM-1 kinase docking complex, and Vincristine-PIM-1 kinase docking complex.

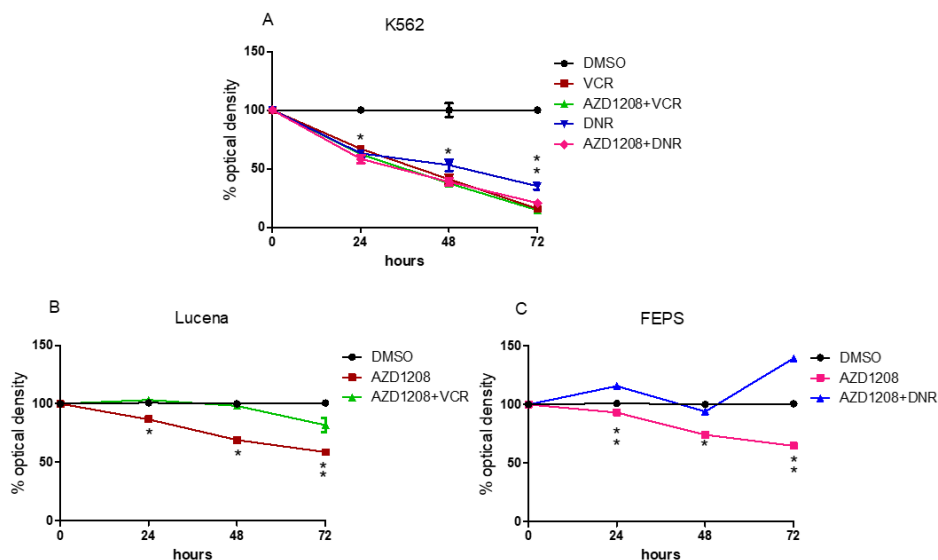


Figure 1

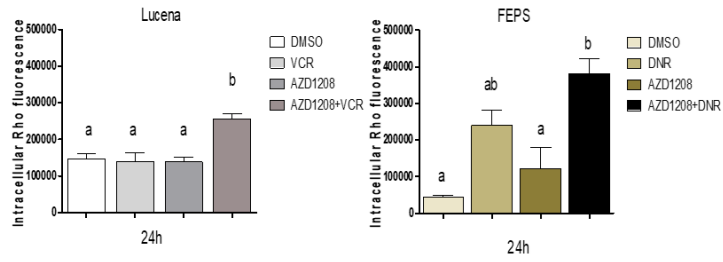


Figure 2

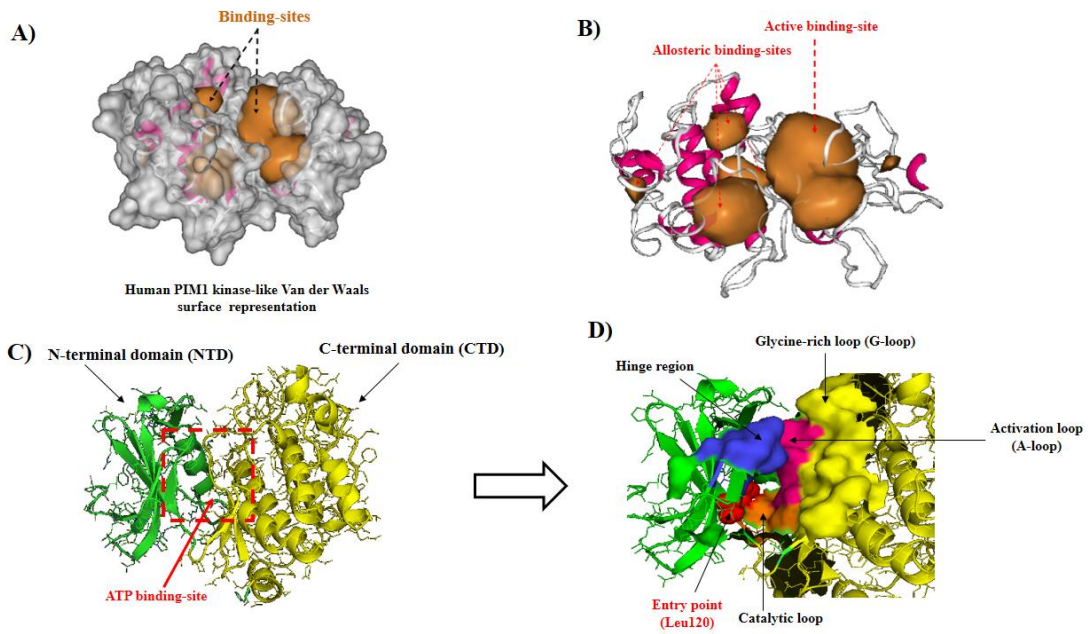


Figure 3

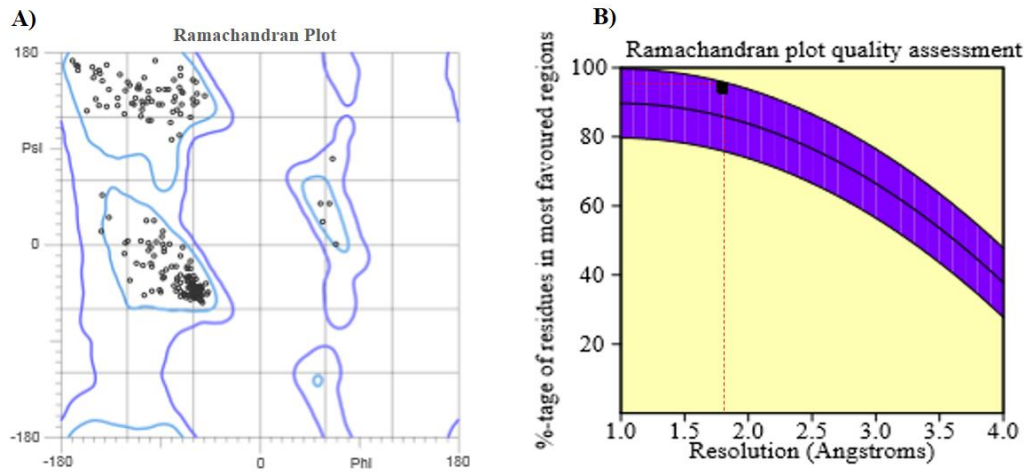


Figure 4

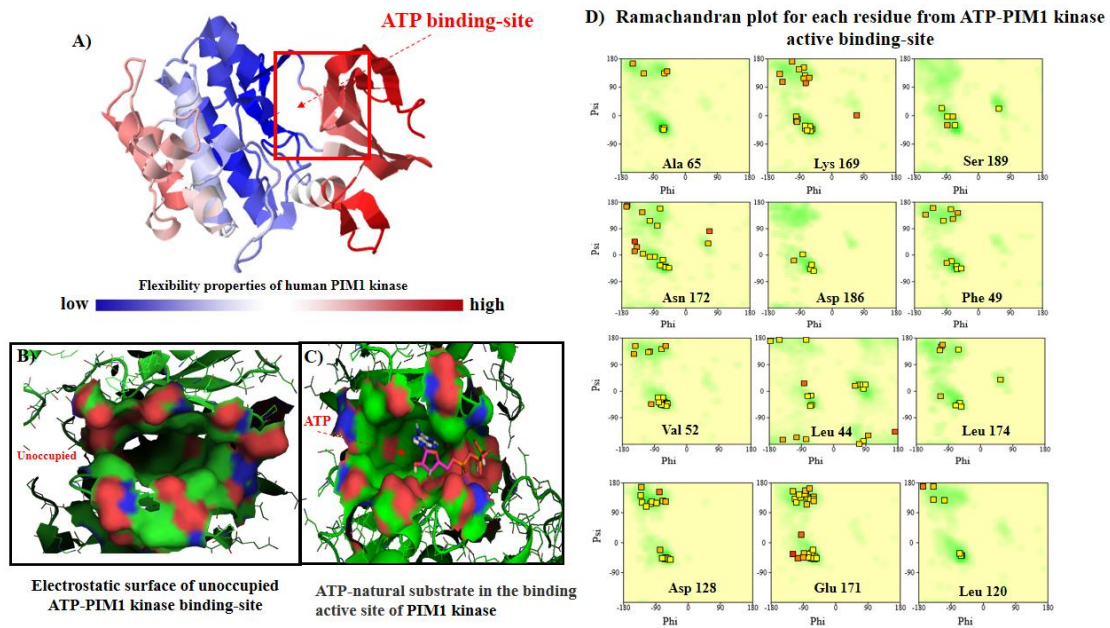


Figure 5

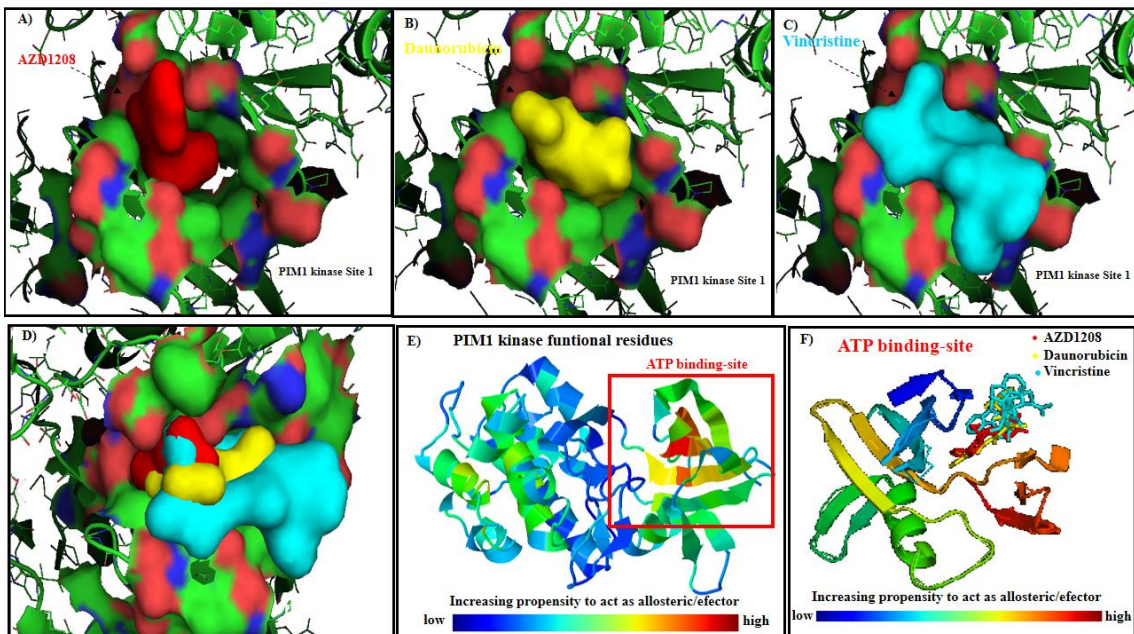
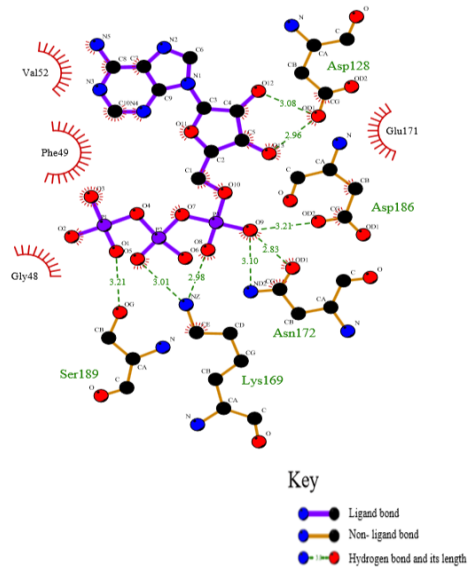
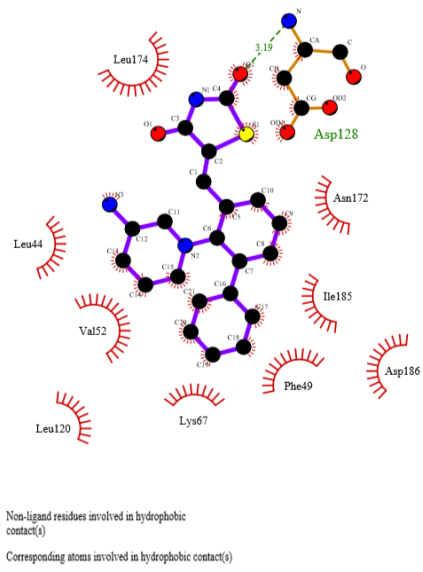


Figure 6

A) ATP-PIM-1\_Lig-Plot interaction diagram

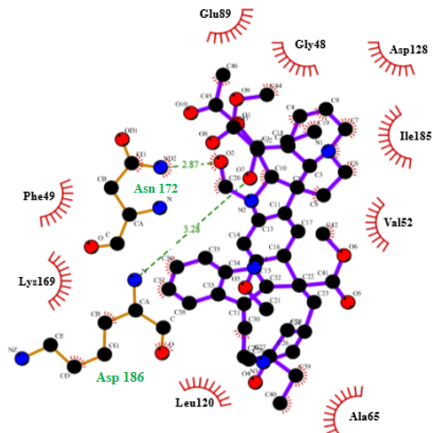


B) AZD1208-PIM-1\_Lig-Plot interaction diagram

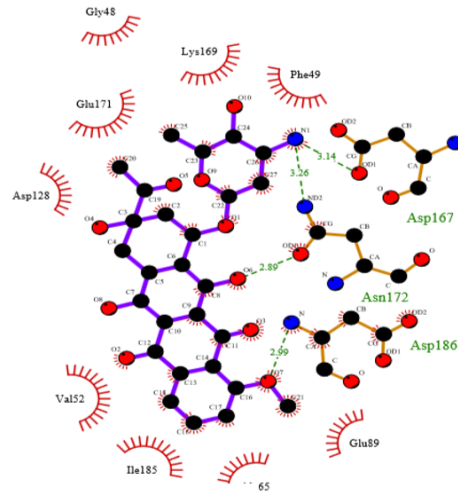


supplementary figure 1

C) Vincristine-PIM-1\_Lig-Plot interaction diagram



D) Daunorubicin-PIM-1\_Lig-Plot interaction diagram



Key

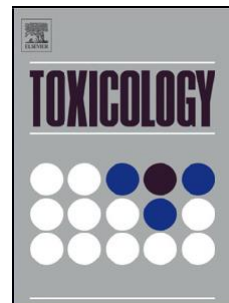
- Ligand bond
- Non-ligand bond
- Hydrogen bond and its length
- Non-ligand residues involved in hydrophobic contact(s)
- Corresponding atoms involved in hydrophobic contact(s)

supplementary figure 3

### 3.3 Artigo 3

## Accepted Manuscript

Title: Modeling Drug-Drug Interactions of AZD1208 with Vincristine and Daunorubicin on Ligand-Extrusion Binding TMD-Domains of multidrug resistance P-glycoprotein (ABCB1)



Authors: Maiara Bernardes Marques, Patricia Viera de Oliveira, Solange Binotto Fagan, Bruno Rodrigues Oliveira, Bruna Félix da Silva Nornberg, Daniela Volcan Almeida, Luis Fernando Marins, Michael González-Durruthy

PII: S0300-483X(18)30194-X  
DOI: <https://doi.org/10.1016/j.tox.2018.10.009>  
Reference: TOX 52110

To appear in: *Toxicology*

Received date: 26-7-2018  
Revised date: 3-10-2018  
Accepted date: 14-10-2018

Please cite this article as: Marques MB, de Oliveira PV, Fagan SB, Oliveira BR, da Silva Nornberg BF, Volcan Almeida D, Marins LF, González-Durruthy M, Modeling Drug-Drug Interactions of AZD1208 with Vincristine and Daunorubicin on Ligand-Extrusion Binding TMD-Domains of multidrug resistance P-glycoprotein (ABCB1), *Toxicology* (2018), <https://doi.org/10.1016/j.tox.2018.10.009> This is a PDF file of an unedited manuscript that has been accepted for publication.

As a service to our customers we are providing this early version of the manuscript. The manuscript will undergo copyediting, typesetting, and review of the resulting proof before it is published in its final form. Please note that during the production process errors may be discovered which could affect the content, and all legal disclaimers that apply to the journal pertain.



Manuscript submitted to Toxicology

Modeling Drug-Drug Interactions of AZD1208 with  
Vincristine and Daunorubicin on Ligand-Extrusion Binding  
TMD-Domains of multidrug resistance P-glycoprotein  
(ABCB1)

Maiara Bernardes Marques<sup>a,\*</sup>, Patricia Viera de Oliveira<sup>b</sup>, Solange  
Binotto Fagan<sup>b</sup>, Bruno Rodrigues Oliveira<sup>a</sup>, Bruna Félix da Silva  
Nornberg<sup>a</sup>, Daniela Volcan Almeida<sup>a</sup>, Luis Fernando Marins<sup>a</sup>,  
Michael González-Durruthy<sup>c,\*</sup>

<sup>a</sup>Laboratory of Molecular Biology, Institute of Biological Sciences,  
Post-Graduation Program in Physiological Sciences, Federal  
University of Rio Grande -FURG, Rio Grande, RS, Brazil.

<sup>b</sup>Post-Graduate Program in Nanoscience- Franciscana University-UFN, RS, Brazil.

<sup>c</sup>Department of Chemistry and Biochemistry, Faculty of Science,  
University of Porto, Porto, Portugal,

\*Correspondence: Institute of Biological Sciences, Post-Graduation Program in  
Physiological Sciences, Federal University of Rio Grande -FURG,  
Rio Grande, Brazil. Phone: +55 53 32336850. Email:  
mai.mbio@gmail.com; Department of Chemistry and Biochemistry,  
Faculty of Science, University of Porto, Porto, Portugal.  
Phone:

+351920276152. Email: michael.durruthy@fc.up.pt

Highlights:

- We present an innovative 3D structure model of the TMDs of ABCB1;
- *in silico* approaches were performed using molecular docking and DTF-*ab initio*;
- This work corroborates with the ethical standards in Toxicology (principle of 3R)
- The study of drug-drug interaction is crucial to the chemotherapy success;

**ABBREVIATIONS:** ABCB1 multiple-drugs resistance P-glycoprotein; AZD1208: PIM inhibitor; DNR: daunorubicin; DTF: Density Functional Theory; NBD: nucleotide binding domain; PIM: proto-oncogene serine/threonine-protein kinase; PDB: Protein data bank; RDD: rational drugs-design; TMD: transmembrane domains; VCR: vincristine; VP: verapamil;

## ABSTRACT

In the present study, the molecular docking mechanism based on pharmacodynamic interactions between the ligands AZD1208 and recognized chemotherapy agents (Vincristine and Daunorubicin) with human ATP-binding cassette (ABC) transporters (ABCB1) was investigated. For the first time, we combined an *in silico* approaches like molecular docking and *ab initio* computational simulation based on Density Functional Theory (DFT) to explain the drug-drug interaction mechanism of aforementioned chemotherapy ligands with the transmembrane ligand extrusion binding domains (TMDs) of ABCB1. In this regard, the theoretical pharmacodynamic interactions were characterized by using the Gibbs free energy (FEB, Kcal/mol) from the best ABCB1-ligand docking complexes. The molecular docking results pointing that for the three chemotherapy ABCB1-ligand complexes are mainly based in non-covalent hydrophobic and hydrogen-bond interactions showing a similar toxicodynamic behavior in terms of strength of interaction (FEB, Kcal/mol) and very close free binding energies when compared with the FEB-values of the ABCB1 specific-inhibitor (Rhodamine B) = - 6.0 Kcal/mol used as theoretical docking control to compare with FEB (AZD1208-ABCB1) ~ FEB (Vincristine-ABCB1) ~ FEB (Daunorubicin-ABCB1) - 6.2 Kcal/mol as average. Ramachandran plot suggests that the 3D-crystallographic structure from ABCB1 transporter can be efficiently-modeled with conformationally-favored Psi *versus* Phi dihedral angles for all key TMDs-residues. Though, the results of DFT-simulation corroborate the existence of drug-drug interaction between (AZD1208/Vincristine) > (AZD1208/Daunorubicin). These theoretical pieces of evidence

have preclinical relevance potential in the design of the new drugs to understand the polypharmacology influence in the molecular mechanism of multiple-drugs resistance, contributing with a higher success in chemotherapy and prognosis of cancer patients.

**Keywords:** ABC transporters; pharmacodynamic; molecular docking; DFT- simulation

## 1. INTRODUCTION

Cancer disease is recognized as a second most lethal pathology in the world after heart disease based on its high morbidity/mortality rates. According to the National Cancer Institute (NIH) the cancer is defined as a collection of diseases in which abnormal cells can divide and invade other tissues, causing metastasis (Roser et al., 2018). In this regard, multiple efforts have been performed to elucidate the mechanisms that confer simultaneous resistance to different chemotherapeutic drugs, with different targets and versatile chemical structures during the last 35 years. Therefore, it is clear that resistance to chemotherapy is one of the main factor of lack of success in cancer treatment (Gottesman et al., 2002)(Holohan et al., 2013).

In this context, ATP-binding cassette (ABC)-transporters constitute a large superfamily of integral membrane transport proteins that are directly involved in the mechanism of multiple-drugs resistance due to their main-function as ligand-extrusion. One of most widely studied (ABC)-transporters is the P-glycoprotein ABCB1 which is about 170 KDa, encoded by the MDR1/ABCB1 gene (Gottesman and Ling, 2006). The ABCB1 overexpression results in the active efflux of chemotherapeutic drugs, resulting in low therapeutic efficacy due to low pharmacokinetic bioavailability of many chemotherapeutic drugs in several types of human cancers (Szakács et al., 2006) According to this idea, from the structural-function point of view ABCB1 protein, transduces the ATP-gained from ATP-hydrolysis to translocate substrates (drugs) into the cancer cell cytoplasm (drugs-import

mechanism) or out of the cytoplasm (drugs-extrusion mechanism) (Chen et al., 2003) (Davidson and Chen, 2004). The drugs-import molecular mechanism is catalyzed by ATP hydrolysis in the named nucleotide-binding sub-domains (NBDs) from ABCB1. While the drugs-extrusion is facilitated by a pair of transmembrane domains (TMDs) in a unidirectional way from a central cavity between the TMDs facing outward. Herein, structurally conserved  $\alpha$ -helices, which are part of the TMDs domains, are present in all reported crystal structure of ATP-binding cassette (ABC)-transporters (drugs-extrusion domains) which are invariably fused to the NBDs (Jones and George, 2004) (Hollenstein et al., 2007) (Locher, 2009). Besides that, the discover new anti-cancer drugs that inhibit oncogenes like proto-oncogene serine/threonine-protein kinase (PIM), (Isaac et al., 2011) (Wang et al., 2001) (Santio et al., 2015) are being developed by combining several and accurately molecular modeling techniques for rational drugs-design (RDD) (Pogacic et al., 2007) (Asati et al., 2018) (Ren et al., 2011) (Li et al., 2016).

Several inhibitors of PIM kinase have been synthesized. Some quinone derivatives are being studied for treatment of prostate cancer (Li et al., 2016); others like imidazole [1,2] pyridazines have been described by the antiproliferative effects in acute leukemia (Pogacic et al., 2007). However, the multiple-drugs resistance induced by (ABC)-transporters continues to be a problem from the pharmacokinetics point of view to ensure the blood bioavailability and reduce adverse effects of many chemotherapeutic agents (PIM kinase inhibitors) (Pogacic et al., 2007)(Asati et al., 2018) (Ren et al., 2011)

In this context, one of the most potent PIM inhibitors is the AZD1208, that showed high efficacy in a preclinical model inhibiting cell growth and leading to apoptosis, by inhibiting the suppression of phosphorylation (p70S6K, 4EBP128) in patient samples with acute myeloid leukemia (Keeton et al., 2014), and other types of cancer as prostate (N. Kirschner et al., 2015) and hepatoblastoma (Stafman et al., 2018). However, studies

demonstrate that an AZD1208 has limited activity when used as a single agent. For this instance, AZD1208 showed a strong synergistic pharmacologic effect (cytotoxic activity) by combining with the AKT-inhibitor (like AZD5363) (Amson et al., 1989) (Meja et al., 2014).

Despite extensive studies of new PIM-inhibitors it is still unclear how the AZD1208 molecule interacts with multiple-drugs resistance protein (ABCB1) and how a concomitant pharmacodynamic interaction with other chemotherapeutic cancer-drugs could enhance the AZD1208-cytotoxicity regarding the ABCB1 inhibition (Keeton et al., 2014). Following this idea, multidisciplinary approaches supported on significant advances in emerging areas like Computational Toxicology and Chemoinformatics have allowed a better understanding of the molecular mechanisms of interaction and significantly reduce the use of animals in experimentation according to the ethical standards in Toxicology based on the principle of 3R (*Reduction, Refinement and Replacement* of animal testing) (Erkekoglu et al., 2011).

In this context, considering the complexity of the problem, we propose for the first time, the use of *in silico* tools based on docking and Density Functional Theory (*ab initio* DFT-simulation) which analyze the structural and electronic properties of a given system the as an efficient alternatives to explain the potential pharmacodynamic interactions of AZD1208 with recognized-chemotherapeutic drugs (like Vincristine and Daunorubicin) (Slater et al., 1986) in the TMDs-ligand extrusion binding domains (TMDs) of multiple-drugs resistance P-glycoprotein (ABCB1) protein, (Dawson et al., 2007) and in this way advance in understanding of the molecular mechanisms involved in the pharmacodynamic interactions toward to decrease the potential AZD1208-multiple cytotoxic drugs-resistance, improve its rational design previous to clinical use and increase the benefit/risk relationships in the human cancer therapies toward to “Precision Oncology” (Levi et al., 2013) (Salgado et al., 2018) (Sophia et al., 2018).

## 2. MATERIALS AND METHODS

## 2.1 Performed molecular docking simulation

To evaluate the binding-interaction between the human multiple-drugs resistance protein isoform 1 (ABC-transporter or ABCB1) (GenBank: NCBI Reference Sequence: NP\_001335874.1) and the different types of ABCB1-chemotherapy ligand substrates (AZD1208, Vincristine and Daunorubicin), molecular docking approach was performed. The first step consists of preparing the ABCB1-protein structure-file (receptor), which was obtained using Phyre2 Protein Fold Recognition Server as PDB x-ray structures model (Kelly et al., 2015). Before the docking experiments, ABCB1-protein structure was optimized using the AutoDock Tools 4 software for AutoDock Vina. The ABCB1-protein-hydrogen atoms were added, according to appropriate hybridization geometry, to those atoms based on built-in modules to add partial charges, protonation states followed by bond orders assignment and set up rotatable bonds of the ABCB1-protein like pdb x-ray crystallography-structure (Trott and Olson, 2010)(Forli et al., 2016).

In the second step, the different types of ABCB1-chemotherapy ligand structures, were obtained from Pubchem Data Base Chemical Structure Search as: Vincristine (PubChem CID: 5978), Daunorubicin (PubChem CID: 30323) and AZD1208 (PubChem CID: 58423153) (Kim et al., 2016). The optimization of all the ABCB1-chemotherapy ligand structures was performed using the MOPAC extension for geometry optimization based on the AM1-Hamiltonian method (Kramer et al., 1997) (Trott and Olson, 2010) (Forli et al., 2016) (de Ruyck et al., 2016) (Kim et al., 2016).

To evaluate the formed complexes like ABCB1-chemotherapy ligand interactions the Gibbs free energy of binding or affinity (FEB in Kcal/mol) was calculated from Autodock Vina flexible molecular docking, an open source software developed by Trott & Olson (2010). In this context, the ABCB1-chemotherapy ligand free energy of binding (FEB) were calculated using a scoring function which approximates the chemical potentials

( $\Delta G_{\text{bind}}$ ). To this end, the implemented  $\Delta G$  scoring function combines the knowledge-based potential and empirical information obtained from experimental binding affinity measurements with Autodock Vina scoring function using default Amber force-field parameters. Conformational relaxation (flexible docking) favors a significant gain of enthalpy of ABCB1-protein-ligand complexes non-associated with ligand intra-molecular deformation or vibrational decrease within ABCB1-protein active binding sites (Kramer et al., 1997) (Trott and Olson, 2010) (Forli et al., 2016) (de Ruyck et al., 2016) (Kim et al., 2016).

The potential ABCB1-active binding sites were previously predicted through DeepSite (freely available at [www.playmolecule.org](http://www.playmolecule.org)) (Jiménez et al., 2017). This step is defined as identifying and delimiting ABCB1-cavities, potentially at the Van der Waals surface that are likely to bind to a small ligand like Vincristine, Daunorubicin and AZD1208. For this instance, DeepSite analyses all the molecular descriptor related to protein (ABCB1-enzyme). The implementation of 3D-deep convolutional neural networks (DCNNs) was validate using deep learning library with an extensive test set based on more than 7000 proteins of the scPDB database (Kellenberger et al., 2006) (Jiménez et al., 2017). The ABCB1 binding-pocket predictions as well as the ABCB1-volumetric map prediction were determined to establish the cartesian coordinates of docking box simulation like ABCB1-grid box size, with dimensions of  $X=40 \text{ \AA}$ ,  $Y= 40 \text{ \AA}$ ,  $Z= 40 \text{ \AA}$  and the ABCB1- grid box center with dimension of  $X=-13.088 \text{ \AA}$ ,  $Y= 18.658 \text{ \AA}$ ,  $Z= -25.464 \text{ \AA}$  (Feinstein and Brylinski, 2015). Several runs starting from random conformations were carried out, and the iterations number in a run was adapted according with exhaustiveness parameter of 100 (average accuracy) in each docking calculation (Trott and Olson, 2010) (Forli et al., 2016) (Xie and Hwang, 2010).



The docking free energy of binding output results is defined by  $\Delta G_{\text{bind}}$  values for all docked poses of the formed complexes (ABCB1-ligands) and include the internal steric energy of a given ABCB-ligands (Vincristine, Daunorubicin and AZD1208) which can be expressed as the sum of individual molecular mechanics terms of standard-chemical potentials like: van der Waals interactions ( $\Delta G_{\text{vdW}}$ ), hydrogen bond ( $\Delta G_{\text{H-bond}}$ ), electrostatic interactions ( $\Delta G_{\text{electrost}}$ ), and intra-molecular ligands interactions ( $\Delta G_{\text{internal}}$ ) from empirically validated Autodock Vina scoring function based on default Amber force-field parameters. Furthermore, Autodock Vina scoring function considers optimal-linear free binding energy coefficients from experimentally determined chemical potentials ( $\Delta G_{\text{internal}}$ ) (Trott and Olson, 2010) (Forli et al., 2016). It is important to note that overall docking parameters are based on distance-dependent atom-pair interactions ( $d_{ij}$ ) according to the general thermodynamic equations depicted below:

(1)

$$FEB_{\text{dock}} \approx \Delta G_{\text{bind}} = \Delta G_{\text{vdW}} + \Delta G_{\text{H-bond}} + \Delta G_{\text{electrost}} + \Delta G_{\text{int}}$$

(2)

$$FEB_{\text{dock}} \approx \Delta G_{\text{bind}} = \Delta G_{\text{vdW}} \sum_{\text{lig-ABC}} \left( \frac{A_{ij}}{d_{ij}^{12}} - \frac{B_{ij}}{d_{ij}^6} \right) + \Delta G_{\text{H-bond}} \sum_{\text{lig-ABC}} E(t) \left( \frac{C_{ij}}{d_{ij}^{12}} - \frac{D_{ij}}{d_{ij}^{10}} \right) + \Delta G_{\text{elec}} \sum_{\text{lig-ABC}} \frac{q_i q_j}{(d_{ij}) d_{ij}} +$$

$$\Delta G_{\text{internal}} \left\{ \sum_{\text{lig}} \frac{A_{ii}}{d_{ii}^{12}} - \frac{B_{ii}}{d_{ii}^6} + \sum_{\text{lig}} E(t) \times \left( \frac{C_{ii}}{d_{ii}^{12}} - \frac{D_{ii}}{d_{ii}^{10}} \right) + \sum_{\text{lig}} \frac{q_i q_i}{4(d_{ii}) d_{ii}} + \sum_{\text{lig}_i} \gamma_k (1 + \cos(\varpi_k \theta_k - \theta_{0k})) \right\}$$

The  $\Delta G = -RT (\ln K_i)$ , R (gas constant) is  $1.98 \text{ cal} \cdot (\text{mol} \cdot \text{K})^{-1}$ , and  $K_i$  represents the predicted ABCB1-inhibition constants at  $T = 298.15 \text{ K}$ . The first term of a 12-6/Lennard-Jones potential describes the *van der Waals* binding-interaction as  $A_{ij}/d_{ij}^{12}$  and  $B_{ij}/d_{ij}^6$  (hyperbolic function or repulsion term) to represent a typical Lennard-Jones interactions

(ABCB1-ligands), provided the Gaussian term is negative and the parabolic positive,  $d_{ij}$  is the surface distance calculated as  $d_{ij} = r_{ij} - R_i - R_j$ , where  $r_{ij}$  is the interatomic distance and  $R_i$  and  $R_j$  are the radii of the atoms in the pair of interaction of ABCB1<sub>(i)</sub>-ligands<sub>(j)</sub> atoms.

The second term is the pair consisting of an H-bond donor and an H-bond acceptor as a directional 12-10 hydrogen-bonding potential term such as  $B_{ij}/d_{ij}^{12}$  and  $C_{ij}/d_{ij}^{10}$ , where  $E(t)$  is an angular weight factor which represents the directionality of the hydrogen bonds and  $d_{ij}$  follows the criteria mentioned above. The third term represents the Coulomb electrostatic potential stored in the formed complex (ABCB1-ligands)  $ij$  of  $N$  charges ( $q_i, q_j$ ) of pairs of charged atoms of ABCB1<sub>(i)</sub> and chemotherapy ligand structures<sub>(j)</sub>. For this purpose, appropriated Gasteiger partial atomic charges of the ABCB1-protein were assigned (Trott and Olson, 2010)(Forli et al., 2016). Herein,  $d_{ij}$  is the interatomic distance between the point charges as the reference positions of interaction based on distance-dependent dielectric constant. The fourth term of the equation (3) as ( $\Delta G_{\text{internal}}$ ) was used to validate the internal steric energy of each ABCB1-ligand including dispersion-repulsion energy and a torsional energy through the sum of the default Amber force field parameters (chemotherapy ligand conformation-independent parameters of the Autodock Vina scoring function (Trott and Olson, 2010).

Moreover, the electrostatic components were considered, and the ligand-partial atomic charges were properly assigned with the Gasteiger-Huckel algorithm using partial equalization of orbital electronegativities (PEOE) after the addition of polar and non-polar hydrogen atoms. Molecular docking dimensionality based on degree of freedom (DOF) of the each member of the ABCB1-ligand data set like: ligand-atom position/translation ( $x_i, y_i, z_i = 3$ ), ligand-atom orientation/quaternion ( $q(x_i), q(y_i), q(z_i), q(w_i) = 4$ ), ligand-number of rotatable bonds/torsion ( $\text{tor}_1, \text{tor}_2, \dots, \text{tor}_n = N_{\text{tor}}$ ) and ligand-total dimensionality (total DOF =  $3 + 4 + n$ ) not have a significant weight in the  $\text{FEB}_{\text{dock}}$  based on the very small intramolecular contributions of force field parameters of the ABCB1-ligand which were considered as rigid and considering the aforementioned ligand-geometry optimization based

on the  $\Delta G_{\text{internal}}$  minimization of all the ABCB1-ligands used in the present study (Trott and Olson, 2010) (Kramer et al., 1997).

ABCB1-ligand conformations with the lowest Gibbs docking free energy of binding (FEB negatives value) were obtained. The best root-mean-square deviation (RMSD) was considered as a criterion of correct docking-pose accuracy below 2Å according to the equation (3) (Trott and Olson, 2010)(Forli et al., 2016).

$$RMSD(\text{pose}_{i\text{-ligands}}, \text{pose}_{j\text{-ABC}}) = \sqrt{\frac{\sum (atom_{(i\text{-ligand})} - atom_{(j\text{-ABC})})^2}{n}} \quad (3)$$

Lastly, the next step consists of analyzing the interaction data obtained from the molecular docking with respect to the final free energy of binding (FEB values) for the ABCB1-ligand complexes of each docking simulation. Besides, the Rhodamine B-molecule was used as reference controls on ABCB1 active-binding pockets (Xie and Hwang, 2010)

## 2.2 Lig-Plot interactions diagrams

To determinate the relevant intermolecular interaction between chemotherapeutic-ligand (AZD1208, Vincristine and Daunorubicin) with the protein-receptor (ABCB1) the corresponding Lig-Plot analyses was performed. For this aim, a software named Lig-Plot, was used. This software evaluates is a software that evaluates the non-covalent intermolecular interactions that occur in a given ABCB1-chemotherapeutic ligand complex. Then, Lig-Plot automatically generates schematic 2D diagrams of interactions showing the type of interaction that took place like (hydrophobic, hydrogen bond and electrostatic interaction) for all the docking simulations and show details describing all the inter-atomic contacts (Laskowski and Swindells, 2011).

## 2.3 Drugs-drugs interactions of AZD1208 based on DFT-modeling

We carried out an *ab initio*-DFT approach to mimicking the pharmacodynamic interaction between two interacting systems like **1)** AZD1208/Vincristine, and **2)** AZD1208/Daunorubicin, which could be in the same biophysical environment after the docking interaction in the ABCB1-binding active site. To this purpose, the electronic and structural properties of the interacting systems were calculated like DFT-binding energy (eV), the Highest Occupied Molecular Orbital/Lowest Unoccupied Molecular Orbital difference usually recognized as HOMO/LUMO difference ( $\Delta H/L$ ) and the previously calculated interatomic distance  $D(\text{\AA})$  from docking simulation ( $d_{ij}$ ) were evaluated. For this goal, the *ab initio*-DFT approach was performed by using the SIESTA software (Spanish Initiative for Electronic Simulations with Thousands of Atoms) code that performs self-

consistent calculations to solve the Kohn-Sham equations (Soler et al., 2002)(Kohn and Sham, 1965). This system allow the simulation of many bodies, it is necessary to use some approaches such as the Born-Oppenheimer approximation, norm-conserving pseudopotential, supercell and base function (Perdew and Zunger, 1981). In all calculations, the local density approximation (LDA) was parameterized by Perdew and Zunger (1981). The work of Bevilaqua et al., (2010) was used to describe the exchange and correlation potential. The pseudopotential model was based on the work of Troullier and Martins (1991), and the orbitals were described with a set of DZP localized bases, cutting radius of 200 Ry for the mesh (grid) of the ABCB1-ligands real space of interaction. All interacting systems studied have a neutral charge in the electron configuration and their atomic structures were relaxed until the residual forces were less than 0.05 eV/Å for all the atoms in the system (Soler et al., 2002). To calculate DFT-binding energy between the molecules, we use the equation (4).

$$E_b = E[A+B]_{\text{total}} - E [A] - E [B] \quad (4)$$

Where  $E [A + B]_{\text{total}}$  is the total energy (eV) of the AZD1208 vs. ABCB1-chemotherapy ligands (Vincristine or Daunorubicin),  $E [A]$  total energy from isolated AZD

1208 system and  $E [B]$  is the energy from the isolated molecules (Vincristine or Daunorubicin).

### 3. RESULTS AND DISCUSSION

#### 3.1 The results of structural prediction/identification of the ABCB1 binding-site

An important task to ensure accuracy of theoretical docking data consists in the prediction of suitable ABCB1-active binding sites. Several algorithms for detecting protein-binding cavities have been performed over the years based on structural, geometric, and chemical protein 3D-features (ABCB1). According to this idea, in the present work the prediction of binding active-sites from the human multiple-drugs resistance protein isoform 1 (ABCB1) was performed by using machine learning algorithm-based 3D-deep convolutional neural networks (DeepSite-CNNs chemoinformatic tool) (Jiménez et al., 2017) which was previously validated by providing an extensive test set based > 7000 proteins structure from the scPDB database (Jiménez et al., 2017) (Chen et al., 2010). The results on structural prediction/identification of the ABCB1 binding-site are shown in **Figure 1**.

Next, to validate the 3D X-ray crystallographic structure of the ABCB1 protein model the Ramachandran plot analysis was performed. The Ramachandran plot is a 2D-projection on the plane from 3D-structure and all the possible conformations of each ABCB1-residue including the active binding sites residues which are defined based on the torsion dihedral angles (Psi) and (Phi) around the peptide-bond of the ABCB1-protein residues which can be depicted by 2D-Ramachandran diagram (Chen et al., 2010). Here in, allowed torsion values of Psi *versus* Phi of a given ABC-transporter residue is found within the Ramachandran colored contour ABCB1-transporter conformationally-favored residues. Otherwise, is considered as ABCB1 transporter sterically-disallowed residue and the torsion

values of dihedral angles Psi versus Phi appear outside of the Ramachandran colored contour (conformationally non-favored residues) see **Figure 2**.

After that, we carried out the molecular docking simulation to obtain the Gibbs free energy of binding (FEB or affinity in Kcal/mol) for the complexes formed between the ABCB1 and the chemotherapy agents (ligand: AZD1208, Vincristine, and Daunorubicin). Docking results are considered as energetically-unfavorable when the Gibbs free energy of binding for ABCB1-ligand complexes  $\geq 0$  Kcal/mol, pointing either extremely low or complete absence of affinity otherwise is synonymous of the presence of docking interactions from medium to medium to high affinity. The results obtained showed that all tested ligands (AZD1208, Vincristine, and Daunorubicin) are able to interact with ABCB1-proteins as shown in **Table 1**, where negative FEB values are presented.

According to the obtained *in silico* docking results, a mechanistic interpretation from the best ABC-chemotherapy ligand conformations from (AZD1208, Vincristine, and Daunorubicin) based on the affinity in Kcal/mol allowed to expand our understanding on AZD1208 interaction mechanism with human leukemia multiple-drugs resistance ABCB1 transporter. For the first-time, theoretical evidences could help explain the influence of the AZD1208 from a structural, electronic and pharmacodynamic point of view in the context of an *in silico* approach. In general terms, the best docking binding-interaction (RMSD  $< 2$  Å) for three chemotherapy ABCB1-ligand conformation complexes suggest similar theoretic toxicodynamic behavior in terms of strength of interaction (FEB, Kcal/mol) like FEB (AZD1208-ABCB1)  $\sim$  FEB (Vincristine-ABCB1)  $\sim$  FEB (Daunorubicin-ABCB1)  $\sim -6.2$  Kcal/mol with very close interaction energies when compared with the binding affinities (FEB values) of the specific ABCB1-inhibitor (Rhodamine B) used as control of simulations (or theoretical control). In this regard, it is well known that, Rhodamine B can influence ABCB1 activity by increasing the membrane permeability for ions associated to changes in



the ATP-intracellular levels, which is the source of energy for the ABCB1 physiological function (Bartosiewicz and Krasowska 2009).

This aspect is very important from the toxicodynamic point of view because suggests similar properties of the chemotherapy ABCB1-ligand (AZD1208) if it considered that the free energy of binding is a function of the inhibition constant ( $K_i$ ) as mentioned above. See **Material and Methods** section like FEB (Kcal/mol)  $\approx \Delta G = -RT (\ln K_i)$ . The best binding-poses and the corresponding lig-plot diagrams-based docking interaction from of ABCB1-chemotherapy ligand docking complexes are showed on **Figure 3**.

Besides, to avoid obtaining false positives on docking interactions (AZD1208-ABCB1-protein) we verified the absence of restricted-flexibility for each ABCB1-residues obtained from the lig-plot analysis of AZD1208-ligand. In order to check this, the crystallographic validation using the Ramachandran plot analysis based in allowed torsion values of  $\Psi$  (Psi) versus  $\Phi$  (Phi) of each AZD1208-interacting-residue was performed (Chen et al., 2010). In this regard, were not identified as Ramachandran outliers. Then, the absence of false positives on AZD1208-docking interactions was corroborated. See **Figure 4**.

The potential cytotoxicity docking-mechanism of AZD1208 is fundamentally based on hydrophobic interactions with active binding-site residues like (Glu 756, Leu 721, Asp 891, Ile 718, Gln 894, Ser 716, Glu 171 and Ala 883 from ABCB1-TMD domain) and for the chemotherapy ligand the hydrophobic contact for Vincristine are (Ser 716, Glu 194, Glu 717, Ile 718, Lys 715, Gly 882, Ala 882, Ala 883, Ser 714, Leu 721, Glu 756) and for Daunorubicin are (Thr 968, Asn 973, Lys 965, Glu 596, Ala 551) as showed in the lig-plot diagrams (**Figure 3**). The presence of hydrogen bond contacts is very low and quantitatively similar for the three ABCB1-ligands (AZD1208, Vincristine and Daunorubicin). Besides, other interactions contribute to the stability of the formed ligand-ABCB1 complexes, however the interaction showed a more heterogeneous pattern of interactions affinity based

on non-covalent hydrogen-bond and electrostatic interaction. However, according to the obtained docking results, we could suggest that the AZD1208-ligand has similar irreversibility-binding properties (cytotoxicity potential) to interact with ABCB1-protein than the chemotherapy agent Vincristine and Daunorubicin. The best docking-pose conformation of the AZD1208-ligand showed that can interact (-6.2 Kcal/mol) at the same biophysical environment of Vincristine, Daunorubicin and Rhodamine B (theoretical docking control). See **Figure 5**.

### 3.2 Results of drugs-drugs interactions of AZD1208 based on DFT-simulation

Herein and according to the molecular docking results, we hypothesize that the AZD1208 could pharmacodynamically interact with the chemotherapy-ligands Vincristine and Daunorubicin. Following this idea, we firstly studied the isolated ligand (AZD1208, Vincristine, and Daunorubicin) in order to analyze the individual structural and electronic properties, before the interaction (AZD1208-Vincristine, and AZD1208-Daunorubicin) applied a DFT-approach. In this regard, the DFT-parameter like HOMO-LOMO difference ( $\Delta H / L$ ) (eV) for each isolated-ligand was calculated as control reference before carrying out the study between interacting systems (AZD1208-Vincristine and AZD1208-Daunorubicin). See **Figure 6**.

The results show that in the case of AZD1208-ligand the concentration of charges in the LUMO orbital is located in the N-atom, S-atom and several H and ( $sp^2$ )-C-atoms from the AZD1208-benzene rings. For AZD1208 the HOMO orbital the concentration of charges occurs in the N-atom and also in some H and ( $sp^2$ )-C-atoms of the molecule. For the Vincristine molecule the obtained  $\Delta H/L = 2.17$  eV, indicated that the density of charges for the Vincristine-LUMO orbital was mainly distributed in the H-atoms from  $sp^2/sp^3$  C-atoms, and also O-atoms in several parts of the Vincristine-molecule (LUMO orbital). The Vincristine-HOMO orbital showed the density of charges concentrated in another part of the molecule. In the case of Daunorubicin the obtained energy level  $\Delta H/L$  was 1.25 eV, and the

density of charges in the LUMO-orbital were distributed in oxygen and  $sp^2$ -C-atoms from the benzene rings, and for the Daunorubicin-HOMO orbital were localized in a small region of the structure formed by C, H and O atoms. It is important to note that this distribution of charges-based HOMO/LUMO differences is decisive to understand which regions of the ligand-molecules are more favored for the interaction from the electronic point of view. Because, reveals which atoms are the most susceptible to interactions based in their electron donor or acceptor properties (Soler et al., 2002).

Following this idea, to test the first part of our hypothesis (*in silico*) a DFT-simulation experiments were performed considering the following interacting systems **1)** AZD1208/Vincristine and **2)** AZD1208/Daunorubicin by considering three potential conformations-based interatomic distances values ( $d_{ij}$ , or  $D(\text{Å})$ ) between the ABCB1-ligands (AZD1208/Vincristine and AZD1208/Daunorubicin) interacting systems where (i) is a (C, H, N, O, N)-atom from AZD1208 and (j) is a (C, H, N, O, N)-atom from Vincristine or Daunorubicin) at the final relative docking position. See **Figure 7**.

Next, several DFT-parameters were calculated like DFT-binding energy  $E_b$  (eV), interatomic distances ( $D$  (Å)) and the band gap or HOMO-LOMO difference ( $\Delta H / L$ ) (eV). The *in silico* DFT-parameters for the three configurations I, II, III from the interacting systems analyzed are showed in the **Table 2**.

According to the obtained results, we observed that the most stable configuration for the first interacting system (AZD1208 + Vincristine) was configuration III, which is considered the most stable because it modularly has the highest binding-energy value ( $E_b = -0.98$  with high probability to induce interaction compared with the configurations II (-0.89 eV) > configuration I (0.47 eV), with the lowest distance between (AZD1208/Vincristine)-atoms between the AZD1208 hydrogen-atom and the Vincristine

oxygen-atom of 2.15 Å, and HOMO/LUMO difference ( $\Delta H/L$ ) of 1.00 eV see more details

**Figure 8.**

As for the second interacting for the second interacting system like AZD1208/Daunorubicin the most stable was the configuration I, which has the highest binding-energy value ( $E_b$ ) of - 0.74 which could suggest high potential to induce drug-drug interactions in the previously modeled ABCB1-docking binding site in this conditions compared with the remaining II and III with low  $E_b$  of -0.19 eV and 0.50 eV respectively, the lowest distance between (AZD1208/Daunorubicin)-atoms between was 2.1 Å involving the hydrogen-atom from AZD1208b and the oxygen-atom from Daunorubicin. For this instance, the obtained HOMO/LUMO difference ( $\Delta H/L$ ) was of 1.44 eV see more details in

**Figure 9.**

Drug-drug interactions are a concern in the treatment of cancer. These interactions may inhibit the action of chemotherapeutic agents, which prevents optimization of the antitumor effect in the treatments and minimization of their toxicity to normal tissue. If both chemotherapies act on the same binding site the probability of their effects, diminishing in the target cell is high and may result in overlapping mechanisms of action. It is important that potential interactions between chemotherapeutics be identified early in the drug development process to allow for improvements in in vitro model systems. That is why docking and DTF testing are essential tools for evaluating these interactions (Scripture and Figg, 2006)

Lastly, it is important to highlight that theoretical study of drug-drug interactions is crucial for testing and development of drugs with a higher success rate in chemotherapy. Considering that the pharmacokinetic interactions between chemotherapeutics are one of the problems of resistance to chemotherapy, there is still a long way to go when we analyze this

problem in the context of MDR phenotype and rational drug design, where a rigorous analysis of the molecular mechanism involved is always a great challenge.

#### 4. CONCLUSION

In the present study, an *in silico* mechanistic investigation based on molecular docking and DFT-*ab initio* simulation approaches were performed for the first time, to study the drug-drug interactions-associated of binding of AZD1208 xenobiotic with two recognized chemotherapy-agents like Vincristine and Daunorubicin on TMD-domains from P-glycoprotein (ABCB1) which is involved in the multiple drugs resistance. Such investigation revealed that these molecules may have great levels of interaction, which can block, inhibit or even enhance their effects on cells by changing its pharmacodynamics and, therefore, missing the goal of treatments. These theoretical pieces of evidence have preclinical relevance potential in the design of the new drugs and to understand the polypharmacology influence in the molecular mechanism in the context of cancer. Such investigation revealed that these molecules may have great levels of interaction, which can block, inhibit or even enhance their effects on cells by changing its pharmacodynamics and, therefore, missing the goal of treatments. These *in silico* results open new horizons for pharmacological evaluation based-molecular docking according to 3R principles of animal testing (Replacement, Reduction and Refinement), aiming to ensure more quality of the cancer therapies with higher coefficients benefit/risk and costs for success in farmacointeraccion drug-drug. Finally, this work intends to divulge a new "methodology" that help in the design of new drugs that surpass the phenotype of resistance to multiple drugs and in order to improve the prognosis of cancer patients.

#### Conflicts of interest

The authors declare that they have no competing interests.

#### Acknowledgements

M.B.M acknowledges Ph.D fellowship from Brazilian Agencies CAPES. M.G.D acknowledges Research fellowship from Interreg Sudoe–NanoDesk-SOE/P1/E02015. P.V.O acknowledges to SGI cluster Altix 1350/450 from the Centro Nacional de Processamento de Alto Desempenho em São Paulo (CENAPAD-SP), Brazil. L. F. M is a research fellow from CNPq (Proc. No. 305928/2015-5).

## REFERENCES

- Amson, R., Sigaux, F., Przedborski, S., Flandrin, G., Givol, D., Telerman, A., 1989. The human protooncogene product p33pim is expressed during fetal hematopoiesis and in diverse leukemias. *Proc. Natl. Acad. Sci.* 86, 8857–8861. <https://doi.org/10.1073/pnas.86.22.8857>
- Asati, V., Thakur, S.S., Upmanyu, N., Bharti, S.K., 2018. Virtual Screening, Molecular Docking, and DFT Studies of Some Thiazolidine-2,4-diones as Potential PIM-1 Kinase Inhibitors. *ChemistrySelect* 3, 127–135. <https://doi.org/10.1002/slct.201702392>
- Bevilaqua, R.C.A., Zanella, I., Fagan, S.B., 2010. Chlorophyll a and pheophytin a as gas sensors of CO<sub>2</sub> and O<sub>2</sub> molecules. *Chem. Phys. Lett.* 496, 310–315. <https://doi.org/10.1016/j.cplett.2010.07.066>
- Chen, J., Lu, G., Lin, J., Davidson, A.L., Quioco, F.A., 2003. A tweezers-like motion of the ATP-binding cassette dimer in an ABC transport cycle. *Mol. Cell* 12, 651–661. <https://doi.org/10.1016/j.molcel.2003.08.004>
- Chen, V.B., Arendall, W.B., Headd, J.J., Keedy, D.A., Immormino, R.M., Kapral, G.J., Murray, L.W., Richardson, J.S., Richardson, D.C., 2010. MolProbity: All-atom structure validation for macromolecular crystallography. *Acta Crystallogr. Sect. D Biol. Crystallogr.* 66, 12–21. <https://doi.org/10.1107/S0907444909042073>
- Davidson, A.L., Chen, J., 2004. ATP-Binding Cassette Transporters in Bacteria. *Annu. Rev. Biochem.* 73, 241–268. <https://doi.org/10.1146/annurev.biochem.73.011303.073626>
- Dawson, R.J.P., Hollenstein, K., Locher, K.P., 2007. Uptake or extrusion: Crystal structures of full ABC transporters suggest a common mechanism. *Mol. Microbiol.* 65, 250–257. <https://doi.org/10.1111/j.1365-2958.2007.05792.x>
- de Ruyck, J., Brysbaert, G., Blossey, R., Lensink, M.F., 2016. Molecular docking as a popular tool in drug design, an in silico travel. *Adv. Appl. Bioinform. Chem.* 9, 1–11. <https://doi.org/10.2147/AABC.S105289>
- Erkekoglu, P., Giray, B.K., Ba??aran, N., 2011. 3R principle and alternative toxicity testing methods. *Fabad J. Pharm. Sci.* 36, 101–117.
- Feinstein, W.P., Brylinski, M., 2015. Calculating an optimal box size for ligand docking and virtual screening against experimental and predicted binding pockets. *J. Cheminform.* 7, 18. <https://doi.org/10.1186/s13321-015-0067-5>
- Forli, S., Huey, R., Pique, M.E., Sanner, M., Goodsell, D.S., Arthur, J., 2016. HHS Public Access 11, 905–919. <https://doi.org/10.1038/nprot.2016.051>. Computational

- Gottesman, M.M., Fojo, T., Bates, S.E., 2002. Multidrug Resistance in Cancer: Role of Atp-Dependent Transporters. *Nat. Rev. Cancer* 2, 48–58.  
<https://doi.org/10.1038/nrc706>
- Gottesman, M.M., Ling, V., 2006. The molecular basis of multidrug resistance in cancer: The early years of P-glycoprotein research. *FEBS Lett.* 580, 998–1009.  
<https://doi.org/10.1016/j.febslet.2005.12.060>
- Hollenstein, K., Dawson, R.J., Locher, K.P., 2007. Structure and mechanism of ABC transporter proteins. *Curr. Opin. Struct. Biol.* 17, 412–418.  
<https://doi.org/10.1016/j.sbi.2007.07.003>
- Holohan, C., Van Schaeybroeck, S., Longley, D.B., Johnston, P.G., 2013. Cancer drug resistance: an evolving paradigm. *Nat. Rev. Cancer* 13, 714–726.  
<https://doi.org/10.1038/nrc3599>
- Isaac, M., Siu, A., Jongstra, J., 2011. The oncogenic PIM kinase family regulates drug resistance through multiple mechanisms. *Drug Resist. Updat.* 14, 203–211.  
<https://doi.org/10.1016/j.drug.2011.04.002>
- Jiménez, J., Doerr, S., Martínez-Rosell, G., Rose, A.S., De Fabritiis, G., 2017. DeepSite: Protein-binding site predictor using 3D-convolutional neural networks. *Bioinformatics* 33, 3036–3042. <https://doi.org/10.1093/bioinformatics/btx350>
- Jones, P.M., George, A.M., 2004. The ABC transporter structure and mechanism: perspectives on recent research. *Cell. Mol. Life Sci.* 61, 682–699.  
<https://doi.org/10.1007/s00018-003-3336-9>
- Keeton, E.K., Mceachern, K., Dillman, K.S., Palakurthi, S., Cao, Y., Grondine, M.R., Kaur, S., Wang, S., Chen, Y., Wu, A., Shen, M., Gibbons, F.D., Lamb, M.L., Zheng, X., Stone, R.M., Deangelo, D.J., Plataniias, L.C., Dakin, L. a, Chen, H., Lyne, P.D., Huszar, D., 2014. AZD1208 , a potent and selective pan-Pim kinase inhibitor , demonstrates ef fi cacy in preclinical models of acute myeloid leukemia. *Blood* 123, 905–914. <https://doi.org/10.1182/blood-2013-04-495366>.The
- Kellenberger, E., Muller, P., Schalon, C., Bret, G., Foata, N., Rognan, D., 2006. sc-PDB: an annotated database of druggable binding sites from the Protein Data Bank. *J. Chem. Inf. Model.* 46, 717–27. <https://doi.org/10.1021/ci050372x>
- Kelly, L.A., Mezulis, S., Yates, C., Wass, M., Sternberg, M., 2015. The Phyre2 web portal for protein modelling, prediction, and analysis. *Nat. Protoc.* 10, 845–858.  
<https://doi.org/10.1038/nprot.2015-053>
- Kim, S., Thiessen, P.A., Bolton, E.E., Chen, J., Fu, G., Gindulyte, A., Han, L., He, J., He, S., Shoemaker, B.A., Wang, J., Yu, B., Zhang, J., Bryant, S.H., 2016. PubChem substance and compound databases. *Nucleic Acids Res.* 44, D1202–D1213.  
<https://doi.org/10.1093/nar/gkv951>
- Kohn, W., Sham, L.J., 1965. Self-Consistent Equations Including Exchange and Correlation Effects. *Phys. Rev.* 140, A1134–A1138.  
<https://doi.org/http://dx.doi.org/10.1103/PhysRev.140.A1133>
- Kramer, B., Rarey, M., Lengauer, T., 1997. CASP2 Experiences with Docking Flexible Ligands Using FlexX. *PROTEINS: Structure, Function and Genetics* 1: 221-225.
- Laskowski, R.A., Swindells, M.B., 2011. LigPlot+: Multiple Ligand–Protein Interaction

- Diagrams for Drug Discovery. *J. Chem. Inf. Model.* 51, 2778–2786.  
<https://doi.org/10.1021/ci200227u>
- Levi A. Garraway, Jaap Verweij, and Karla V. Ballman *Journal of Clinical Oncology* 2013  
31:15, 1803-1805
- Li, K., Li, Y., Zhou, D., Fan, Y., Guo, H., Ma, T., Wen, J., Liu, D., Zhao, L., 2016.  
Synthesis and biological evaluation of quinoline derivatives as potential anti-prostate  
cancer agents and Pim-1 kinase inhibitors. *Bioorganic Med. Chem.* 24, 1889–1897.  
<https://doi.org/10.1016/j.bmc.2016.03.016>
- Locher, K.P., 2009. Structure and mechanism of ATP-binding cassette transporters. *Philos.  
Trans. R. Soc. B Biol. Sci.* 364, 239–245. <https://doi.org/10.1098/rstb.2008.0125>
- Meja, K., Stengel, C., Sellar, R., Huszar, D., Davies, B.R., Gale, R.E., Linch, D.C.,  
Khwaja, A., 2014. PIM and AKT kinase inhibitors show synergistic cytotoxicity in  
acute myeloid leukaemia that is associated with convergence on mTOR and MCL1  
pathways. *Br. J. Haematol.* 167, 69–79. <https://doi.org/10.1111/bjh.13013>
- N. Kirschner, A., Wang, J., Van Der Meer, R., Anderson, P.D., Franco-Coronel, O.E.,  
Kushner, M.H., Everett, J.H., Hameed, O., Keeton, E.K., Ahdesmaki, M., Grosskurth,  
S.E., Huszar, D., Abdulkadir, S.A., 2015. PIM kinase inhibitor AZD1208 for  
treatment of MYC-driven prostate cancer. *J. Natl. Cancer Inst.* 107, 1–11.  
<https://doi.org/10.1093/jnci/dju407>
- Perdew, J.P., Zunger, A., 1981. Self-interaction correction to density-functional  
approximations for many-electron systems. *Phys. Rev. B* 23, 5048–5079.  
<https://doi.org/10.1103/PhysRevB.23.5048>
- Pogacic, V., Bullock, A.N., Fedorov, O., Filippakopoulos, P., Gasser, C., Biondi, A.,  
Meyer-Monard, S., Knapp, S., Schwaller, J., 2007. Structural analysis identifies  
imidazo[1,2-b]pyridazines as PIM kinase inhibitors with in vitro antileukemic  
activity. *Cancer Res.* 67, 6916–6924. <https://doi.org/10.1158/0008-5472.CAN-07-0320>
- Ren, J.X., Li, L.L., Zheng, R.L., Xie, H.Z., Cao, Z.X., Feng, S., Pan, Y.L., Chen, X., Wei,  
Y.Q., Yang, S.Y., 2011. Discovery of novel Pim-1 kinase inhibitors by a hierarchical  
multistage virtual screening approach based on svm model, pharmacophore, and  
molecular docking. *J. Chem. Inf. Model.* 51, 1364–1375.  
<https://doi.org/10.1021/ci100464b>
- Roser, M., Ritchie, H., 2018 - "Cancer". Published online at OurWorldInData.org.  
Retrieved from: '<https://ourworldindata.org/cancer>' [Online Resource] accessed in 25<sup>nd</sup>  
may, 2018.
- Salgado, R., Moore, H., Martens, J.W.M., Lively, T., Malik, S., McDermott, U., Michiels,  
S., Moscow, J.A., Tejpar, S., McKee, T., Lacombe, D., 2018. Steps forward for  
cancer precision medicine. *Nat. Rev. Drug Discov.* 17, 1–2.  
<https://doi.org/10.1038/nrd.2017.218>
- Santio, N.M., Eerola, S.K., Paatero, I., Yli-Kauhaluoma, J., Anizon, F., Moreau, P.,  
Tuomela, J., Haärkönen, P., Koskinen, P.J., 2015. Pim kinases promote migration and  
metastatic growth of prostate cancer xenografts. *PLoS One* 10, 1–20.  
<https://doi.org/10.1371/journal.pone.0130340>



- Scripture, C.D., Figg, W.D., 2006. Drug interactions in cancer therapy. *Nat. Rev. Cancer* 6, 546–558. <https://doi.org/10.1038/nrc1887>
- Slater, L.M., Sweet, P., Stupecky, M., Gupta, S., 1986. Cyclosporin A reverses vincristine and daunorubicin resistance in acute lymphatic leukemia in vitro. *J. Clin. Invest.* 77, 1405–1408. <https://doi.org/10.1172/JCI112450>
- Sophia CK and Kent WM. Applying Precision Oncology Principles in Radiation Oncology. 2018. *JCO Precision Oncology*. doi.org/10.1200/PO.18.00034.
- Soler, J.M., Artacho, E., Gale, J.D., García, A., Junquera, J., Ordejón, P., Sánchez-Portal, D., 2002. The SIESTA method for ab initio order- N materials simulation. *J. Phys. Condens. Matter* 14, 2745–2779. <https://doi.org/10.1088/0953-8984/14/11/302>
- Stafman, L.L., Mruthyunjappa, S., Waters, A.M., Garner, E.F., Aye, J.M., Stewart, J.E., Yoon, K.J., Whelan, K., Mroczek-Musulman, E., Beierle, E.A., 2018. Targeting PIM kinase as a therapeutic strategy in human hepatoblastoma. *Oncotarget* 9. <https://doi.org/10.18632/oncotarget.25205>
- Szakács, G., Paterson, J.K., Ludwig, J. a, Booth-Genthe, C., Gottesman, M.M., 2006. Targeting multidrug resistance in cancer. *Nat. Rev. Drug Discov.* 5, 219–34. <https://doi.org/10.1038/nrd1984>
- Trott, O., Olson, A., 2010. NIH Public Access. *J. Comput. Chem.* 31, 455–461. <https://doi.org/10.1002/jcc.21334>.AutoDock
- Troullier, N., Martins, J.L., 1991. Efficient pseudopotentials for plane-wave calculations. II. Operators for fast iterative diagonalization N. 43, 8861–8869. <https://doi.org/doi.org/10.1103/PhysRevB.43.8861>
- Wang, Z., Bhattacharya, N., Weaver, M., Petersen, K., Meyer, M., Gapter, L., Magnuson, N.S., 2001. Pim-1: a serine/threonine kinase with a role in cell survival, proliferation, differentiation and tumorigenesis. *J. Vet. Sci.*
- Xie, Z.R., Hwang, M.J., 2010. An interaction-motif-based scoring function for protein-ligand docking. *BMC Bioinformatics* 11. <https://doi.org/10.1186/1471-2105-11-298>

## CAPTIONS

**Figure 1. A)** Representation of X-ray crystallographic molecular structure model from human leukemia multi-drugs resistance protein isoform 1 (ATP-binding Cassette ABCB1 transporter) showing the transmembrane domain (TMD) embedded in the membrane lipid bilayer with outward-facing conformation for ligand-extrusion pockets and ABCB1-nucleotide-binding domains (NBD). **B)** DeepSite prediction of topological cavities of ABCB1 transporter active binding-sites as volumetric orange regions and **C)** Van der Waals surface representation of the ABCB1-active binding site localized in TMD region label color

is related to acidic residue (red), basic residue (blue) and neutral (green) in the ABCB1-active binding site.

**Figure 2.** **A)** Representation of Ramachandran diagrams and spatial distribution of Ramachandran outliers (Glycine) in the modeled pdb x-ray structure of human multiple-drugs resistance protein isoform 1 (ABCB1). All the possible combinations of dihedral angles of torsion like Psi *versus* Phi of each amino acid residues of ABCB1 protein are showed. **B)** Ramachandran plot quality assessment (ABCB1 model quality) is measured by the percentage of the ABCB1-residues that are in the most favored, or core, regions of the Ramachandran plot *versus* resolution (Å). For such purpose, is showed a good model structure for ABCB1-protein, modeled with high resolution of 2.3 Å, with expected percentage of favored region (including the ABCB1-ligand extrusion pockets) over 90% (red dotted line). However, it is important to note that as the resolution gets poorer, so this figure decreases - as might be expected. The shaded region reflects this expected decrease with worsening resolution.

**Figure 3.** On the left Van der Waals surface representation for each chemotherapy ABCB1-ligand complexes for the best docking pose (RMSD < 2Å) in the TMD domain region of active binding-site (ABCB1-ligand extrusion pocket) like **A)** AZD1208-ABCB1 complex (light blue), **B)** Vincristine-ABCB1 complex (yellow), and **C)** Daunorubicin-ABCB1 complex (violet). The Van der Waals color-labels as red region denotes negative charge, blue region positive charge and green region like neutral for the ABCB1-binding-site residues. On the right Lig-plot diagrams of interactions for the formed complexes like: **D)** AZD1208-ABCB1 complex, **E)** Vincristine-ABCB1 complex and **F)** Daunorubicin-ABCB1 complex. All the Lig-plot diagrams are related to the ABCB1-active bind site for the best docking poses of the ligand studied and are representing non-covalent interaction like (hydrophobic and hydrogen-bond interaction) (Laskowski and Swindells, 2011). The

corresponding Rhodamine B-ABCB1-docking complex (Rhodamine B specific ABCB1 inhibitor) used as control of docking simulation experiment can see as **Supplementary material SM1(A)**

**Figure 4.** Validation based on Ramachandran diagrams for each AZD1208-lig-plot interacting residues from ABCB1-protein. More details refer **Figure 3-D**.

**Figure 5.** Van der Waals surface representation of superimposed ABCB1-ligand docking complexes with the best docking pose ( $\text{RMSD} < 2\text{\AA}$ ) showing the drug-drug interaction in the ligand-extrusion binding TMD-Domains of multiple-drugs resistance P-glycoprotein (ABCB1) like: **A)** ABCB1 showing the unoccupied-active binding-site (white dotted circle) from ligand extrusion pocket. **B)** AZD1208/Vincristine/ABCB1 interaction complex with color-label: light-blue/yellow/green respectively), **C)** AZD1208/Daunorubicin/ABCB1 complex with color-label as: light-blue/violet/green respectively). Additional information of the control simulation like superimposed AZD1208/Rhodamine/ABCB1 complex can be found in the **Supplementary material SM1 (A)**.

**Figure 6.** DFT-results on HOMO/LUMO difference ( $\Delta H / L$ ) (eV) used as control simulation for the three isolated ligands **A)** AZD1208- $(\Delta H / L) = 1.78$  eV, **B)** Vincristine- $(\Delta H / L) = 2.17$  eV and **C)** Daunorubicin- $(\Delta H / L) = 1.25$  eV. Herein, empty spheres are to represent the empty energy-levels and the filled-spheres as filled-energy levels from the ligands. The plot of charges was performed at  $0.0001509 \text{ eV/\AA}^3$  and the atoms-type are showing on the right by color label like: carbon-atoms (dark gray), hydrogen-atoms (light gray), nitrogen-atoms (blue), oxygen-atoms (red) and sulfur-atoms (yellow).

**Figure 7.** Final configurations obtained for the interacting systems-based DFT-simulation like **A)** AZD1208/Vincristine and **B)** AZD1208/Daunorubicin and the corresponding obtained configuration I, II, III.

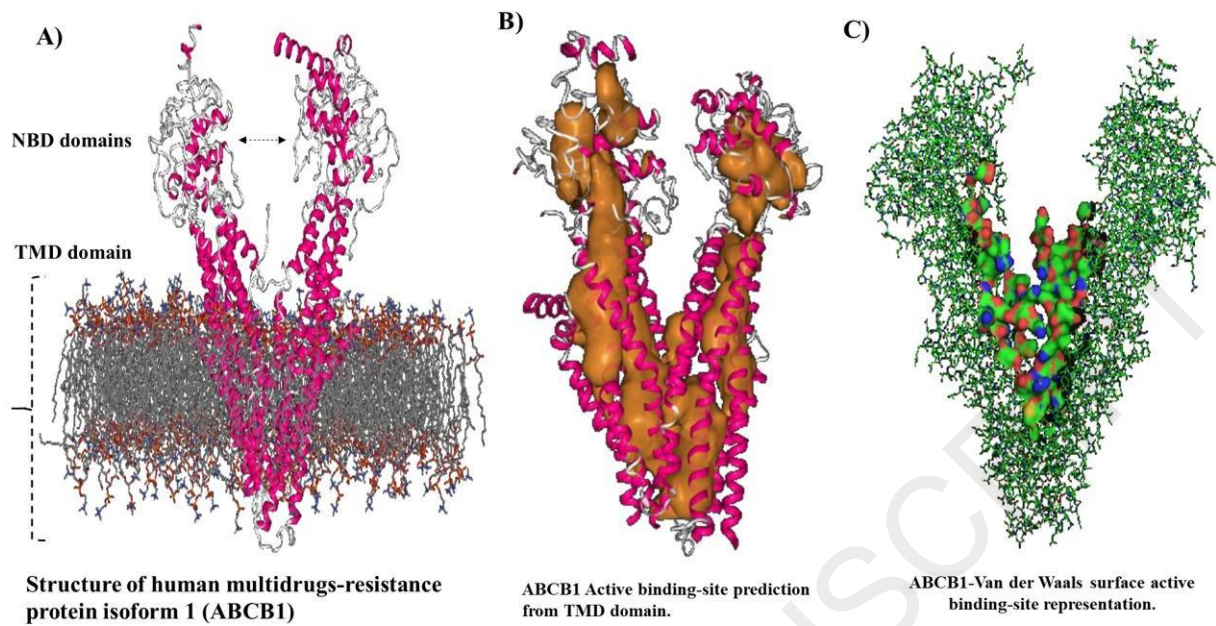
**Figure 8.** Graphical representation of drug-drug interaction based on DFT-results for the AZD1208/Vincristine interacting system showing the most stable configuration (III), energy levels-based HOMO/LUMO energy gap difference ( $\Delta H/L$ ). The corresponding plot of charges is represented regarding the HOMO/LUMO interaction orbitals from drug-drug interacting-systems (AZD1208/Vincristine). Herein, empty spheres are to represent the empty energy-levels and the filled-spheres as filled-energy levels from the drug-drug interacting-systems. Note that the concentration of charges in the lowest unoccupied molecular orbital (LUMO) is only localized in the Vincristine molecule. However, the highest occupied molecular orbital (HOMO) the electronic charge density was observed in the AZD1208 molecule allowing explaining potential drug-drug interactions. The plot of charges was performed at  $0.0001509 \text{ eV/\AA}^3$  and the atoms-type is showing on the right by color label like: carbon-atoms (dark gray), hydrogen-atoms (light gray), nitrogen-atoms (blue), oxygen-atoms (red) and sulfur-atoms (yellow).

**Figure 9.** Graphical representation of drug-drug interaction based on DFT-results for the AZD1208/Daunorubicin interacting system showing the most stable configuration (I), energy levels-based HOMO/LUMO gap difference ( $\Delta H/L$ ). Herein, empty spheres are to represent the empty energy-levels and the filled-spheres as filled-energy levels from the interacting-systems. The corresponding plot of charges is represented regarding the HOMO/LUMO interaction orbitals from drug-drug interacting-systems (AZD1208/Daunorubicin). Note that the electronic charge density in the lowest unoccupied molecular orbital (LUMO) is only localized in the AZD1208 molecule. Herein, for the highest occupied molecular orbital (HOMO) the density of charges was observed in parts of the AZD1208 molecule. The electronic charge density plot was performed at  $0.0001509 \text{ eV/\AA}^3$  and the atoms-type is showing on the right by color label like: carbon-atoms (dark

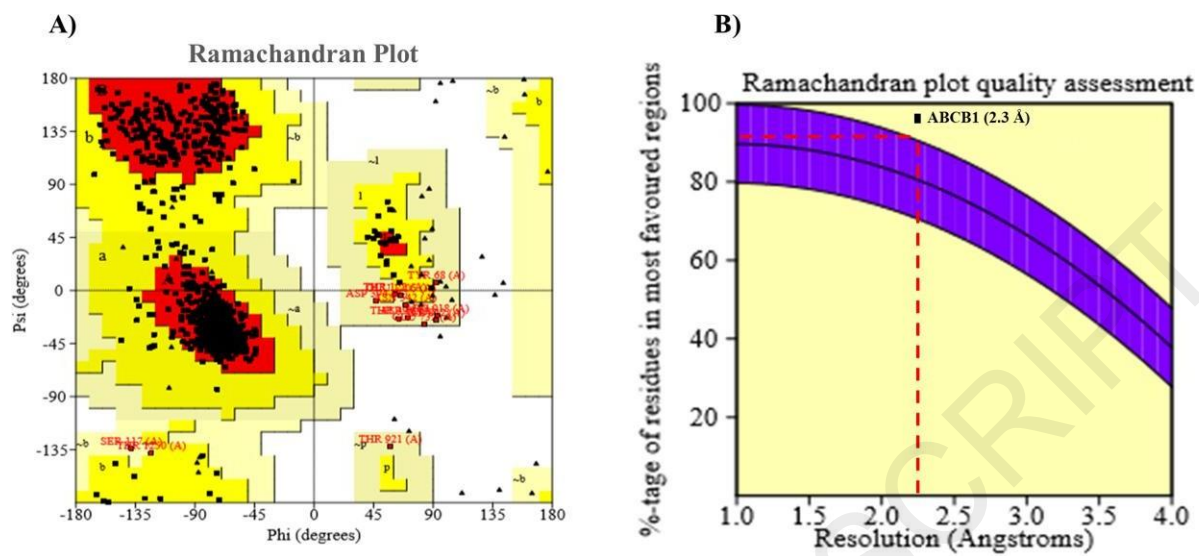
gray), hydrogen-atoms (light gray), nitrogen-atoms (blue), oxygen-atoms (red) and sulfur-atoms (yellow).

ACCEPTED MANUSCRIPT

Figr-1



Figr-2



Figr-3

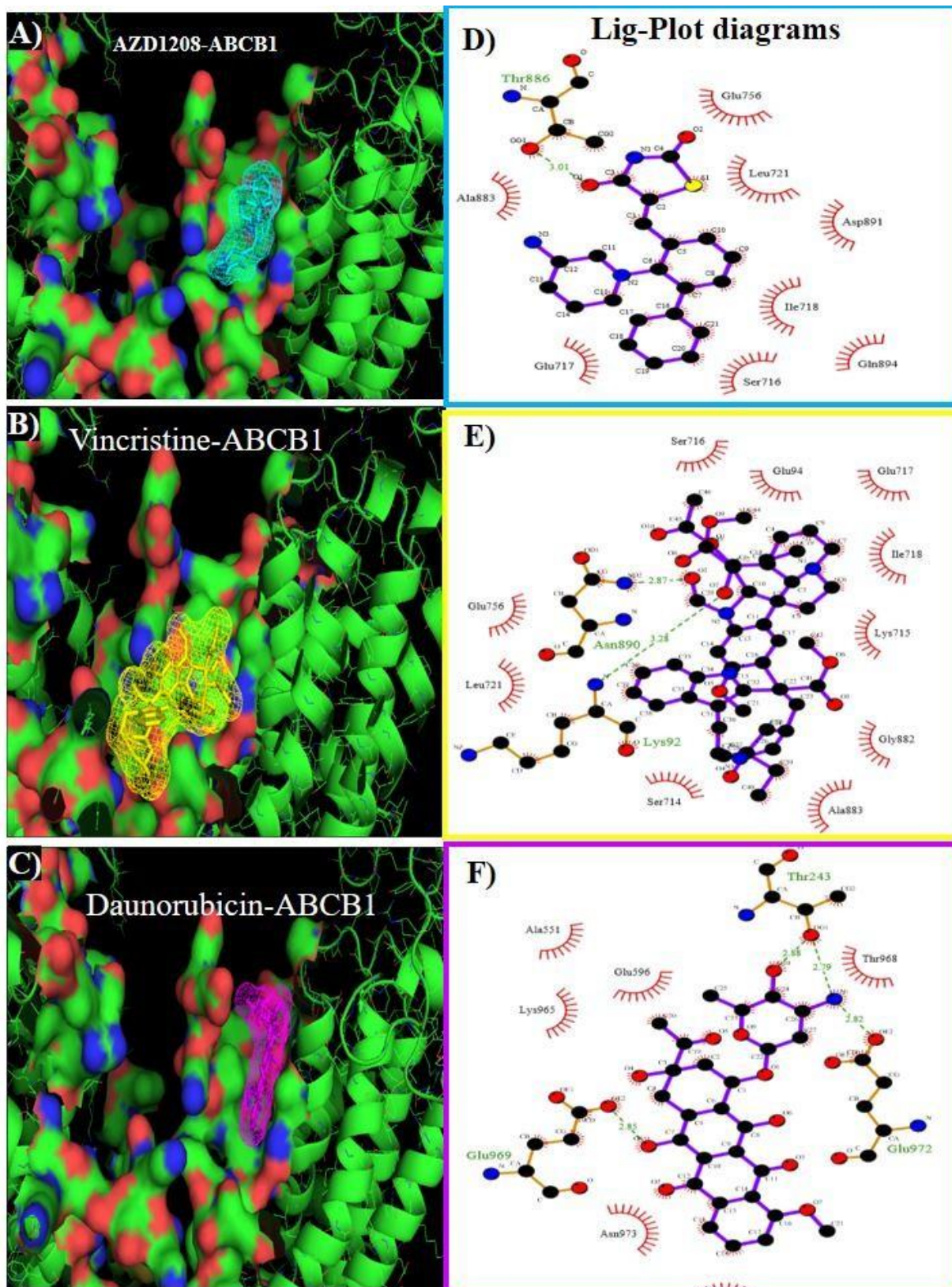
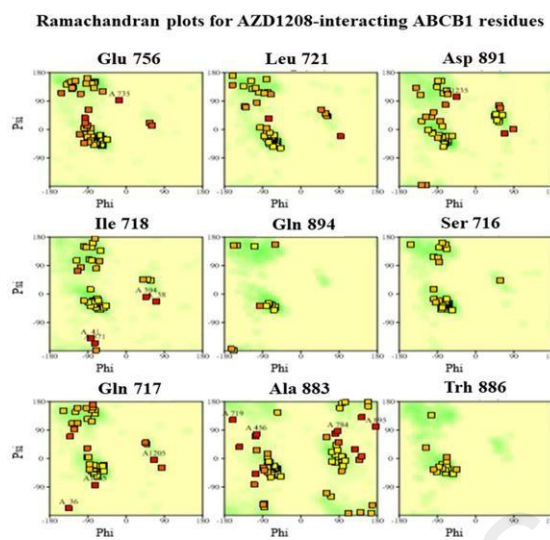
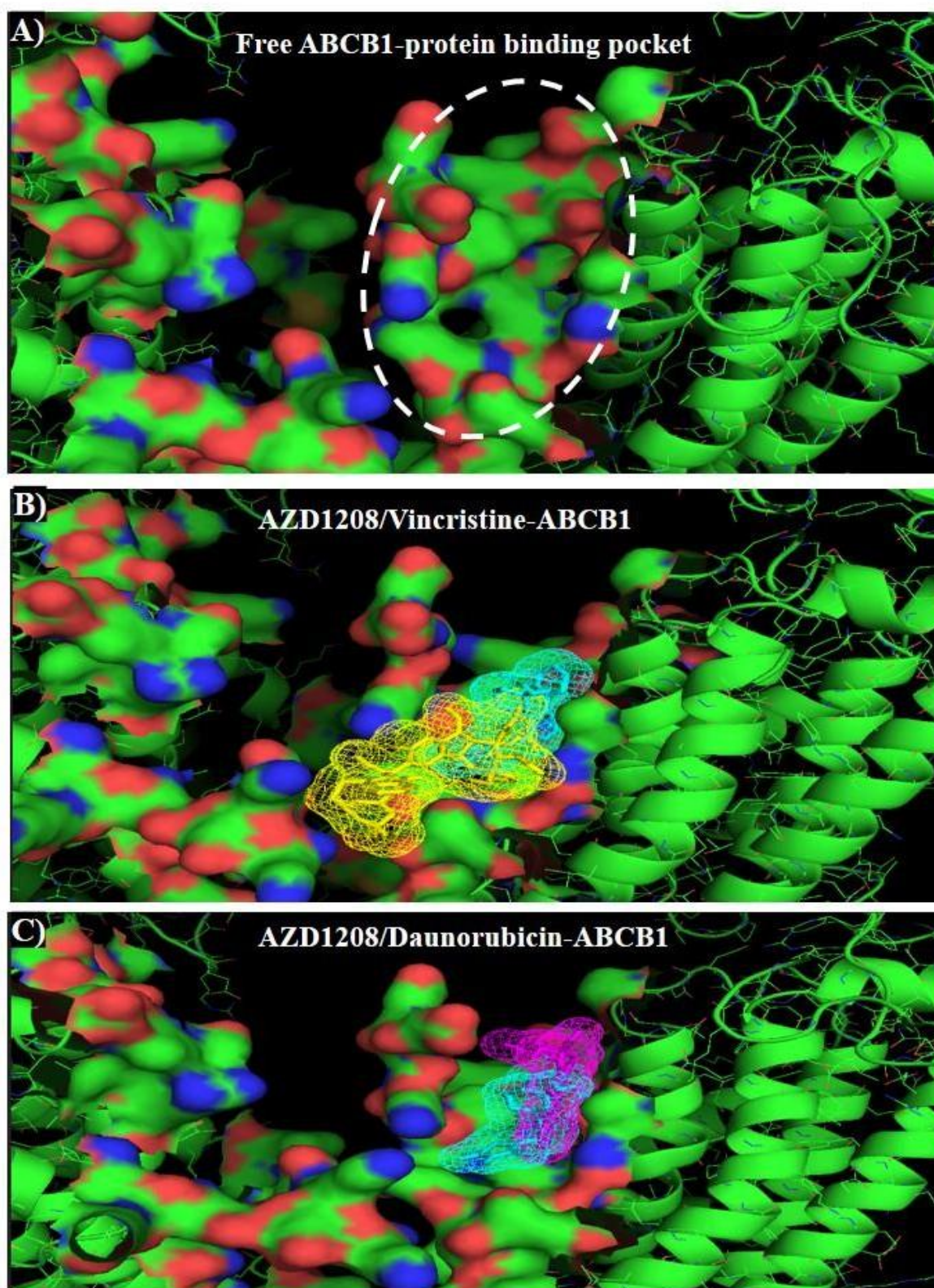




Fig-4



Figr-5



Figr-6

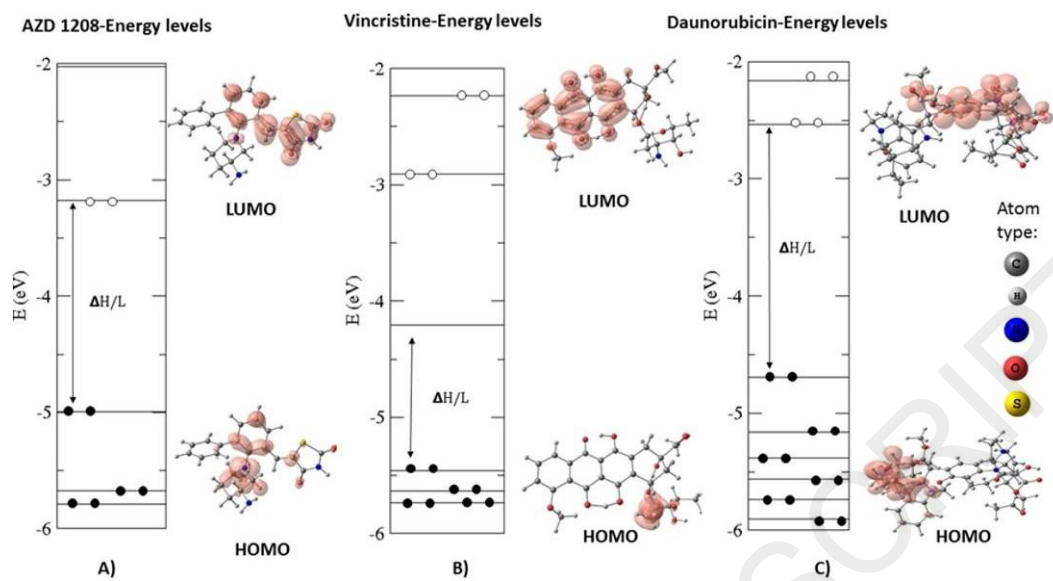
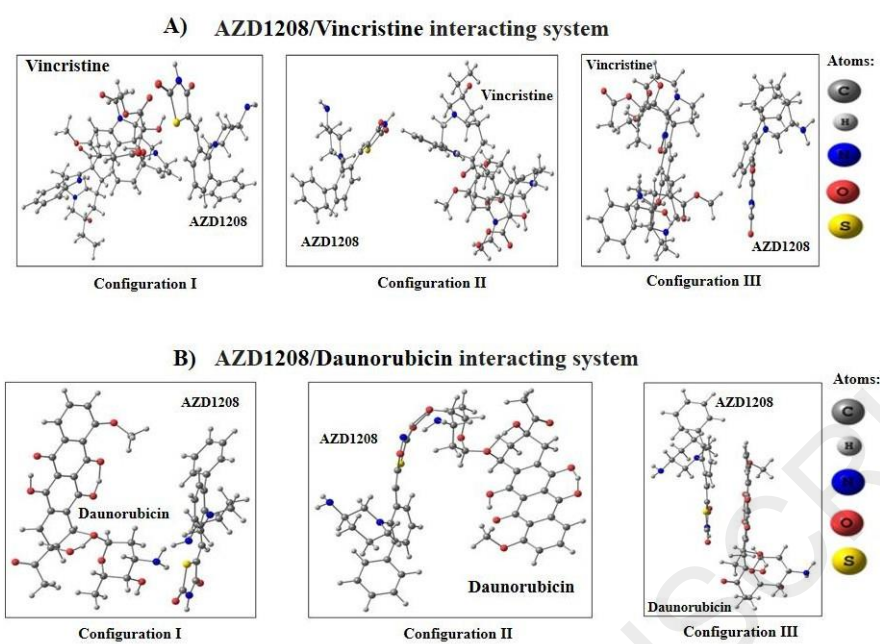
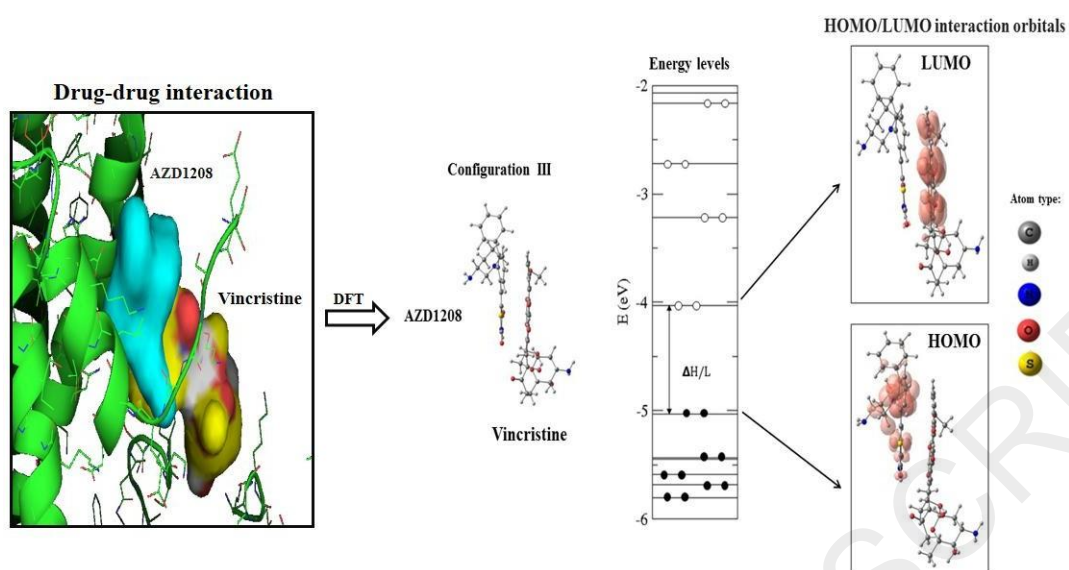


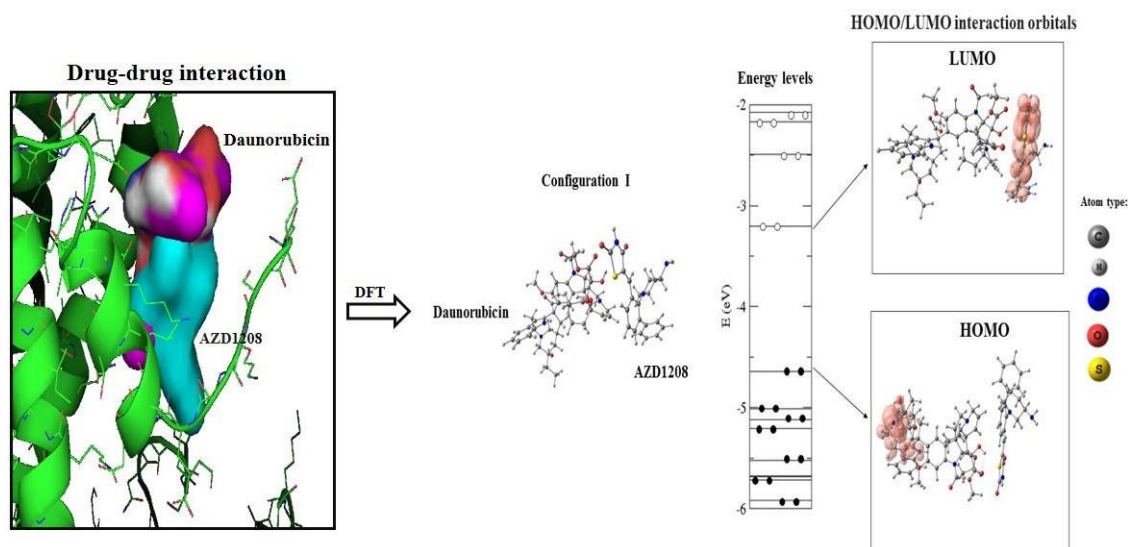
Fig-7



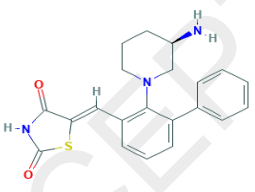
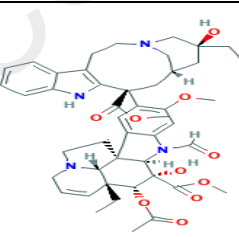
Figr-8

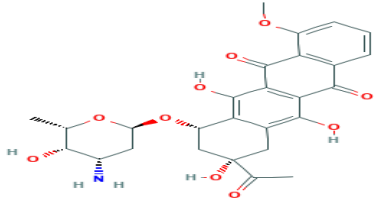
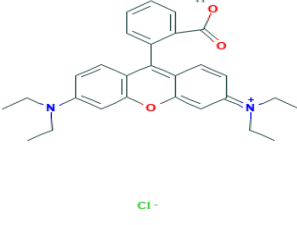


Figr-9



**Table 1.** Results of docking complexes of interaction for the best ABCB1-ligand conformations based on the affinity in Kcal/mol. Please, note that the docking simulation of Rhodamine B-molecule was used as reference controls on ABCB1 active-binding pockets.

ABC-Ligand Structures	Docking Complexes	Docking Affinity (FEB:Kcal/mol)	R.M.S.D (Å)
	AZD1208-ABCB1 protein	-6.2	3.462
	Vincristine-ABCB1 protein	-6.1	1.781

	Daunorubin-ABCB1 protein	-6.5	1.991
	Rhodamine B-ABCB1 protein (Specific ABCB1-inhibitor)	-6.0	1.217

**Table 2.** DFT-Results by considering the performed three configurations (I, II, and III) of each interacting system as AZD1208/Vincristine and AZD1208/Daunorubicin. The most stable interacting systems (configurations) are marked with an asterisk (\*).

Ligand interacting-systems	$E_b$ (eV)	D (Å)	$\Delta H/L$ (eV)
AZD1208 + Vincristine (I)	-0.47	2.35 H-O	0.91
AZD1208 + Vincristine (II)	-0.89	1.77 H-O	0.98
AZD1208 + Vincristine (III)*	-0.98	2.15 H-O	1.00
AZD1208+Daunorubicin (I)*	-0.74	2.10 H-O	1.44
AZD1208+Daunorubicin (II)	-0.19	2.10 N-O	1.37
AZD1208+Daunorubicin (III)	0.50	2.78 H-S	1.27

#### 4. DISCUSSÃO GERAL E CONCLUSÕES

As principais conclusões que encontramos na tese permitiram propor um novo mecanismo de ação. Mostramos que o efeito de diferentes drogas quimioterápicas podem selecionar células com diferentes capacidades antioxidantes, o que altera o metabolismo oxidativo tumoral, logo o aumento da demanda de ATP. Cabe ressaltar que a DNR seleciona células com expressão constitutiva de importantes fatores de transcrição que comandam genes relacionados com o estresse oxidativo e com o fenótipo MDR. Com relação ao sistema de fosforilação, a PIM-1 é uma quinase que tem sido relacionada aos processos oncogênicos como sobrevivência celular, proliferação e resistência a múltiplos fármacos (MDR). Esta quinase vem sendo relacionada com o fenótipo MDR por fosforilar membros da família ABC (STOLARCZYK et al., 2011).

O AZD1208 é um inibidor da quinase PIM-1. Nesse sentido, acreditávamos que a associação de dois quimioterápicos (AZD1208 mais VCR ou AZD1208 mais DNR) poderiam atuar bloqueando a PIM-1 e por consequência disso, inativar a fosforilação da proteína ABCB1, causando um efeito citotóxico maior nas linhagens resistentes, Lucena e FEPS, do que o AZD1208 sozinho. No entanto, isso não foi observado. A associação dos quimioterápicos aumentou a viabilidade celular das duas linhagens resistentes MDRs.

Quando analisamos a atividade de ABCB1, o AZD1208 sozinho não foi capaz de afetar a extrusão da bomba. Diferentemente, a coexposição de AZD1208 e DNR ou VCR prejudicou a atividade de ABCB1. No entanto, mesmo com a ação da ABCB1 prejudicada, as células resistentes ainda apresentaram um aumento na viabilidade celular. Nesse sentido, uma das hipóteses para explicar esse resultado é que provavelmente que o gene *abcb1* esteja compensando o aumento da atividade da ABCB1. Outra hipótese é que possivelmente alguma outra bomba de extrusão está



superexpressa, como a MRP-1. PIM-1 também pode estar fosforilando a proteína MRP1.

Para analisar se os quimioterápicos poderiam estar interagindo com PIM-1 realizamos *docking molecular* para investigar o mecanismo molecular do PIM-1. A análise de *docking molecular* mostrou que o AZD1208 é capaz de interagir, teoricamente, com o VCR e o DNR no mesmo ambiente biofísico da PIM-1, no sítio de ligação ao ATP. Esta evidência sugere que o AZD1208 possa induzir a interação farmacodinâmica com VCR e DNR, enfraquecendo seu potencial citotóxico no sítio de ligação do ATP da PIM-1, o que poderia explicar o que observamos nos resultados *in vitro*. Já que esta interação farmacodinâmica pode resultar em competição pelo mesmo sítio ativo de PIM-1, isso pode diminuir a ação dessa quinase pois, teoricamente, a mesma está ocupada. Logo, a ação citotóxica dos quimioterápicos é perdida pelo efluxo dos mesmos. Corroborando com as conclusões apresentadas até aqui, o último trabalho mostrou através de *docking molecular* e teoria de densidade funcional (DTF-*ab initio*) que os três quimioterápicos também apresentam uma interação farmacodinâmica no sítio de ligação da região TMD da proteína ABCB1. Esses dados complementam os nossos achados até aqui, no sentido de que se tanto a PIM-1 quando a ABCB1 são alvos de competição inibitória dos três quimioterápicos.

A resistência múltipla a drogas (MDR) é uma das principais causas de insucesso no tratamento do câncer, levando a alterações no metabolismo celular e consequente desregulação de vias oxidativas, que estão relacionadas à agressividade tumoral e ao baixo prognóstico do câncer. Geralmente, mais de um tipo de agente quimioterápico é combinado para ser usado nos tratamentos clínicos contra o câncer. Essa tese mostra a importância de testar quimioterápicos clássicos (VCR e DNR) juntamente novos quimioterápicos (como o AZD1208), a fim de analisar as interações farmacodinâmicas

que podem ocorrer entre eles. Se ambos agentes quimioterápicos agem no mesmo sítio ativo da proteína efetora (que pode ser tanto a PIM-1 quanto a ABCB1) é provável que seus efeitos diminuam na célula-alvo, podendo resultar em mecanismos de ação sobrepostos. É crucial que as interações potenciais entre os quimioterápicos sejam identificadas no início do processo de desenvolvimento de drogas.

Finalmente, nessa tese propomos um novo mecanismo de ação de interação farmacodinâmica entre quimioterápicos que podem selecionar células com diferentes capacidades antioxidantes, atuar sobre o mecanismo de fosforilação de uma importante quinase PIM-1, interagindo sobre a principal bomba do fenótipo MDR, a proteína ABCB1. Esses dados, em conjunto, podem ser considerados uma ferramenta pré-clínica nas estratégias de pesquisa de novos inibidores que possam ultrapassar o fenótipo MDR e melhorar os prognósticos dos pacientes com câncer.

## REFERÊNCIAS GERAIS

- Ambudkar, S. V., Kim, I.-W., Sauna, Z.E., 2006. The power of the pump: mechanisms of action of P-glycoprotein (ABCB1). *Eur. J. Pharm. Sci.* 27, 392–400. <https://doi.org/10.1016/j.ejps.2005.10.010>
- Amson, R., Sigaux, F., Przedborski, S., Flandrin, G., Givol, D., Telerman, A., 1989. The human protooncogene product p33pim is expressed during fetal hematopoiesis and in diverse leukemias. *Proc. Natl. Acad. Sci.* 86, 8857–8861. <https://doi.org/10.1073/pnas.86.22.8857>
- Asati, V., Thakur, S.S., Upmanyu, N., Bharti, S.K., 2018. Virtual Screening, Molecular Docking, and DFT Studies of Some Thiazolidine-2,4-diones as Potential PIM-1 Kinase Inhibitors. *ChemistrySelect* 3, 127–135. <https://doi.org/10.1002/slct.201702392>
- Bachmann, M., Möröy, T., 2005. The serine/threonine kinase Pim-1. *Int. J. Biochem. Cell Biol.* 37, 726–730. <https://doi.org/10.1016/j.biocel.2004.11.005>
- Bertram, J.S., 2000. The molecular biology of cancer. *Mol. Aspects Med.* 21, 167–223. [https://doi.org/10.1016/S0098-2997\(00\)00007-8](https://doi.org/10.1016/S0098-2997(00)00007-8)
- Bevilaqua, R.C.A., Zanella, I., Fagan, S.B., 2010. Chlorophyll a and pheophytin a as gas sensors of CO<sub>2</sub> and O<sub>2</sub> molecules. *Chem. Phys. Lett.* 496, 310–315. <https://doi.org/10.1016/j.cplett.2010.07.066>
- Chen, J., Lu, G., Lin, J., Davidson, A.L., Quijcho, F.A., 2003. A tweezers-like motion of the ATP-binding cassette dimer in an ABC transport cycle. *Mol. Cell* 12, 651–661. <https://doi.org/10.1016/j.molcel.2003.08.004>
- Chen, L.S., Redkar, S., Taverna, P., Cortes, J.E., Gandhi, V., 2011. Mechanisms of cytotoxicity to Pim kinase inhibitor, SGI-1776, in acute myeloid leukemia. *Blood* 118, 693–702. <https://doi.org/10.1182/blood-2010-12-323022>
- Chen, V.B., Arendall, W.B., Headd, J.J., Keedy, D.A., Immormino, R.M., Kapral, G.J., Murray, L.W., Richardson, J.S., Richardson, D.C., 2010. MolProbity: All-atom structure validation for macromolecular crystallography. *Acta Crystallogr. Sect. D Biol. Crystallogr.* 66, 12–21. <https://doi.org/10.1107/S09074444909042073>
- Daflon-Yunes, N., Pinto-Silva, F.E., Vidal, R.S., Novis, B.F., Berguetti, T., Lopes, R.R.S., Polycarpo, C., Rumjanek, V.M., 2013. Characterization of a multidrug-resistant chronic myeloid leukemia cell line presenting multiple resistance mechanisms. *Mol. Cell. Biochem.* 383, 123–35. <https://doi.org/10.1007/s11010-013-1761-0>
- Davidson, A.L., Chen, J., 2004. ATP-Binding Cassette Transporters in Bacteria. *Annu. Rev. Biochem.* 73, 241–268. <https://doi.org/10.1146/annurev.biochem.73.011303.073626>
- Dawson, R.J.P., Hollenstein, K., Locher, K.P., 2007. Uptake or extrusion: Crystal structures of full ABC transporters suggest a common mechanism. *Mol. Microbiol.*

65, 250–257. <https://doi.org/10.1111/j.1365-2958.2007.05792.x>

- de Ruyck, J., Brysbaert, G., Blossey, R., Lensink, M.F., 2016. Molecular docking as a popular tool in drug design, an in silico travel. *Adv. Appl. Bioinform. Chem.* 9, 1–11. <https://doi.org/10.2147/AABC.S105289>
- Diehn, M., Cho, R.W., Lobo, N.A., Kalisky, T., Dorie, M.J., Kulp, A.N., Qian, D., Lam, J.S., Ailles, L.E., Wong, M., Joshua, B., Kaplan, M.J., Wapnir, I., Dirbas, F.M., Somlo, G., Garberoglio, C., Paz, B., Shen, J., Lau, S.K., Quake, S.R., Brown, J.M., Weissman, I.L., Clarke, M.F., 2009. Association of reactive oxygen species levels and radioresistance in cancer stem cells. *Nature* 458, 780–783. <https://doi.org/10.1038/nature07733>
- Engh, R.A., Bossemeyer, D., 2001. The Protein Kinase Activity Modulation Sites: Mechanism for Cellular Regulation - Targets for Therapeutic Intervention. *Adv. Enzyme Regul.* 41, 121–149. [https://doi.org/10.1016/S0065-2571\(00\)00010-8](https://doi.org/10.1016/S0065-2571(00)00010-8)
- Erkekoglu, P., Giray, B.K., Ba??aran, N., 2011. 3R principle and alternative toxicity testing methods. *Fabad J. Pharm. Sci.* 36, 101–117.
- Feinstein, W.P., Brylinski, M., 2015. Calculating an optimal box size for ligand docking and virtual screening against experimental and predicted binding pockets. *J. Cheminform.* 7, 18. <https://doi.org/10.1186/s13321-015-0067-5>
- Forli, S., Huey, R., Pique, M.E., Sanner, M., Goodsell, D.S., Arthur, J., 2016. HHS Public Access 11, 905–919. <https://doi.org/10.1038/nprot.2016.051>. *Computational*
- Garraway, L.A., Verweij, J., Ballman, K. V., 2013. Precision oncology: An overview. *J. Clin. Oncol.* 31, 1803–1805. <https://doi.org/10.1200/JCO.2013.49.4799>
- Gewirtz, D.A., 1999. A critical evaluation of the mechanisms of action proposed for the antitumor effects of the anthracycline antibiotics adriamycin and daunorubicin. *Biochem. Pharmacol.* 57, 727–741. [https://doi.org/10.1016/S0006-2952\(98\)00307-4](https://doi.org/10.1016/S0006-2952(98)00307-4)
- Gottesman, M.M., Fojo, T., Bates, S.E., 2002. Multidrug Resistance in Cancer: Role of Atp-Dependent Transporters. *Nat. Rev. Cancer* 2, 48–58. <https://doi.org/10.1038/nrc706>
- Gottesman, M.M., Ling, V., 2006. The molecular basis of multidrug resistance in cancer: The early years of P-glycoprotein research. *FEBS Lett.* 580, 998–1009. <https://doi.org/10.1016/j.febslet.2005.12.060>
- Hanahan, D., Weinberg, R. a, 2011. Hallmarks of cancer: the next generation. *Cell* 144, 646–74. <https://doi.org/10.1016/j.cell.2011.02.013>
- Hanahan, D., Weinberg, R.A., Francisco, S., 2000. The Hallmarks of Cancer Review University of California at San Francisco 100, 57–70.
- Harder, B., Jiang, T., Wu, T., Tao, S., de la Vega, M.R., Tian, W., Chapman, E., Zhang, D.D., 2015. Molecular mechanisms of Nrf2 regulation and how these influence chemical modulation for disease intervention. *Biochem. Soc. Trans.* 43, 680–686.

<https://doi.org/10.1042/BST20150020>

- Hollenstein, K., Dawson, R.J., Locher, K.P., 2007a. Structure and mechanism of ABC transporter proteins. *Curr. Opin. Struct. Biol.* 17, 412–418.  
<https://doi.org/10.1016/j.sbi.2007.07.003>
- Hollenstein, K., Frei, D.C., Locher, K.P., 2007b. Structure of an ABC transporter in complex with its binding protein. *Nature* 446, 213–216.  
<https://doi.org/10.1038/nature05626>
- Holohan, C., Van Schaeybroeck, S., Longley, D.B., Johnston, P.G., 2013. Cancer drug resistance: an evolving paradigm. *Nat. Rev. Cancer* 13, 714–726.  
<https://doi.org/10.1038/nrc3599>
- Housman, G., Byler, S., Heerboth, S., Lapinska, K., Longacre, M., Snyder, N., Sarkar, S., 2014. Drug Resistance in Cancer: An Overview. *Cancers (Basel)*. 6, 1769–1792. <https://doi.org/10.3390/cancers6031769>
- Isaac, M., Siu, A., Jongstra, J., 2011. The oncogenic PIM kinase family regulates drug resistance through multiple mechanisms. *Drug Resist. Updat.* 14, 203–211.  
<https://doi.org/10.1016/j.drug.2011.04.002>
- Jaramillo, M., Zhang, D., 2013. The emerging role of the Nrf2–Keap1 signaling pathway in cancer. *Genes Dev.* 27, 2179–2191.  
<https://doi.org/10.1101/gad.225680.113>
- Jiménez, J., Doerr, S., Martínez-Rosell, G., Rose, A.S., De Fabritiis, G., 2017. DeepSite: Protein-binding site predictor using 3D-convolutional neural networks. *Bioinformatics* 33, 3036–3042. <https://doi.org/10.1093/bioinformatics/btx350>
- Jones, P.M., George, A.M., 2004. The ABC transporter structure and mechanism: perspectives on recent research. *Cell. Mol. Life Sci.* 61, 682–699.  
<https://doi.org/10.1007/s00018-003-3336-9>
- Jones, P.M., George, A.M., 2002. Mechanism of ABC transporters: A molecular dynamics simulation of a well characterized nucleotide-binding subunit. *Proc. Natl. Acad. Sci.* 99, 12639–12644. <https://doi.org/10.1073/pnas.152439599>
- Keane, N.A., Reidy, M., Natoni, A., Raab, M.S., O’Dwyer, M., 2015. Targeting the Pim kinases in multiple myeloma. *Blood Cancer J* 5, e325.  
<https://doi.org/10.1038/bcj.2015.46>
- Keeton, E.K., Mceachern, K., Dillman, K.S., Palakurthi, S., Cao, Y., Grondine, M.R., Kaur, S., Wang, S., Chen, Y., Wu, A., Shen, M., Gibbons, F.D., Lamb, M.L., Zheng, X., Stone, R.M., Deangelo, D.J., Plataniias, L.C., Dakin, L. a, Chen, H., Lyne, P.D., Huszar, D., 2014. AZD1208 , a potent and selective pan-Pim kinase inhibitor , demonstrates efficacy in preclinical models of acute myeloid leukemia. *Blood* 123, 905–914. <https://doi.org/10.1182/blood-2013-04-495366>.The
- Kellenberger, E., Muller, P., Schalon, C., Bret, G., Foata, N., Rognan, D., 2006. sc-PDB: an annotated database of druggable binding sites from the Protein Data Bank. *J. Chem. Inf. Model.* 46, 717–27. <https://doi.org/10.1021/ci050372x>

- Kelly, L.A., Mezulis, S., Yates, C., Wass, M., Sternberg, M., 2015. The Phyre2 web portal for protein modelling, prediction, and analysis. *Nat. Protoc.* 10, 845–858. <https://doi.org/10.1038/nprot.2015-053>
- Kim, S., Thiessen, P.A., Bolton, E.E., Chen, J., Fu, G., Gindulyte, A., Han, L., He, J., He, S., Shoemaker, B.A., Wang, J., Yu, B., Zhang, J., Bryant, S.H., 2016. PubChem substance and compound databases. *Nucleic Acids Res.* 44, D1202–D1213. <https://doi.org/10.1093/nar/gkv951>
- Kohn, W., Sham, L.J., 1965. Self-Consistent Equations Including Exchange and Correlation Effects. *Phys. Rev.* 140, A1134–A1138. <https://doi.org/http://dx.doi.org/10.1103/PhysRev.140.A1133>
- Laskowski, R.A., Swindells, M.B., 2011. LigPlot+: Multiple Ligand–Protein Interaction Diagrams for Drug Discovery. *J. Chem. Inf. Model.* 51, 2778–2786. <https://doi.org/10.1021/ci200227u>
- Li, J., Hu, X.F., Loveland, B.E., Xing, P.X., 2009. Pim-1 expression and monoclonal antibody targeting in human leukemia cell lines. *Exp. Hematol.* 37, 1284–1294. <https://doi.org/10.1016/j.exphem.2009.08.002>
- Li, K., Li, Y., Zhou, D., Fan, Y., Guo, H., Ma, T., Wen, J., Liu, D., Zhao, L., 2016. Synthesis and biological evaluation of quinoline derivatives as potential anti-prostate cancer agents and Pim-1 kinase inhibitors. *Bioorganic Med. Chem.* 24, 1889–1897. <https://doi.org/10.1016/j.bmc.2016.03.016>
- Liu, L., Ning, X., Sun, L., Zhang, H., Shi, Y., Guo, C., Han, S., Liu, J., Sun, S., Han, Z., Wu, K., Fan, D., 2008. Hypoxia-inducible factor-1 $\alpha$  contributes to hypoxia-induced chemoresistance in gastric cancer. *Cancer Sci.* 99, 121–128. <https://doi.org/10.1111/j.1349-7006.2007.00643.x>
- Locher, K.P., 2009. Structure and mechanism of ATP-binding cassette transporters. *Philos. Trans. R. Soc. B Biol. Sci.* 364, 239–245. <https://doi.org/10.1098/rstb.2008.0125>
- Lozzio, C., Lozzio, B., 1975. Human With Chronic Positive. *Blood* 45, 321–334.
- Marmiroli, S., Fabbro, D., Miyata, Y., Pierobon, M., Ruzzene, M., 2015. Phosphorylation, Signaling, and Cancer: Targets and Targeting. *Biomed Res. Int.* 2015, 3–6. <https://doi.org/10.1155/2015/601543>
- Martin, J., Anamika, K., Srinivasan, N., 2010. Classification of protein kinases on the basis of both kinase and non-kinase regions. *PLoS One* 5, 1–12. <https://doi.org/10.1371/journal.pone.0012460>
- Meja, K., Stengel, C., Sellar, R., Huszar, D., Davies, B.R., Gale, R.E., Linch, D.C., Khwaja, A., 2014. PIM and AKT kinase inhibitors show synergistic cytotoxicity in acute myeloid leukaemia that is associated with convergence on mTOR and MCL1 pathways. *Br. J. Haematol.* 167, 69–79. <https://doi.org/10.1111/bjh.13013>
- Meng, X.-Y., Zhang, H.-X., Mezei, M., Cui, M., 2011. Molecular Docking: A Powerful Approach for Structure-Based Drug Discovery. *Curr. Comput. Aided-Drug Des.* 7,

146–157. <https://doi.org/10.2174/157340911795677602>

- N. Kirschner, A., Wang, J., Van Der Meer, R., Anderson, P.D., Franco-Coronel, O.E., Kushner, M.H., Everett, J.H., Hameed, O., Keeton, E.K., Ahdesmaki, M., Grosskurth, S.E., Huszar, D., Abdulkadir, S.A., 2015. PIM kinase inhibitor AZD1208 for treatment of MYC-driven prostate cancer. *J. Natl. Cancer Inst.* 107, 1–11. <https://doi.org/10.1093/jnci/dju407>
- Nowell, P.C., 1976. The Clonal Evolution of Tumor Cell Populations. *Science* (80- ). <https://doi.org/10.1126/science.959840>
- Pavlova, N.N., Thompson, C.B., 2016. The Emerging Hallmarks of Cancer Metabolism. *Cell Metab.* 23, 27–47. <https://doi.org/10.1016/j.cmet.2015.12.006>
- Peng, C., Wang, X., Chen, J., Jiao, R., Wang, L., Li, Y.M., Zuo, Y., Liu, Y., Lei, L., Ma, K.Y., Huang, Y., Chen, Z.Y., 2014. Biology of ageing and role of dietary antioxidants. *Biomed Res. Int.* 2014. <https://doi.org/10.1155/2014/831841>
- Perdew, J.P., Zunger, A., 1981. Self-interaction correction to density-functional approximations for many-electron systems. *Phys. Rev. B* 23, 5048–5079. <https://doi.org/10.1103/PhysRevB.23.5048>
- Pogacic, V., Bullock, A.N., Fedorov, O., Filippakopoulos, P., Gasser, C., Biondi, A., Meyer-Monard, S., Knapp, S., Schwaller, J., 2007. Structural analysis identifies imidazo[1,2-b]pyridazines as PIM kinase inhibitors with in vitro antileukemic activity. *Cancer Res.* 67, 6916–6924. <https://doi.org/10.1158/0008-5472.CAN-07-0320>
- Ren, J.X., Li, L.L., Zheng, R.L., Xie, H.Z., Cao, Z.X., Feng, S., Pan, Y.L., Chen, X., Wei, Y.Q., Yang, S.Y., 2011. Discovery of novel Pim-1 kinase inhibitors by a hierarchical multistage virtual screening approach based on svm model, pharmacophore, and molecular docking. *J. Chem. Inf. Model.* 51, 1364–1375. <https://doi.org/10.1021/ci100464b>
- Rumjanek, V.M., Trindade, G.S., Wagner-souza, K., 2001. Multidrug resistance in tumour cells : characterisation of the multidrug resistant cell line K562-Lucena 1 \* 73.
- Salgado, R., Moore, H., Martens, J.W.M., Lively, T., Malik, S., McDermott, U., Michiels, S., Moscow, J.A., Tejpar, S., McKee, T., Lacombe, D., 2018. Steps forward for cancer precision medicine. *Nat. Rev. Drug Discov.* 17, 1–2. <https://doi.org/10.1038/nrd.2017.218>
- Santio, N.M., Eerola, S.K., Paatero, I., Yli-Kauhaluoma, J., Anizon, F., Moreau, P., Tuomela, J., Haärkönen, P., Koskinen, P.J., 2015. Pim kinases promote migration and metastatic growth of prostate cancer xenografts. *PLoS One* 10, 1–20. <https://doi.org/10.1371/journal.pone.0130340>
- Scripture, C.D., Figg, W.D., 2006. Drug interactions in cancer therapy. *Nat. Rev. Cancer* 6, 546–558. <https://doi.org/10.1038/nrc1887>
- Slater, L.M., Sweet, P., Stupecky, M., Gupta, S., 1986. Cyclosporin A reverses

- vincristine and daunorubicin resistance in acute lymphatic leukemia in vitro. *J. Clin. Invest.* 77, 1405–1408. <https://doi.org/10.1172/JCI112450>
- Soler, J.M., Artacho, E., Gale, J.D., García, A., Junquera, J., Ordejón, P., Sánchez-Portal, D., 2002. The SIESTA method for ab initio order- N materials simulation. *J. Phys. Condens. Matter* 14, 2745–2779. <https://doi.org/10.1088/0953-8984/14/11/302>
- Song, K., Li, M., Xu, X.J., Xuan, L., Huang, G.N., Song, X.L., Liu, Q.F., 2014. HIF-1a and GLUT1 gene expression is associated with chemoresistance of acute myeloid leukemia. *Asian Pacific J. Cancer Prev.* 15, 1823–1829. <https://doi.org/10.7314/APJCP.2014.15.4.1823>
- Sosa, V., Moliné, T., Somoza, R., Paciucci, R., Kondoh, H., LLeonart, M.E., 2013. Oxidative stress and cancer: An overview. *Ageing Res. Rev.* <https://doi.org/10.1016/j.arr.2012.10.004>
- Stafman, L.L., Mruthyunjayappa, S., Waters, A.M., Garner, E.F., Aye, J.M., Stewart, J.E., Yoon, K.J., Whelan, K., Mroczek-Musulman, E., Beierle, E.A., 2018. Targeting PIM kinase as a therapeutic strategy in human hepatoblastoma. *Oncotarget* 9. <https://doi.org/10.18632/oncotarget.25205>
- Szakács, G., Paterson, J.K., Ludwig, J. a, Booth-Genthe, C., Gottesman, M.M., 2006. Targeting multidrug resistance in cancer. *Nat. Rev. Drug Discov.* 5, 219–34. <https://doi.org/10.1038/nrd1984>
- Theo Cuypers, H., Selten, G., Quint, W., Zijlstra, M., Maandag, E.R., Boelens, W., van Wezenbeek, P., Melief, C., Berns, A., 1984. Murine leukemia virus-induced T-cell lymphomagenesis: Integration of proviruses in a distinct chromosomal region. *Cell* 37, 141–150. [https://doi.org/10.1016/0092-8674\(84\)90309-X](https://doi.org/10.1016/0092-8674(84)90309-X)
- Trott, O., Olson, A., 2010. NIH Public Access. *J. Comput. Chem.* 31, 455–461. <https://doi.org/10.1002/jcc.21334>.AutoDock
- Troullier, N., Martins, J.L., 1991. Efficient pseudopotentials for plane-wave calculations. II. Operators for fast iterative diagonalization N. 43, 8861–8869. <https://doi.org/doi.org/10.1103/PhysRevB.43.8861>
- TURSYNBAY, Y., ZHANG, J., LI, Z., TOKAY, T., ZHUMADILOV, Z., WU, D., XIE, Y., 2016. Pim-1 kinase as cancer drug target: An update. *Biomed. Reports* 4, 140–146. <https://doi.org/10.3892/br.2015.561>
- Wacker, S. a, Houghtaling, B.R., Elemento, O., Kapoor, T.M., 2012. Using transcriptome sequencing to identify mechanisms of drug action and resistance. *Nat. Chem. Biol.* 8, 235–7. <https://doi.org/10.1038/nchembio.779>
- Wang, Z., Bhattacharya, N., Mixter, P.F., Wei, W., Sedivy, J., Magnuson, N.S., 2002. Phosphorylation of the cell cycle inhibitor p21 Cip1 / WAF1 by Pim-1 kinase. *Biochem. Biophys. Acta* 1593, 45–55. [https://doi.org/10.1016/S0167-4889\(02\)00347-6](https://doi.org/10.1016/S0167-4889(02)00347-6)
- Wang, Z., Bhattacharya, N., Weaver, M., Petersen, K., Meyer, M., Gapter, L.,



- Magnuson, N.S., 2001. Pim-1: a serine/threonine kinase with a role in cell survival, proliferation, differentiation and tumorigenesis. *J. Vet. Sci.*
- Wu, Q., Yang, Z., Nie, Y., Shi, Y., Fan, D., 2014. Multi-drug resistance in cancer chemotherapeutics: Mechanisms and lab approaches. *Cancer Lett.* 347, 159–166. <https://doi.org/10.1016/j.canlet.2014.03.013>
- Xie, Y., Burcu, M., Linn, D.E., Qiu, Y., Baer, M.R., 2010. Pim-1 kinase protects P-glycoprotein from degradation and enables its glycosylation and cell surface expression. *Mol. Pharmacol.* 78, 310–8. <https://doi.org/10.1124/mol.109.061713>
- Xie, Y., Xu, K., Linn, D.E., Yang, X., Guo, Z., Shimelis, H., Nakanishi, T., Ross, D.D., Chen, H., Fazli, L., Gleave, M.E., Qiu, Y., 2008. The 44-kDa Pim-1 kinase phosphorylates BCRP/ABCG2 and thereby promotes its multimerization and drug-resistant activity in human prostate cancer cells. *J. Biol. Chem.* 283, 3349–3356. <https://doi.org/10.1074/jbc.M707773200>
- Xie, Z.R., Hwang, M.J., 2010. An interaction-motif-based scoring function for protein-ligand docking. *BMC Bioinformatics* 11. <https://doi.org/10.1186/1471-2105-11-298>
- Zhukova, Y.N., Alekseeva, M.G., Zakharevich, N. V, Shtil, A.A., Danilenko, V.N., 2011. Pim family of protein kinases: Structure, functions, and roles in hematopoietic malignancies. *Mol. Biol.* 45, 695–703. <https://doi.org/10.1134/S0026893311040170>